THE ROLE OF HMG-COA REDUCTASE IN AHR-MEDIATED, TCDD-INDUCED LIVER INJURY

By

Amanda Michelle Jurgelewicz

A DISSERTATION

Submitted to
Michigan State University
in partial fulfillment of the requirements
for the degree of

Pharmacology and Toxicology – Environmental Toxicology – Doctor of Philosophy

2023

ABSTRACT

Non-alcoholic fatty liver disease (NAFLD) impacts 25% of the world's population and is expected to become the leading cause for liver transplantation; however, there are currently no recommended pharmaceutical interventions available for treatment. Exposure to environmental contaminants, such as 2,3,7,8-tetrachlorodibenzo-p-dioxin (TCDD), can elicit hepatopathologies in rodents that resemble NAFLD in humans. Most, if not all, of the toxic effects of exposure to TCDD are mediated by the aryl hydrocarbon receptor (AHR). Exposure to TCDD can also alter cholesterol homeostasis in mice and is implicated in increased prevalence of metabolic syndrome in humans, which are also leading risk factors for NAFLD development. Therefore, the primary goal of this dissertation was to gain a better understanding of the connection between AHR-mediated signaling, dysregulation of cholesterol and TCDD-induced liver injury in an effort to discover potential therapeutic options for treating NAFLD in the future.

First, a genome-wide association study (GWAS) was carried out to characterize regions of the genome that might be linked to TCDD-induced metabolic and physiological changes in mice. The goal of this GWAS was to identify key genes and/or pathways implicated in liver injury. Linear regression implicated 7 genes, 2 of which were novel, that were significantly associated with TCDD liver burden. Notably, TCDD-induced changes in body weight were associated with HMG-CoA reductase *(Hmgcr)*, which encodes the rate limiting step for cholesterol biosynthesis.

Secondly, a mouse study was undertaken to deduce the role of HMGCR in modulating TCDD-induced liver injury. This study used simvastatin, a competitive inhibitor of HMGCR, in the presence and absence of TCDD to determine if inhibition of cholesterol synthesis could affect TCDD-induced hepatosteatosis. Interestingly, simvastatin co-treatment was found to be

protective against AHR-mediated steatosis in both sexes. However, co-treatment induced sex-specific injury by increasing hepatic glycogen in females and exacerbating TCDD-induced liver injury in males. These results suggest that people who take statins are at greater risk of toxicant-induced liver injury.

Finally, single-nuclei RNA sequencing (snRNAseq) was utilized in mouse liver to gain a mechanistic understanding for statin-induced changes to TCDD-induced liver injury. Although co-treatment did not significantly alter liver pathology compared to TCDD alone, it was shown to alter relative proportions of distinct liver cell (sub)types and promote decreased immune cell infiltration. While these changes could be protective against liver injury, statin co-treatment was also associated with wasting and death, suggesting that taking statins as a treatment for NAFLD may lead to adverse consequences.

The results outlined in this dissertation provide insight on the role of cholesterol homeostasis in liver injury. Furthermore, while statin drugs have been suggested as a possible treatment for NAFLD, this work demonstrates how statins directly impact liver cell (sub)types proportions during toxicant-induced liver injury and suggests that they may have unintentional side effects in vulnerable populations. Although the impact of statins will need to be further evaluated in human NAFLD, we hope that the outcomes of this research can be used to inform the development of new treatment options for NAFLD patients.

To My Parents

ACKNOWLEDGEMENTS

There are many people that I would like to thank that made this research possible. First, I would like to thank my Ph.D. mentor, Dr. John LaPres. John has cultivated a great research environment to work in, and I have enjoyed my time working with him. John always has an optimistic outlook on science that helped through the many challenges I faced throughout my research. There were many times where it felt easier to give up, but his support and willingness to always help when I needed it were essential for me to stay confident in myself and my project. I am thankful to have been a member of his lab throughout my time at MSU in addition to his support as the director of both the BioMolecular Sciences and EITS programs.

I would also like to thank both past and present members of the LaPres lab that have been great peer mentors and help to me in my research. Dr. Peter Dornbos trained me when I joined the lab, was integral to a lot of the research presented in this dissertation and was also very helpful when learning how to write manuscripts and present my research. Even after he graduated from MSU, he was still willing to help me and give me advice. I appreciate the time he spent mentoring me to become a more independent scientist. I would also like to thank Michelle Steidemann. Not only did Michelle help me a lot with cell culture and western blotting advice, but we were both the only graduate students in the lab for most of my time at MSU. I appreciate her company, peer support and feedback. We also had many undergraduate students that worked in our lab over the years, and I want to thank them for helping me whenever they could with my project. Anooj Arkatkar was especially helpful with our computational work in Chapter 2, and Zach D'Haem was a big help with cell work. It has been a great experience to be a mentor to other students, and I hope that I have helped you all as much as you have helped me.

I want to thank our Superfund collaborators, especially Dr. Tim Zacharewski and his lab, who have been integral in all the *in vivo* work I have done. Dr. Rance Nault was essential computational help for processing our large sequencing datasets for downstream analysis and trained me in some of the techniques that I used in my research. Other past and present members of the lab, such as Drs. Kelly Fader, Russ Fling, and Giovan Cholico, have also been great help in performing and wrapping up our mouse studies. I also want to acknowledge and thank the NIEHS Superfund Program for providing funding for our research.

I want to thank my committee members, Drs. Norbert Kaminski, Jamie Bernard, and Sudin Bhattacharya. I appreciate all your great suggestions to aid my research progress as well as the time you took to be a part of my committee.

I want to thank the Pharmacology & Toxicology department and the EITS program for their support throughout my Ph.D. Drs. Anne Dorrance and Karen Liby were both helpful past and current graduate directors during my time in Pharm/Tox. Jake Wier and Meagan Kroll were extremely helpful as the past and current academic coordinators in Pharm/Tox to aid me in finishing my degree. The EITS program provided a lot of my funding throughout my time at MSU through the T32 fellowship, summer support and travel support for conferences. Kasey Baldwin and Amy Swagart in EITS/IIT were great help for any EITS-related questions. I want to thank the BioMolecular Sciences Program for inviting me to become a student at MSU and for their support during the first year, and the Biochemistry & Molecular Biology department for their facilities.

Last, but not least, I want to thank my friends and family. My parents have always been supportive throughout my life, especially through my journey to getting a Ph.D. Even though they are not scientists, they were always willing to learn as much as they could about my research. I

appreciate their never-ending support throughout everything I do. I also want to thank my grandma, who unfortunately passed during my time at MSU, for always showing me love and support in everything that I did. I hope I made you proud. I want to thank my partner, Earl. He has had to deal with the brunt of the good and the bad that comes with being a graduate student, and I appreciate his support through it all. I'm looking forward to our next chapter as graduate school comes to an end. Thank you to all my friends who have also been great moral support for me, especially Katie and Morgan. Also, thank you to my dog, Freddy, who has always found a way to cheer me up when I needed it. My road to getting a Ph.D. would have been a much more difficult journey if I did have the support and care from my family and friends. Thank you to everyone who has helped me in any way throughout my Ph.D. I appreciate all your assistance and support.

TABLE OF CONTENTS

LIST OF ABBREVIATIONS

ABCA1	ATP Binding Cassette Subfamily A Member 1
ABHD2	Abhydrolase Domain Containing 2, Acylglycerol Lipase
ACNAT1	Acyl-Coenzyme A Amino Acid N-Acyltransferase 1
ACSL4	Acyl-Coenzyme A Synthetase Long Chain Family Member 4
ACTB	Beta(β)-Actin
ADK	Adenosine Kinase
AHR	Aryl Hydrocarbon Receptor
ALT	Alanine Aminotransferase
ANGPTL3	Angiopoietin Like 3
ANOVA	Analysis of Variance
APOA1	Apolipoprotein A1
APOC2	Apolipoprotein C2
Ara9	AHR-Interacting Protein
ARNT	Aryl Hydrocarbon Receptor Nuclear Translocator
bHLH	Basic Helix-Loop-Helix
C1RA	Complement C1, R Subcomponent A
C3	Complement 3
C4B	Complement 4B
C4BP	Complement 4 Binding Protein
CD74	HLA Class II Histocompatibility Antigen Gamma Chain; Cluster of Differentiation 74

CYP1A1	Cytochrome P450 1a1
CYP1A2	Cytochrome P450 1a2
CYP1B1	Cytochrome P450 1b1
CYP4A10	Cytochrome P450 4a10
CYP4A14	Cytochrome P450 4a14
CYP51	Cytochrome P450 51
DAVID	Database for Annotation, Visualization and Integrated Discovery
DCs	Dendritic Cells
DEGs	Differentially Expressed Genes
DHCR7	7-dehydrochloesterol Reductase
DIO1	Iodothyronine Deiodinase 1
DREs	Dioxin Response Elements
ECL	Enhanced Chemiluminescence
ER	Endoplasmic Reticulum
FC	Free Cholesterol
FDFT1	Squalene Synthase
FDPS	Farnesyl Diphosphate Synthase
FDR	False Detection Rate
GBE1	1,4-Alpha-Glucan Branching Enzyme 1
GC/MS	Gas Chromatography / Mass Spectrometry
GC/MS/MS	Gas Chromatograph/High Efficiency Triple-Quadrupole Mass Spectrometry
GEO	Gene Expression Omnibus

GH	Growth Hormone
GUSB	Beta(β)-Glucuronidase
GYS2	Glycogen Synthase 2
HCC	Hepatocellular Carcinoma
HDL	High-Density Lipoprotein
H&E	Hematoxylin and Eosin
HK1	Hexokinase 1
HMGCR	3-hydroxy-3-methylglutaryl (HMG) Coenzyme A (CoA) Reductase
HMGCS1	3-hydroxy-3-methylglutaryl (HMG) Coenzyme A (CoA) Synthase
HP	Haptoglobin
HPRT	Hypoxanthine Phosphoribosyltransferase
HSCs	Hepatic Stellate Cells
HSP90	Heat Shock Protein 90
HTATIP2	HIV-1 Tat Interactive Protein 2
IDI1	Isopentenyl Diphosphate Delta Isomerase 1
IGF	Insulin-Like Growth Factor
IGF1	Insulin-Like Growth Factor 1
IGFBP1	Insulin-Like Growth Factor Binding Protein 1
IL-6	Interleukin-6
IRAK4	Interleukin 1 Receptor Associated Kinase 4
ELOVL6	ELOVL Fatty Acid Elongase 6
FC	Free Cholesterol

FICZ	6-formylindolo(3,2-b)carbazole
JNK	c-Jun N-terminal Kinase
KCs	Kupffer Cells
LCAT	Lecithin-Cholesterol Acyltransferase
LCS	Lab Control Spike
LDL	Low-Density Lipoprotein
LDLR	Low-Density Lipoprotein Receptor
LGALS9	Galectin 9
LIPG	Lipase G
LOD	Log of the Odds
LSECs	Liver Sinusoidal Endothelial Cells
LSS	Lanosterol Synthase
MAP3K8	Mitogen-Activated Protein Kinase Kinase Kinase 8
MAFFT	Multiple Alignment using Fast Fourier Transform
MB	Method Blank
MetS	Metabolic Syndrome
MIATE	Minimum Information about Animal Toxicology Experiments
MVD	Mevalonate Diphosphate Decarboxylase
MVK	Mevalonate Kinase
NAFLD	Non-Alcoholic Fatty Liver Disease
NASH	Non-Alcoholic Steatohepatitis
NHANES	National Health and Nutrition Examination Survey

NF-κB	Nuclear Factor Kappa-Light-Chain-Enhancer of Activated B Cells
NFKB1	Nuclear Factor Kappa B Subunit 1
NFE2L2	Nuclear Factor Erythroid 2-Related Factor 2
NLRP3	Nucleotide-Binding Domain, Leucine-Rich Repeat Family Pyrin Domain Containing 3 Inflammasome
NPTX1	Neuronal Pentraxin 1
PAFAH2	Platelet Activating Factor Acetylhydrolase 2
PAS	Per-Arnt-Sim
PASS	Periodic acid-Schiff Stain
PCBs	Polychlorinated Biphenyls
PDCs	Plasmacytoid Dendritic Cells
PEMT	Phosphatidylethanolamine N-Methyltransferase
PGM1	Phosphoglucomutase 1
PMM1	Phosphomannomutase 1
PMVK	Phosphomevalonate Kinase
PNPLA3	Patatin-like Phospholipase Domain-Containing Protein 3
PP	Pyrophosphate
PPAR	Proliferator-Activated Receptor
PPARA/α	Proliferator-Activated Receptor Alpha
PRKCB	Protein Kinase C Beta
PTMS	Parathymosin
PYGL	Glycogen Phosphorylase L

ORO	Oil Red O
QTL	Quantitative Trait Loci
QuHAnT	Quantitation Histological Analysis Tool
RIPA	Radioimmunoprecipitation Assay
ROS	Reactive Oxygen Species
SCAP	SREBP-Cleavage Activating Protein
SDS-PAGE	Sodium Dodecyl Sulfate-Polyacrylamide Gel Electrophoresis
SLC46A3	Solute Carrier Family 46 Member 3
SLCO1A4	Solute Carrier Organic Anion Transporter Family 1a4
SERPING1	Serpin Family G Member 1
snRNAseq	Single-Nuclei RNA Sequencing
SREBP2	Sterol Regulatory Element-Binding Protein 2
SQLE	Squalene Epoxidase
TBST	Tris-Buffered Saline with 0.05% Tween 20
TC	Total Cholesterol
TCDD	2,3,7,8-tetrachlorodibenzo-ρ-dioxin
TCDF	1,2,7,8-tetrachlorodibenzofuran
TNF	Tumor Necrosis Factor
TRAF3	TNF Receptor Associated Factor 3
T+S	TCDD and Simvastatin
UGP2	UDP-Glucose Pyrophosphorylase
UMAP	Uniform Manifold Approximation and Projection

Chapter 1: Introduction

Non-Alcoholic Fatty Liver Disease

Pathogenesis and Epidemiology

Non-alcoholic fatty liver disease (NAFLD) is an umbrella term that encompasses a spectrum of progressive liver pathologies ranging from fat accumulation (steatosis) or fat accumulation with inflammation (steatohepatitis or NASH) to irreversible changes such as fibrosis or cirrhosis that is caused by conditions outside of excessive alcohol use (Figure 1.1A).[1–4] NAFLD has become a global epidemic and prevalence continues to rise over time. It is estimated that it may affect as many as 25% of the world's population or as many as 1 billion individuals.[1,2,4] However, a recent report suggests that the worldwide prevalence may even be as high as 32.8%.[4] It is important to note that many epidemiology studies consider NAFLD prevalence to be steatosis specifically, so these values could be higher when considering cases of NASH, fibrosis or cirrhosis. The highest prevalence rates have been reported in the Middle East and South American countries (~30%), and the lowest prevalence has been seen in Africa (13%); however, the studies in African countries remain limited.[1,2] The prevalence in the United States and Europe is about the same at ~24-25%, or 64 million and 52 million people, respectively.[2,5] In Asian countries, there is a wide range of NAFLD prevalence (7.9%-43.3%), but it is particularly rising in areas with increasing urbanized lifestyles and changes to a more Western diet.[2,6] For example, in Shanghai, prevalence increased from 12.9% to 43.3% from 2003 to 2016, but the less urbanized areas in southern China have a prevalence of 9.1% as of 2012.[6] Racial disparities for NAFLD prevalence are mostly noted in studies conducted in the United States. It is estimated that the proportion of Americans with NAFLD of Hispanic descent have the highest prevalence (45%) followed by Americans of European descent (33%) and then Americans of African descent (24%).[2,6] The larger

prevalence in Hispanic Americans may be due, in part, to having a higher frequency of genetic variants in genes like *Pnpla3*.[1,2] It is unclear if sex influences NAFLD prevalence as there are some reports suggesting that prevalence is higher in females and some suggesting that it is higher in males.[2,4] However, NAFLD is strongly correlated to age. Older individuals are more likely to have more progressive liver injury and mortality possibly due to a longer duration of disease.[2]

Figure 1.1: Schematic of NAFLD progression. (A) A diagram of how NAFLD progresses from a healthy liver to carcinoma. (B) A representation of how free fatty acid accumulation can lead to the development of NASH that is partially adapted from figure 1 in Dowman *et. al*, 2010.[3] This figure was created using Biorender.com.

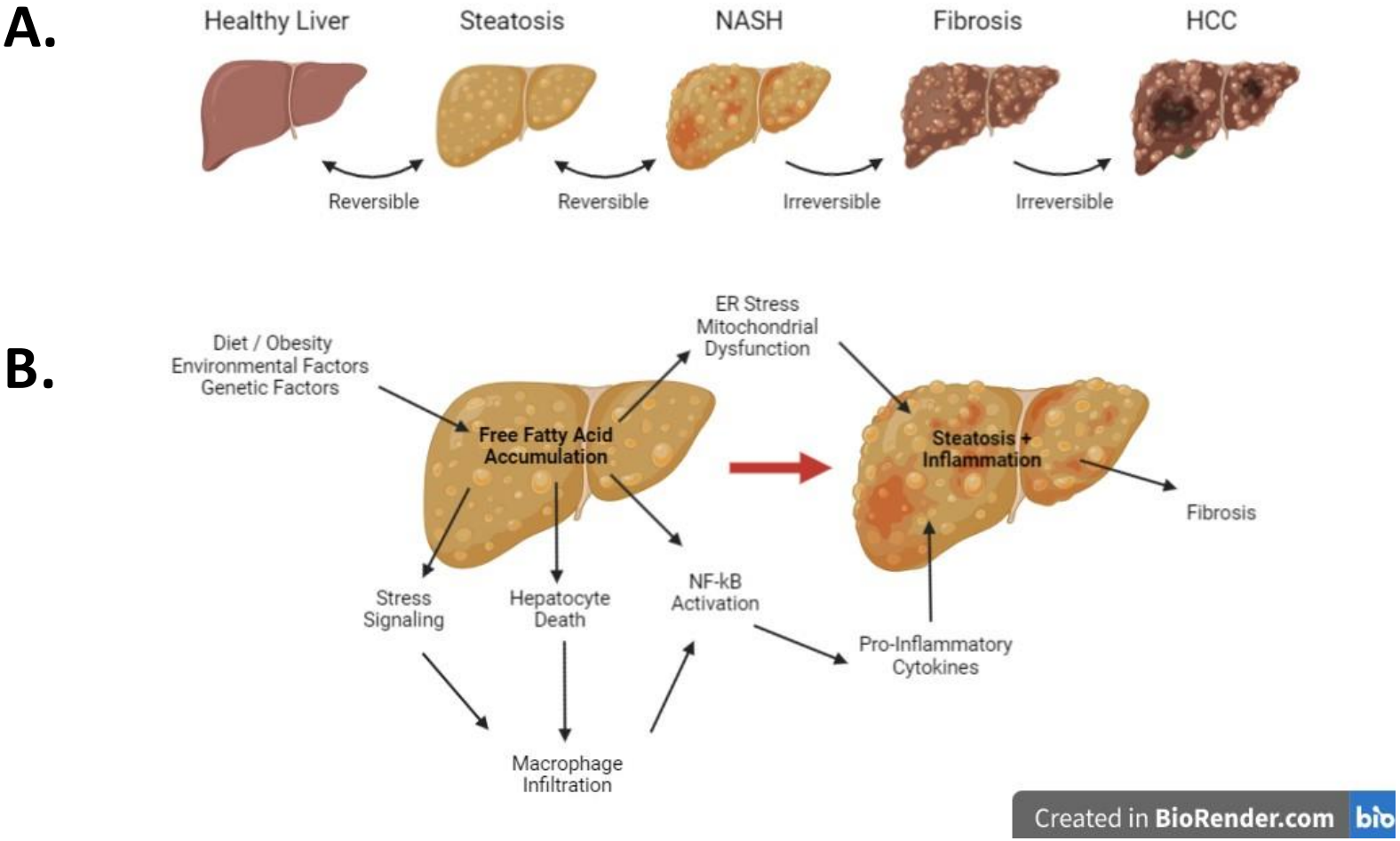

Liver injury is commonly thought of as a "multiple-hit" phenomenon.[1,3,7,8] The multiple "hits" is what can transform early stages of steatosis to NASH and then subsequent forms of damage (Figure 1.1B). The "first hit" in NAFLD is caused by an imbalance between fat delivery and its metabolism or secretion by the liver that can occur from multiple environmental factors such as weight gain, diet, increased free fatty acid mobilization to the liver or genetic factors like variants in *Pnpla3* that are associated with NAFLD development.[3,8] This results in fat accumulation in hepatocytes that predisposes them to increased susceptibility to secondary injuries or additional "hits" that lead to the development of NASH. These secondary "hits" can include pro-inflammatory cytokine production by Kupffer cells (KCs), mitochondrial dysfunction, oxidative stress and endoplasmic reticulum (ER) stress that contribute to the development of inflammation.[3,8–10] For example, fat deposition can initially protect hepatocytes from lipotoxicity; however, when the fat storage limit has exceeded, free fatty acids can activate hepatocyte oxidative stress or other stressors such as activation of NF-κB signaling that trigger localized inflammation.[1,3,9] If inflammation is unable to be managed and damage continues to occur to the liver, it can lead to activation of hepatic stellate cells (HSCs) that can induce a fibrogenic response that produces permanent scarring.[3,7,9,11] Advanced fibrosis can result in liver failure, portal hypertension and the need for liver transplantation.[3,11] Activation of HSCs and fibrosis can also influence the development of hepatocellular carcincoma (HCC).[11] For example, extracellular matrix deposits in a fibrotic liver can bind to hepatocyte growth factors and stimulate the growth and survival of transformed cells.[11] NAFLD is currently the leading cause of chronic liver disease worldwide, and it is expected to become the number one cause for liver transplantation.[1–3,6,12]

Early stages of NAFLD are difficult to diagnose due to many patients testing normal in liver function tests and there are no validated non-invasive tests for NASH, thus requiring the need for procedures like liver biopsies for formal diagnosis.[1,2,10,12] Therefore, it is difficult to measure the true prevalence of each stage of NAFLD progression and many diagnostic criteria are not consistent.[5] In the total population of the United States, it is estimated that ~25% has NAFLD defined as greater than 5% hepatic fat accumulation, ~5% has NASH (with or without fibrosis) and ~1.25% has NASH cirrhosis (NASH with the presence of advanced fibrosis) as of a study published in 2021.[5] A prediction model that estimated growth in cases from 2015 to 2030 in the United States estimates that NAFLD prevalence is expected to increase by 21%, NASH prevalence is expected to increase by 63%, incidence of decompensated cirrhosis is predicted to increase by 168% and the incidence of HCC is projected to increase by 137%.[5,13] The mortality rates caused by chronic liver disease are typically low in NAFLD patients. About 4-8% of those will pass from cirrhosis-related complications and 1-5% from developing HCC, and most patients with NAFLD will pass from cardiovascular disease (40%).[1,12] However, there has been a 170% increase in the cases of NASH on the liver transplant waiting list in the United States, and the proportion of total transplants due to NASH increased from 1.2% in 2001 to 9.7% in 2009.[1,12] Currently, the economic burden of NAFLD in terms of direct annual medical costs is estimated to be $103 billion in the United States alone, so NAFLD is a significant public health burden worldwide.[14]

Risk Factors and Treatment Options

There are many risk factors for NAFLD development, but the most common co-morbidities associated with NAFLD are obesity, metabolic syndrome, diabetes, and exposure to

environmental contaminants. The worldwide prevalence of obesity among those with steatosis and NASH is 51% and 81%, respectively.[10] Increased abdominal weight can cause excess fat accumulation promoting steatosis of the liver, and it has been shown that increased areas of visceral adipose tissue were longitudinally associated with higher incidence of NAFLD.[10,15] It's estimated that 95% of severely obese patients undergoing bariatric surgery will have NAFLD.[2] Diabetes, especially type 2, is highly prevalent in NAFLD patients as insulin resistance can also promote liver damage. Globally, 55.5% of patients with type 2 diabetes are estimated to also have NAFLD with the highest prevalence in Europe (68%).[10] There is also a large prevalence of NASH (37%) and advanced fibrosis (37.3%) in individuals with NAFLD and type 2 diabetes.[10] The many type 2 diabetic or obese patients with NAFLD also have metabolic syndrome (MetS), which is a cluster of metabolic conditions that increase the risk for cardiovascular disease.[10] These conditions include excess fat in the waist, high blood pressure, high blood sugar, abnormal cholesterol levels and high triglyceride levels. In a cohort study of over 11,000 Americans, it was shown that while 18.2% of the total cohort had NAFLD, the incidence was much larger in those with MetS (43.2%) and the prevalence increased with the number of MetS criteria met (67% of those meeting all 5 criteria).[10,16] In this same study, advanced fibrosis cases almost doubled in patients with MetS and was almost 5 times greater in patients with all 5 criteria.[10,16] In a global study including over 8.5 million individuals from 22 countries, metabolic comorbidities were very high in those with NAFLD, including obesity (51.34%), type 2 diabetes (22.51%) and metabolic syndrome (42.54%).[12] Thus, metabolic abnormalities greatly increase the risk for development of NAFLD. However, exposure to environmental contaminants also has a strong connection to NAFLD pathogenesis. Xenobiotics including polychlorinated biphenyls (PCBs), hydrocarbons,

dioxins, pesticides, and more are becoming recognized as contributors to liver disease.[17–20] Analysis of the National Health and Nutrition Examination Survey (NHANES) from 2003-2004 indicated that environmental pollutants such as heavy metals and PCBs were associated with dose-dependent increases in alanine aminotransferase (ALT) elevation, a marker of liver injury in humans.[17–20] Furthermore, in rodent studies, various xenobiotics have been shown to induce steatosis, oxidative stress, NASH and even fibrosis.[17,19–22] Human exposure to toxicants, such as dioxins, is also associated with increased incidence of metabolic risk factors of NAFLD including MetS.[23,24] Therefore, although much focus of NAFLD risk is focused on metabolic comorbidities, exposure to environmental contaminants is also an important factor to explore.

While the risk of NAFLD will continue to rise as concern over environmental pollution and cases of metabolic disorders is growing over time, there are currently no recommended pharmaceutical interventions available to directly treat hepatopathologies present in NAFLD patients.[1,12] Therefore, NAFLD is commonly treated through improving the risk factors that are associated with development. This primarily involves dietary management, exercise, or bariatric surgery to promote weight loss and improve conditions associated with MetS.[1,10]

Liver Structure and Functions

The liver is a major organ in the body responsible for many essential biological functions. These functions include, but are not limited to, metabolism (lipids, cholesterol, carbohydrates, etc.), protein synthesis (albumin, clotting factors, etc.), energy homeostasis, detoxification of xenobiotics and enterohepatic circulation. The liver is also the only internal organ capable of regeneration. These roles are enabled due to the spatial organization of distinct liver cell types

in the functional units of the liver known as hepatic lobules. The major liver cell types include, but are not limited to, hepatocytes, Kupffer cells (KCs), hepatic stellate cells, liver sinusoidal endothelial cells (LSECs) and cholangiocytes (Figure 1.2).[25–29] Within liver lobules, nutrient-rich blood from the portal vein and oxygen-rich blood from the hepatic artery travels from the portal triad (zone 1) through the midlobular region (zone 2) to the central vein (zone 3).[25–27] This results in a gradient of oxygen and nutrients across the lobule and thus functional heterogeneity across the gradient to optimize roles for the level of oxygen and nutrients in different regions.[25–27] For example, functions requiring larger amounts of oxygen, such as cholesterol biosynthesis, glucogenogenesis or β-oxidation, take place in zone 1 and functions that do not require as much oxygen, such as xenobiotic metabolism, lipogenesis or glycolysis, take place in zone 3.[25–27] This spatial organization allows for opposing metabolic functions to work effectively.[25–27] However, when the functional relationship between liver cell types becomes disrupted, it can lead to adverse health consequences in the liver, including NAFLD.[28,30] The primary cell types associated with liver injury are hepatocytes, KCs and HSCs. [1,3,7–9]

Figure 1.2: Liver Anatomy in Hepatic Lobules. A diagram depicting the hepatic zonation of liver lobules, the major liver cell types, and aryl hydrocarbon receptor (AHR) expression across the lobule. Nutrient and oxygen-rich blood will travel from the portal triad (zone 1) to the central vein (zone 3) resulting in zone-specific metabolic functions. This figure was adapted from Figure 1 in Cunningham and Porat-Shilom, 2021.[25] This figure was created using Biorender.com.

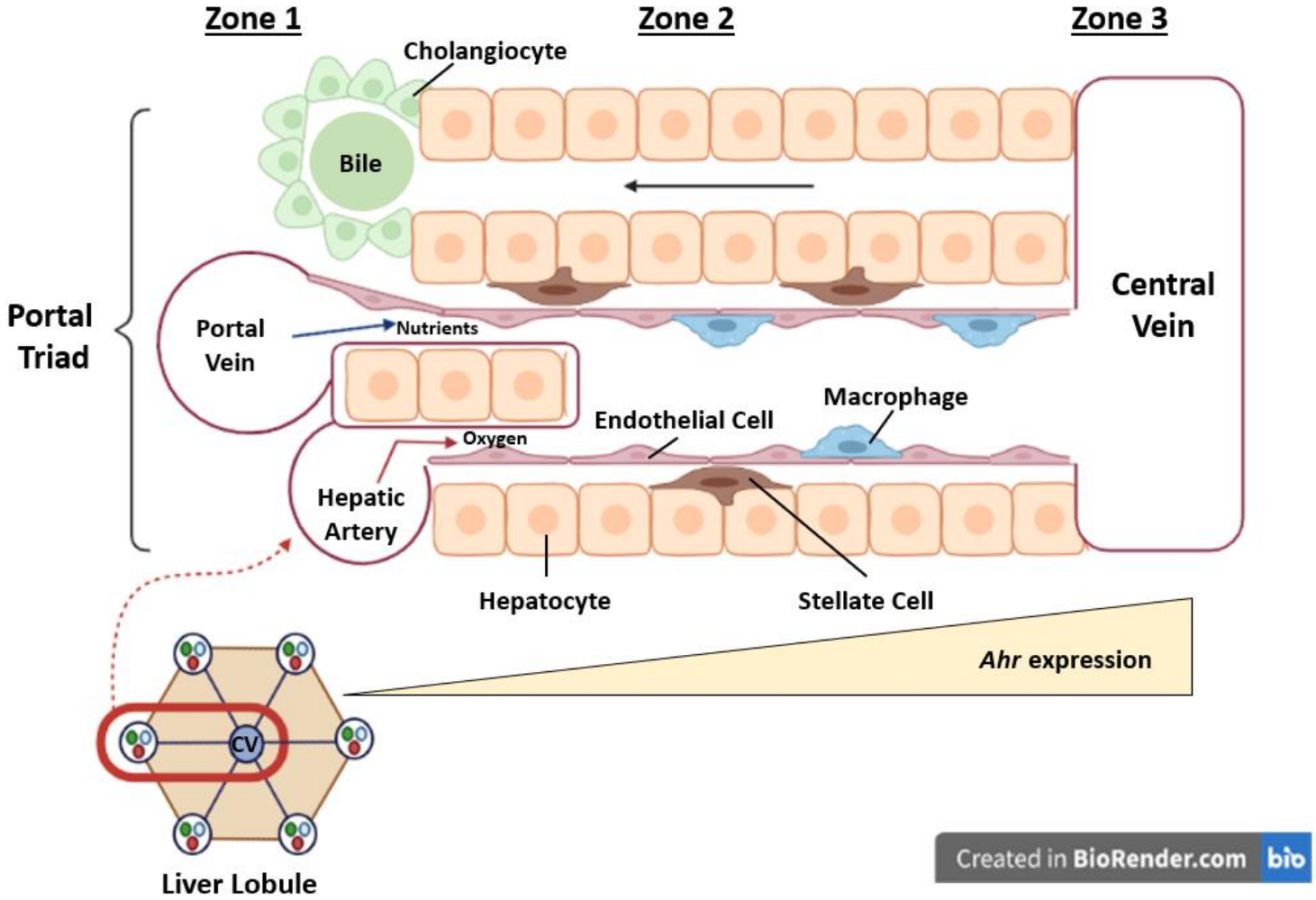

Main Liver Cell Types and Their Functions

Hepatocytes are the main parenchymal cells of the liver, and they make up about 80% of the total mass of the liver. This cell type is responsible for the major functions in the liver including protein synthesis, carbohydrate metabolism, lipid metabolism and detoxification. Due to the spatial division of labor across the lobules to optimize for oxygen and nutrient levels, hepatocytes exist as a gradient across the lobule with functional heterogeneity.[25–27] While periportal hepatocytes and centrilobular hepatocytes both express genes involved in various metabolic pathways, the level of expression will exist as a gradient to correspond to the primary functions in their respective locations.[25–27] In the oxygen and nutrient-rich environment, periportal hepatocytes will display higher expression of genes involved in gluconeogenesis, for example, while centrilobular cells, located in a more hypoxic and nutrient sparce environment, will have higher expression of genes involved in glycolysis.[25–27] Therefore, this gradient of enzyme expression can influence where drugs or toxicants elicit damage within the lobules as it can influence where they will preferentially accumulate.[28,30]

Kupffer cells are the resident macrophages of the liver that are primarily responsible for removing foreign debris. However, they can also produce pro-inflammatory mediators in response to liver injury contributing to the development of inflammation.[3,9] KCs display heterogeneity across liver lobules like hepatocytes even though they are non-parenchymal cells. KCs are more highly expressed in the periportal region due to the direct blood flow into the liver and display more phagocytotic activity in this area.[25,31] Other immune cell types within the liver are also generally more enriched in this region though it remains challenging to map the zonation of less expressed cell types as they can be masked by the abundance of hepatocytes.[25]

Hepatic stellate cells are also an important cell type in the context of progressive liver injury. In normal conditions, HSCs exist in a quiescent state and their function when inactivated remains unclear. However, liver injury like inflammation and hepatocyte damage will send signals to HSCs causing them to become activated.[3,32] Activated HSCs are a major source of extracellular matrix production that is used to produce scarring at sites of injury to protect the liver.[3,32] Prolonged activation of these cells can induce widespread fibrosis that impacts liver function. However, HSCs activation have also been implicated in assisting with liver regeneration such as producing angiogenic factors and factors that promote hepatocyte proliferation.[32]

The other 2 major cell types in the liver are liver sinusoidal endothelial cells (LSECs) and cholangiocytes. LSECs are a permeable barrier separating hepatocytes and HSCs from blood. They primarily regulate vascular tone in the liver, contain fenestrae that filter fluid between blood and the space of Disse containing hepatocytes and HSCs and regulate quiescence of HSCs.[33] Cholangiocytes are another type of endothelial cell that line the bile duct. Their major function is to modulate bile as it is transported along the biliary tree.[34] This process involves a coordinated transport of various proteins, ions, water, and solutes to and from the bile that is modulated by various signaling pathways and molecules.[34] While there are 11 predominant cell types that make up liver lobules, hepatocytes, KCs, HSCs, LSECs and cholangiocytes are the major cell types that contribute to the major functioning of the liver. Additionally, there are many receptors within the liver that contribute to proper functioning and liver development, including the aryl hydrocarbon receptor (AHR).

Aryl Hydrocarbon Receptor (AHR)

The AHR is a transcription factor in the basic helix-loop-helix (bHLH)/Per-Arnt-Sim (PAS) family of environmental sensing proteins. The AHR is primarily known for its role in xenobiotic metabolism, and as a result, it's highly expressed in the centrilobular region (Figure 1.2). It has been suspected to also have some endogenous roles in addition to xenobiotic metabolism.[35,36] AHR-deficient or null mice have been shown to have many impairments including an ~50% reduction in liver size, reduced fertility and several impacts on the immune system such as being defective in T-cell differentiation, suggesting that the AHR may play an important role in the development of the liver, reproductive organs and immune system.[35]

The general structure of the AHR includes 4 conserved domains (Figure 1.3).[35–37] The bHLH region in the N-terminus is required for DNA binding and protein dimerization.[35,36] The PAS domain is located adjacent to the C-terminal end of the bHLH region and contains two sub-domains, PAS-A and PAS-B.[35,36] This PAS domain is a docking site for hetero- or homodimerization of other PAS proteins, such as the aryl hydrocarbon receptor nuclear translocator (ARNT), and also where the chaperone protein, Heat Shock Protein 90 (HSP90), binds to stabilize the AHR in the cytosol.[35,36,38] The PAS-B domain is also where the AHR-interacting protein (ARA9), another chaperone protein, binds to the AHR for stabilization, and it contains a ligand binding site.[35,36,39] The Cryo-EM structure of the AHR showed that the HSP90-ARA9-AHR complex is active upon ligand binding, and the presence of p23, another chaperone protein, is not required for this interaction.[37] The ligand binding domain consists of 5 β-sheets and 4 α-helices, and the site adjacent to the Fα location within the ligand binding pocket in the PAS-B domain is the primary anchor point of AHR ligands with a secondary anchor point near the Cα location in this domain.[37]

This location holds all the structural and molecular determinants that control ligand binding specificity and affinity to the AHR.[37] The final conserved domain is the transactivation domain that can interact with transcriptional co-activators utilized to modulate gene expression.[35,36]

Figure 1.3: General organization of the aryl hydrocarbon receptor. This figure outlines the general positioning and functions of the major 4 domains of found on the AHR. This includes the basic helix-loop-helix (bHLH), the Per-Arnt-Sim (PAS) A and B domains and the transactivation domain (TAD). This figure was adapted from figure 5 in Okey, 2007.[40]

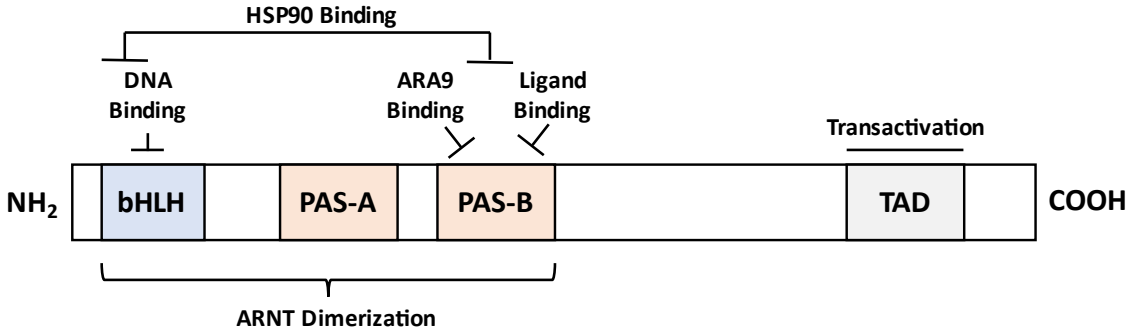

In mice, there are different alleles of the *Ahr*, but the 4 domains are still conserved. The B allele is known as a 'responsive' allele to AHR ligands with high affinity binding sites.[36,41] The D allele is known as a 'non-responsive' allele.[36,41] This is caused by a mutation in the PAS-B domain of D allele mice, particularly due to an amino acid switch from valine, present in responsive strains, to alanine at residue 375.[42] The B allele also has 3 different receptor forms. While all forms are responsive to AHR ligands, they have varied molecular weights of the AHR: B1, 95 kD; B2, 104 kD; and B3, 105 kD.[36] B1, B2 and D alleles are found in *Mus musculus* strains of mice, and B3 allele strains are found in wild-derived species like *Mus spretus.*[36]

The AHR has both exogeneous and endogenous ligands. Exogeneous ligands of the AHR include 2 main classes: halogenated aromatic hydrocarbons and polycyclic aromatic hydrocarbons.[35,36] Halogenated aromatic hydrocarbons include compounds like polychlorinated biphenyls (PCBs) and polychlorinated dibenzodioxins like 2,3,7,8-tetrachlorodibenzo-ρ-dioxin (TCDD). Polycyclic aromatic hydrocarbons include compounds like benzo[a]pyrene and benzoflavones. Exogenous ligands of the AHR are particularly associated with adverse health effects. Endogenous ligands include naturally occurring compounds such as kynurenine or 6-Formylindolo(3,2-b)carbazole (FICZ).[35,36] Discovery of more endogenous ligands of the AHR may lead to more clues on the endogenous roles of the AHR in the future.

Although there are various *Ahr* alleles in mice and ligands for the AHR, ligand exposure and subsequent binding to the AHR will lead the activation of the canonical AHR signaling pathway (Figure 1.4). In the absence of a ligand, the AHR is found in the cytosol bound to its chaperone proteins HSP90 and ARA9 that stabilize it.[37–39,43] Ligands such as TCDD can readily pass through the plasma membrane of the cell once it enters the body and will bind to the AHR in the

cytosol. The chaperone proteins will dissociate from AHR, and the AHR:TCDD complex will translocate into the nucleus and heterodimerize with ARNT.[35,44] The newly formed complex can bind to specific regions on the DNA known as dioxin response elements (DREs), which will lead to changes in gene expression.[36,45] For example, AHR activation will induce expression of xenobiotic metabolizing enzymes like *Cyp1a1* or *Cyp1a2* that are a part of the AHR gene battery. The changes in gene expression in diverse pathways may play an important role in toxicant-induced adverse pathologies seen upon exposure. It has been shown that AHR-deficient mice are relatively unaffected by doses of TCDD 10-fold higher than what is found to induce severe toxic effects in mice expressing a functional AHR.[46]

Figure 1.4: The canonical AHR signaling pathway. TCDD will readily pass through the plasma membrane where it will bind to AHR (1). AHR will dissociate from its chaperone proteins and the AHR:TCDD complex will translocate into the nucleus (2-3). The AHR:TCDD complex will heterodimerize with ARNT (4). This new heterodimer can bind to dioxin response elements (DREs) on DNA leading to changes in gene expression in a variety of pathways, such as induction of the AHR gene battery (5).

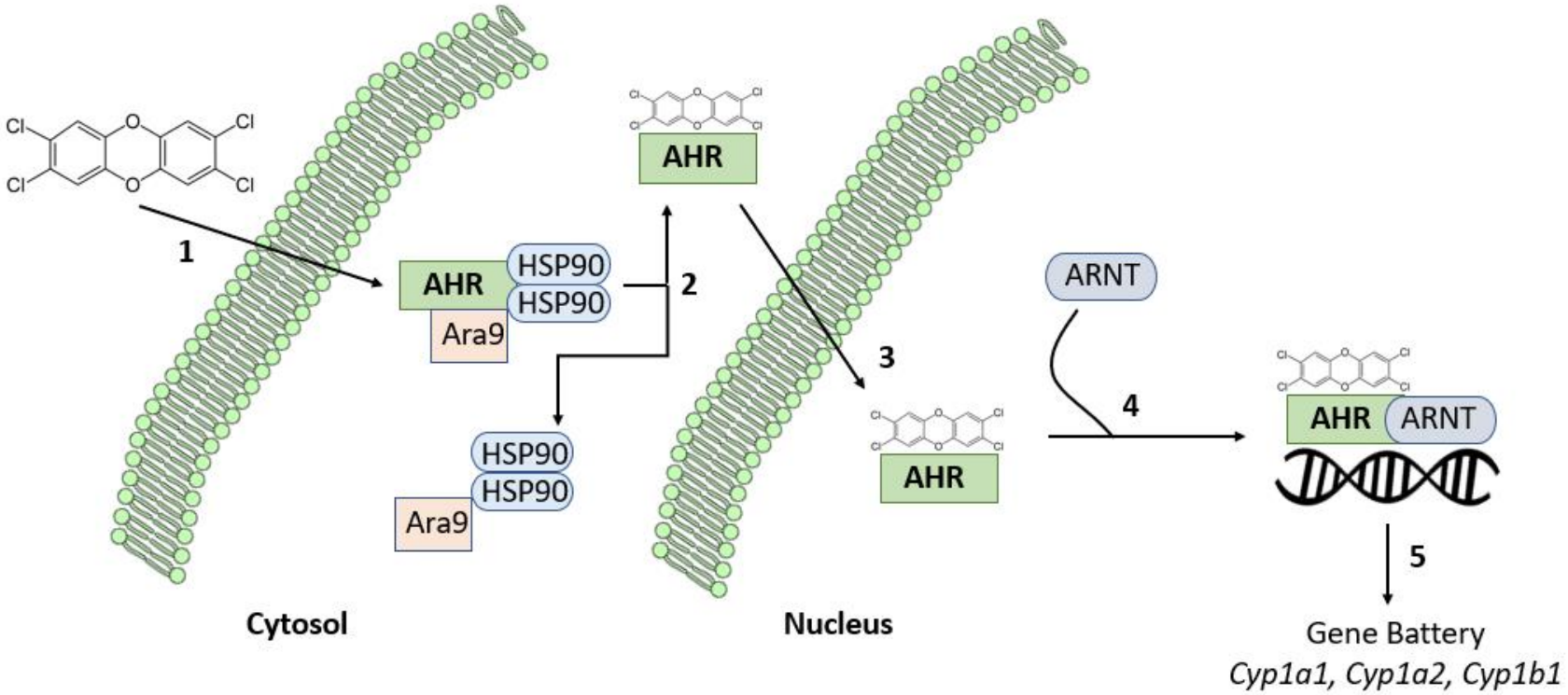

2,3,7,8-Tetrachlorodibenzo-ρ-dioxin (TCDD)

The prototypical and most studied ligand for the AHR is TCDD. TCDD is a persistent, polyhalogenated organic pollutant that is of environmental concern. It is primarily created as an unwanted byproduct of incomplete combustion of organic materials in manufacturing processes such as the creation of herbicides or pesticides but also during waste incineration or chlorine bleaching of paper.[19] It is infamous as being a contaminant in Agent Orange, used during the Vietnam War, and as the poison given to Victor Yushchenko.[47] Very recently, there has been growing concern over the potential release of TCDD and/or other dioxins in East Palestine, Ohio as a result of the burning of vinyl chloride caused by the train derailment in February 2023. The highest known exposure to TCDD in residential populations occurred during the industrial accident in Seveso, Italy in 1976.[23,48] Although these major events led to high levels of TCDD exposure to humans, the background exposure to TCDD is typically quite low, with lipid-adjusted TCDD levels of 1 to 10 ppt in serum.[49] People are most commonly exposed to TCDD through consumption of contaminated foods, especially foods with high fat content such as fish or dairy products, as TCDD is highly lipophilic.[19] Due to its very stable chemical structure, TCDD bioaccumulates in organisms, and its levels are highly correlated with age.[50] Additionally, TCDD has a long half-life in humans of up to 11 years, and as a result, this can lead to long-term health consequences from TCDD exposure.[23,51]

There is strong evidence that TCDD exposures drive adverse health outcomes in humans and rodents through AHR-mediated signaling.[22,46] In humans, TCDD exposure commonly leads to the development of chloracne seen in multiple exposures including the Seveso incident and the poisoning of Victor Yushchenko.[23,47,48] Additionally, TCDD can induce immunosuppression in

humans.[48,52,53] Notably, TCDD exposure has been associated with increased incidence of metabolic disorders in humans including NAFLD, diabetes and metabolic syndrome.[23,24] The impacts of TCDD on liver injury have been well-documented in rodents.[21,22,49,54] TCDD has been shown to elicit dose-dependent increases in hepatic steatosis, NASH and fibrosis.[21,22] When dosing C57Bl6/J mice every 4 days for 92 days, hepatic lipid accumulation can be seen in doses as small as 0.3 μg/kg as well as inflammation at 1 μg/kg and fibrosis at 10 μg/kg.[21] In as short as a 28-day treatment paradigm, lipid accumulation can be seen at 1 μg/kg with inflammation at 10 μg/kg and fibrosis at 30 μg/kg.[21] Interestingly, male mice exhibit greater sensitivity to TCDD-induced hepatotoxicity compared to females and exhibit more severe damage at lower doses.[54] While much remains unclear about this sex-specific difference, it has been shown that the liver transcriptome in males is more dysregulated by TCDD treatment in comparison to females.[55] Although TCDD has been shown to elicit liver damage, much remains unknown about the mechanism for how AHR-mediated signaling drives these toxic effects. Therefore, there have been emerging studies analyzing the impact of TCDD treatment on metabolic pathways that could influence the development of liver injury, such as alterations in cholesterol homeostasis.[49,54,56]

Cholesterol Homeostasis

Regulation of Cholesterol Homeostasis

Cholesterol homeostasis is tightly regulated in the body due to the necessity of cholesterol in various processes. Cholesterol is essential for cell membrane maintenance and fluidity and is a precursor for producing steroids including Vitamin D and sex hormones.[57,58] While

many cells can synthesize cholesterol, at least 50% of total synthesis in the body occurs within hepatocytes in the liver.[57] The body is responsible for producing about 80% of total cholesterol it needs while about 20% comes from dietary sources.

Cholesterol biosynthesis requires a long chain of reactions to produce cholesterol. However, the early stage of converting 3-hydroxy-3-methylglutaryl coenzyme A (HMG-CoA) to mevalonate by HMG-CoA reductase (HMGCR) is the rate-limiting step that will largely control if cholesterol is synthesized.[57,58] Cholesterol biosynthesis is regulated by the sterol regulatory binding-element protein 2 (SREBP2) located in the endoplasmic reticulum (ER), which will sense levels of cholesterol that are present intracellularly.[57,58] Low levels of cholesterol will be detected by the SREBP-cleavage activating protein (SCAP) located on the C-terminal of SREBP2, and this the SCAP-SREBP2 complex will translocate from the ER to the Golgi apparatus to activate SREBP2 via cleaving an N-terminal fragment from the protein.[57,58] The homodimerized, processed form of SREBP2 can enter the nucleus where it functions as a transcription factor and upregulates expression of various enzymes in the cholesterol biosynthesis pathway in addition to the low-density lipoprotein receptor (LDLR) that is responsible for bringing cholesterol back into the cells.[57,58] Low levels of cholesterol will promote translation of proteins like HMGCR for synthesis.[57,58]

If cholesterol levels are high, biosynthesis can be turned off. Increasing levels of cholesterol can signal for degradation of HMGCR, phosphorylation of HMGCR that inhibits activity of the enzyme or inhibition of transcription by not activating SREBP2.[57,58] It can also inhibit synthesis of LDLR to prevent cholesterol from entering the cells.[57,58] Notably, the mevalonate pathway that includes this rate-limiting step is also utilized to make additional

compounds. Farnesyl pyrophosphate is a branching off point that is used to make compounds such as ubiquinone that is used by the mitochondria in the electron transport chain. Thus, it has been suggested that the enzyme squalene epoxidase (SQLE), used to convert squalene to 2,3-oxidosqualene, may be another rate-limiting enzyme after HMGCR in the cholesterol biosynthesis pathway.[57,58] This step occurs after the production of farnesyl pyrophosphate, so degradation of SQLE or inhibition of its transcription by SREBP2 can shut down cholesterol biosynthesis while maintaining synthesis of compounds using farnesyl pyrophosphate.[57,58]

Figure 1.5: The cholesterol biosynthesis pathway. The early stages of cholesterol biosynthesis and the enzymes that are responsible for catalyzing each step. The rate-limiting step is the conversion of HMG-CoA to mevalonic acid, also known as mevalonate.

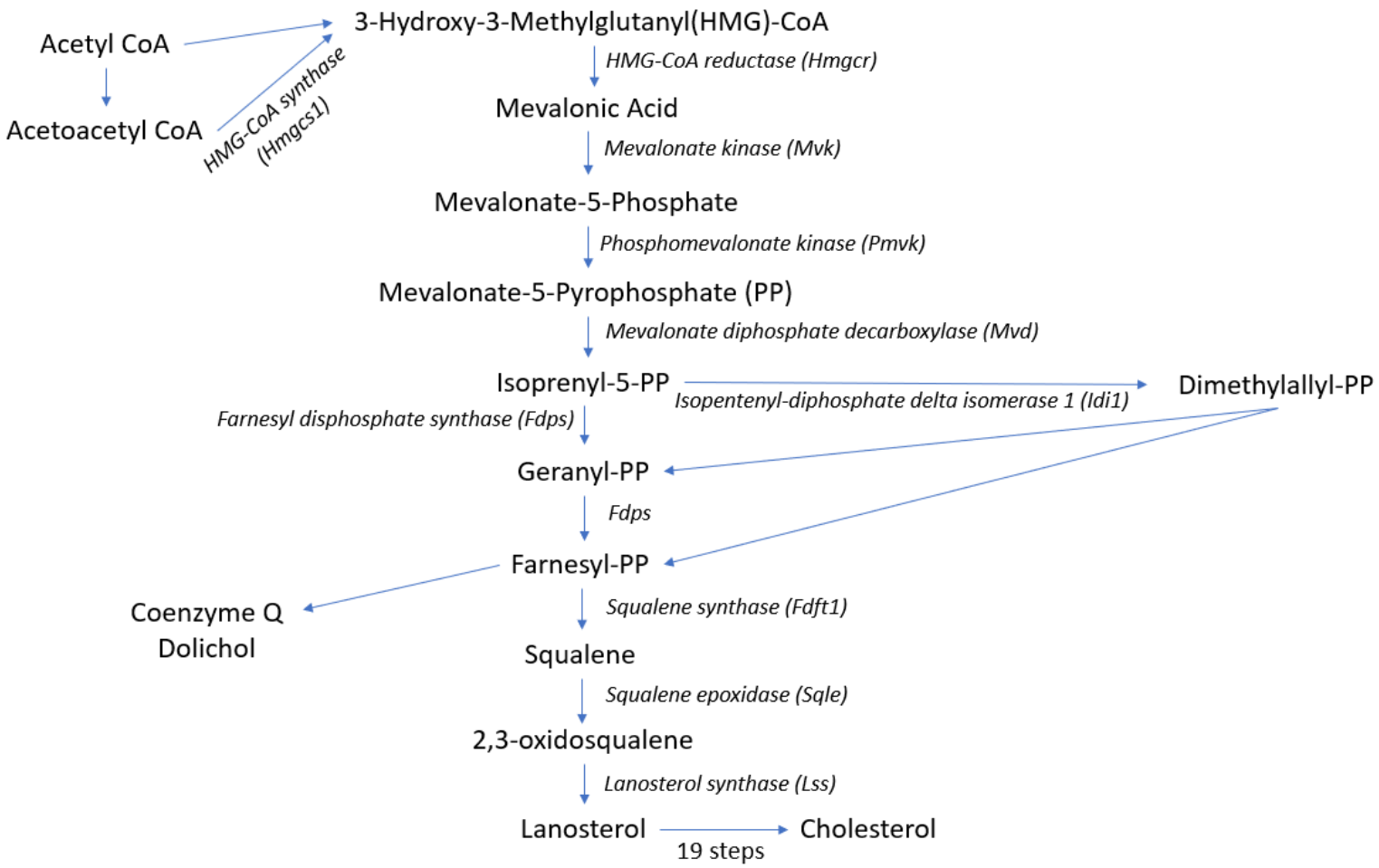

The liver is also largely responsible for cholesterol transport, metabolism, recycling, and excretion. Cholesterol is hydrophobic, so it is packaged into lipoproteins within the liver that can readily travel through the bloodstream to other areas of the body. There are several types of lipoproteins in the blood, but low-density lipoproteins (LDL) and high-density lipoproteins (HDL) are most utilized for cholesterol transportation.[57,58] LDL molecules are the major blood cholesterol carriers and they are recognized by LDL receptors (LDLRs) to bring large amounts of cholesterol back into the cell.[57,58] If cholesterol levels are high within cells or this process becomes dysregulated, LDL molecules will remain in the blood where they can be converted into foam cells by macrophages.[59] Foam cells are highly associated with plaque formation in arteries that may lead to cardiovascular disease due to impaired blood flow.[59] HDL molecules are instead thought to be responsible for reverse cholesterol transport or the process of bringing excess cholesterol from peripheral tissues back to the liver for redistribution or removal.[57,58] Therefore, high circulating levels of LDL is associated with "bad" cholesterol and high circulating levels of HDL is associated with "good" cholesterol in humans. If cholesterol is not needed, it can be oxidized into bile acids where it will be excreted from the liver into bile.[60] The bile will undergo enterohepatic circulation where bile acids can be recycled back to the liver or be excreted from the body.[60]

Dysregulation of Cholesterol and Liver Injury

Cholesterol homeostasis has been shown to be extensively dysregulated in NAFLD. In human liver biopsies of patients with confirmed NAFLD, it has been shown that NAFLD was associated with increased maturation of SREBP2, more mRNA and protein expression of HMGCR,

and decreased phosphorylation of HMGCR.[61] The increased levels of HMGCR corresponded to higher levels of hepatic free cholesterol (FC), worse histological severity of NAFLD and increased levels of serum LDL.[61] Additionally, animal studies have shown that induction of hepatic FC accumulation promotes steatohepatitis and fibrosis and correcting the overload of FC improves disease severity in NASH.[62] Another study showed that cholesterol crystals were present within hepatocytes in both patients with NASH and mice fed a high-fat-high-cholesterol diet, but not in mice with simple steatosis.[63] The high-fat diet fed mice had enlarged KCs containing cholesterol droplets with an appearance similar to foam cells, which was not seen in mice with simple steatosis, suggesting that cholesterol accumulation promotes more severe forms of liver injury.[63]

There have been some suggested mechanisms for how hepatic FC accumulation may be associated with the development of liver injury. One potential mechanism may be due to ER stress. Chronic ER stress is associated with induction of pathways that lead to the development of steatosis, inflammation, and hepatocyte cell death.[62] Reports have suggested that cholesterol accumulation in the ER membrane can induce ER stress, and the unfolded protein response in the ER may be activated in NAFLD through JNK signaling.[62] Another potential mechanism is due to mitochondrial dysfunction. Mitochondria are very sensitive to changes in membrane fluidity due to cholesterol accumulation leading to dysfunction.[62] Increased levels of cholesterol in the mitochondria can lead to decreases in ATP synthesis and decreased stores of mitochondrial-reduced glutathione, an antioxidant that controls reactive oxygen species generation.[62] Thus, cholesterol accumulation can result in hepatocytes being more susceptible to oxidative stress.

Notably, TCDD exposure is associated with alterations in cholesterol homeostasis. TCDD, via the AHR, can suppress expression of key enzymes involved in cholesterol biosynthesis

including HMGCR, SQLE, squalene synthase (FDFT1) and SREBP2, in mice and primary human hepatocytes.[56,64] These changes in expression correlate to alterations in circulating cholesterol levels. TCDD exposure in mice was shown to cause a 20% decrease in circulating total cholesterol and LDL levels and a 30% decrease in HDL levels.[64] Additionally, TCDD exposure is associated with increases in cholesterol and cholesterol ester content in the liver.[49,54] For example, hepatic cholesterol and cholesterol ester levels were shown to increase 9.0- and 11.3-fold, respectively, in male mice treated with TCDD.[49] As dysregulation of cholesterol, especially increases in hepatic cholesterol, are associated with the development of liver injury, it is likely that there is a strong connection between TCDD-induced liver injury and alterations in cholesterol homeostasis.

Statin Drugs as a Treatment for NAFLD

Statins are a class of lipid-lowering medication that are competitive inhibitors of HMGCR.[65] Their purpose is to effectively decrease the levels of circulating LDLs through inhibiting cholesterol biosynthesis in the liver.[65] Inhibition of cholesterol production promotes LDL re-uptake in the liver and peripheral tissues to draw cholesterol out of circulation.[65] Therefore, statins are given to individuals who have high risk of cardiovascular disease in order to lower LDL in the blood to reduce the risk of developing atherosclerosis.

Statins are the most prescribed class of drugs in the United States and are taken by over 100 million people.[66] There are various types of statins that are either fermentation-derived from fungi, such as lovastatin or simvastatin, or synthetically-derived, such as atorvastatin or fluvastatin.[65] However, all statins competitively inhibit HMGCR and mostly differ in terms of half-lives, cost, and their LDL-lowering capabilities.[65] People are typically prescribed statins on an

individual basis depending on their tolerance as some experience adverse side effects like muscle pain.[65] Simvastatin was previously the most prescribed statin, but this has recently changed to atorvastatin.[66] Both of these statins are equally effective at lowering cholesterol when dosed at a moderate intensity, but atorvastatin can achieve this with a smaller dose and has a longer half-life in comparison to simvastatin.[67] However, simvastatin remains a more cost-effective option and is still used by millions of people.

Interestingly, statins have been suggested as a potential therapy for NAFLD.[68,69] Beyond cholesterol-lowering effects, statins have been shown to exert anti-inflammatory properties.[70] For example, statins have been shown to reduce protein prenylation as a result of reducing upstream mediators of cholesterol.[65,70] Additionally, they can lower activity of NF-κB, reduce tumor necrosis factor (TNF) and interleukin 6 (IL-6) levels and possibly deactivate the NLRP3 inflammasome.[65,70] Furthermore, statins have been shown to interact with peroxisome proliferator-activated receptor alpha (PPARα).[71] PPARα is a major regulator of lipid metabolism in the liver and activation can promote lipid uptake, utilization, and catabolism. Through activation of PPARα and their anti-inflammatory properties, statins have been considered as a potential therapy for progressive liver injury. Statins and TCDD are both implicated in altering cholesterol homeostasis and can impact pathways involved in NAFLD, so it's important to deduce their relationship as millions of people not only take statins but are also exposed to TCDD in their environment.

Overview of Specific Aims

The overall focus of this dissertation was to gain more insight on pathways that may play

an important role in NAFLD. More specifically, this research tested the hypothesis that dysregulation of cholesterol plays an important role in TCDD-induced liver injury. Gaining a better understanding of this connection may lead to potential therapeutic options for NAFLD in the future. Furthermore, this dissertation aimed to address the implications of those who take statin drugs and have been exposed to environmental toxicants. While statin has been suggested as a treatment option for NAFLD, it's important to elucidate if vulnerable populations may be at greater risk of toxicity if they take statins.

Specific Aim 1: Identifying Key Genes Implicated in AHR-Mediated Liver Injury

Although exposure to AHR ligands has been linked to many adverse health effects in humans, much remains unknown regarding the mechanism behind how these exposures can drive pleiotropic effects.[47,48,52] However, previous reports have indicated that interstrain differences in response to AHR ligands in mice can be leveraged to identify novel AHR-regulated genes.[72,73] The study outlined in Chapter 2 aimed to identify novel genes that are regulated by AHR-mediated signaling in the liver to point to key genes or pathways that could be important for adverse AHR-mediated phenotypes, such as liver injury. To address this, 14 genetically diverse strains of mice were treated in the presence and absence of 100 ng/kg body weight TCDD for 10 consecutive days, and RNA sequencing was performed in the liver tissue along with TCDD burden. Furthermore, linear regression and QTL analysis were utilized to identify genes significantly associated with TCDD liver burden, TCDD-induced changes in body weight and TCDD-induced changes in body fat percentage. Linear regression indicated that 7 genes were associated with TCDD liver burden, and 1 gene was associated with changes in body fat percentage. QTL analysis

indicated a peak on chromosome 13 that was associated with changes in body weight.

Specific Aim 2: Characterizing the Role of HMGCR Repression in TCDD-Induced Liver Injury

Our mouse panel study indicated through QTL analysis that there was a significant peak at chromosome 13 for TCDD-induced changes in body weight, which was within 0.5 Mb of *Hmgcr.* TCDD exposure has been shown previously to dysregulate cholesterol homeostasis in mice, and dysregulation of cholesterol is highly implicated in the development of progressive injury.[56,61,62,64,74] Therefore, the study outlined in Chapter 3 aimed to better characterize the impact of HMGCR repression on TCDD-induced liver injury. To address this aim, C57Bl/6 male and female mice were treated with vehicle control or 10 µg/kg body weight TCDD for 10 consecutive days and were fed either control or chow laced with simvastatin (500 mg/kg food), a competitive inhibitor of HMGCR. This study confirmed TCDD-induced repression of cholesterol biosynthesis, but also indicated sex-specific adverse differences in response to simvastatin co-treatment.

Specific Aim 3: Characterizing the Impact of Simvastatin on TCDD-Induced Liver Injury

Our initial statin study indicated that TCDD and simvastatin (T+S) co-treated male mice had higher levels of circulating alanine aminotransferase (ALT) levels, a marker for liver injury, and greater AHR activation suggesting exacerbated TCDD-induced liver injury. Millions of individuals take statins and may be exposed to TCDD or other AHR ligands in their environment, so it is important to confirm if statins induce greater risk for liver injury.[66] Therefore, the study outlined in Chapter 4 aimed to confirm if statin does exacerbate TCDD-induced liver injury, and if so, what is the mechanism behind this effect. To address this aim, male C57Bl/6 mice were

treated with vehicle control or 30 µg/kg body weight TCDD every 4 days for 28 days and were fed either control or simvastatin-laced chow (500 mg/kg food). Single-nuclei RNA sequencing (snRNAseq) was utilized in liver tissue to investigate the role of different cell (sub)types that could potentially play a role in differences in liver injury between TCDD alone and simvastatin co-treatment. While we did not see significant differences in histopathological indicators of liver injury between TCDD alone and co-treatment, we did see alterations in liver cell (sub)type proportions and changes in differentially expressed genes (DEGs) that could impact liver injury severity. Furthermore, co-treated mice experienced wasting and had greater AHR activation compared to TCDD alone suggesting that co-treatment had greater AHR-mediated toxicity.

REFERENCES

1. Maurice, J. & Manousou, P. Non-alcoholic fatty liver disease. *Clinical Medicine* **18**, 245–250 (2018).

2. Mitra, S., De, A. & Chowdhury, A. Epidemiology of non-alcoholic and alcoholic fatty liver diseases. *Transl Gastroenterol Hepatol* **5**, 16 (2020).

3. Dowman, J. K., Tomlinson, J. W. & Newsome, P. N. Pathogenesis of non-alcoholic fatty liver disease. *QJM* **103**, 71–83 (2010).

4. Riazi, K. *et al.* The prevalence and incidence of NAFLD worldwide: a systematic review and meta-analysis. *Lancet Gastroenterol Hepatol* **7**, 851–861 (2022).

5. Murag, S., Ahmed, A. & Kim, D. Recent Epidemiology of Nonalcoholic Fatty Liver Disease. *Gut Liver* **15**, 206–216 (2021).

6. Wong, M. C. S. *et al.* The changing epidemiology of liver diseases in the Asia–Pacific region. *Nat Rev Gastroenterol Hepatol* **16**, 57–73 (2019).

7. Akazawa, Y. & Nakao, K. To die or not to die: death signaling in nonalcoholic fatty liver disease. *J Gastroenterol* **53**, 893–906 (2018).

8. El-Zayadi, A.-R. Hepatic steatosis: a benign disease or a silent killer. *World J Gastroenterol* **14**, 4120–6 (2008).

9. Luedde, T. & Schwabe, R. F. NF-κB in the liver—linking injury, fibrosis and hepatocellular carcinoma. *Nat Rev Gastroenterol Hepatol* **8**, 108–118 (2011).

10. Godoy-Matos, A. F., Silva Júnior, W. S. & Valerio, C. M. NAFLD as a continuum: from obesity to metabolic syndrome and diabetes. *Diabetol Metab Syndr* **12**, 60 (2020).

11. Dhar, D., Baglieri, J., Kisseleva, T. & Brenner, D. A. Mechanisms of liver fibrosis and its role in liver cancer. *Exp Biol Med* **245**, 96–108 (2020).

12. Younossi, Z. M. *et al.* Global epidemiology of nonalcoholic fatty liver disease-Meta-analytic assessment of prevalence, incidence, and outcomes. *Hepatology* **64**, 73–84 (2016).

13. Estes, C., Razavi, H., Loomba, R., Younossi, Z. & Sanyal, A. J. Modeling the epidemic of nonalcoholic fatty liver disease demonstrates an exponential increase in burden of disease. *Hepatology* **67**, 123–133 (2018).

14. Witkowski, M. *et al.* The Economic Burden of Non-Alcoholic Steatohepatitis: A Systematic Review. *Pharmacoeconomics* **40**, 751–776 (2022).

15. Kim, D. *et al.* Body Fat Distribution and Risk of Incident and Regressed Nonalcoholic Fatty Liver Disease. *Clinical Gastroenterology and Hepatology* **14**, 132-138.e4 (2016).

16. Jinjuvadia, R., Antaki, F., Lohia, P. & Liangpunsakul, S. The Association Between Nonalcoholic Fatty Liver Disease and Metabolic Abnormalities in The United States Population. *J Clin Gastroenterol* **51**, 160–166 (2017).

17. Rajak, S., Raza, S., Tewari, A. & Sinha, R. A. Environmental Toxicants and NAFLD: A Neglected yet Significant Relationship. *Dig Dis Sci* **67**, 3497–3507 (2022).

18. Cave, M. *et al.* Polychlorinated Biphenyls, Lead, and Mercury Are Associated with Liver Disease in American Adults: NHANES 2003–2004. *Environ Health Perspect* **118**, 1735–1742 (2010).

19. Zheng, S. *et al.* Effects of environmental contaminants in water resources on nonalcoholic fatty liver disease. *Environ Int* **154**, 106555 (2021).

20. Armstrong, L. E. & Guo, G. L. Understanding Environmental Contaminants' Direct Effects on Non-alcoholic Fatty Liver Disease Progression. *Curr Environ Health Rep* **6**, 95–104 (2019).

21. Nault, R. *et al.* Dose-Dependent Metabolic Reprogramming and Differential Gene Expression in TCDD-Elicited Hepatic Fibrosis. *Toxicol Sci* **154**, 253–266 (2016).

22. Pierre, S. *et al.* Aryl hydrocarbon receptor-dependent induction of liver fibrosis by dioxin. *Toxicol Sci* **137**, 114–24 (2014).

23. Warner, M. *et al.* Diabetes, metabolic syndrome, and obesity in relation to serum dioxin concentrations: the Seveso women's health study. *Environ Health Perspect* **121**, 906–11 (2013).

24. Uemura, H. *et al.* Prevalence of metabolic syndrome associated with body burden levels of dioxin and related compounds among Japan's general population. *Environ Health Perspect* **117**, 568–73 (2009).

25. Cunningham, R. P. & Porat-Shliom, N. Liver Zonation – Revisiting Old Questions With New Technologies. *Front Physiol* **12**, (2021).

26. Jungermann, K. Zonation of metabolism and gene expression in liver. *Histochem Cell Biol* **103**, 81–91 (1995).

27. Gebhardt, R. Metabolic zonation of the liver: Regulation and implications for liver function. *Pharmacol Ther* **53**, 275–354 (1992).

28. Nault, R., Fader, K. A., Bhattacharya, S. & Zacharewski, T. R. Single-Nuclei RNA Sequencing Assessment of the Hepatic Effects of 2,3,7,8-Tetrachlorodibenzo-p-dioxin. *Cell Mol*

Gastroenterol Hepatol **11**, 147–159 (2021).

29. Halpern, K. B. *et al.* Single-cell spatial reconstruction reveals global division of labour in the mammalian liver. *Nature* **542**, 352–356 (2017).

30. Nault, R. *et al.* Single-cell transcriptomics shows dose-dependent disruption of hepatic zonation by TCDD in mice. *Toxicological Sciences* (2022) doi:10.1093/toxsci/kfac109.

31. Bykov, I., Ylipaasto, P., Eerola, L. & Lindros, K. O. Functional Differences between Periportal and Perivenous Kupffer Cells Isolated by Digitonin-Collagenase Perfusion. *Comp Hepatol* **3**, S34 (2004).

32. Yin, C., Evason, K. J., Asahina, K. & Stainier, D. Y. R. Hepatic stellate cells in liver development, regeneration, and cancer. *Journal of Clinical Investigation* **123**, 1902–1910 (2013).

33. Poisson, J. *et al.* Liver sinusoidal endothelial cells: Physiology and role in liver diseases. *J Hepatol* **66**, 212–227 (2017).

34. Tabibian, J. H., Masyuk, A. I., Masyuk, T. V., O'Hara, S. P. & LaRusso, N. F. Physiology of Cholangiocytes. in *Comprehensive Physiology* 541–565 (Wiley, 2013). doi:10.1002/cphy.c120019.

35. Abel, J. & Haarmann-Stemmann, T. An introduction to the molecular basics of aryl hydrocarbon receptor biology. *Biol Chem* **391**, 1235–48 (2010).

36. Swanson, H. I. & Bradfield, C. A. The AH-receptor: genetics, structure and function. *Pharmacogenetics* **3**, 213–30 (1993).

37. Gruszczyk, J. *et al.* Cryo-EM structure of the agonist-bound Hsp90-XAP2-AHR cytosolic complex. *Nat Commun* **13**, 7010 (2022).

38. Heid, S. E., Pollenz, R. S. & Swanson, H. I. Role of heat shock protein 90 dissociation in mediating agonist-induced activation of the aryl hydrocarbon receptor. *Mol Pharmacol* **57**, 82–92 (2000).

39. Carver, L. A., LaPres, J. J., Jain, S., Dunham, E. E. & Bradfield, C. A. Characterization of the Ah receptor-associated protein, ARA9. *J Biol Chem* **273**, 33580–7 (1998).

40. Okey, A. B. An aryl hydrocarbon receptor odyssey to the shores of toxicology: the Deichmann Lecture, International Congress of Toxicology-XI. *Toxicol Sci* **98**, 5–38 (2007).

41. Poland, A., Palen, D. & Glover, E. Analysis of the four alleles of the murine aryl hydrocarbon receptor. *Mol Pharmacol* **46**, 915–21 (1994).

42. A Poland & E Glover. Characterization and strain distribution pattern of the murine Ah

receptor specified by the Ahd and Ahdb-3 alleles. *Mol Pharmacol* **38**, 306–312 (1990).

43. Meyer, B. K. & Perdew, G. H. Characterization of the AhR-hsp90-XAP2 core complex and the role of the immunophilin-related protein XAP2 in AhR stabilization. *Biochemistry* **38**, 8907–17 (1999).

44. Nukaya, M., Walisser, J. A., Moran, S. M., Kennedy, G. D. & Bradfield, C. A. Aryl hydrocarbon receptor nuclear translocator in hepatocytes is required for aryl hydrocarbon receptor-mediated adaptive and toxic responses in liver. *Toxicol Sci* **118**, 554–63 (2010).

45. Dere, E., Lo, R., Celius, T., Matthews, J. & Zacharewski, T. R. Integration of genome-wide computation DRE search, AhR ChIP-chip and gene expression analyses of TCDD-elicited responses in the mouse liver. *BMC Genomics* **12**, 365 (2011).

46. Fernandez-Salguero, P. M., Hilbert, D. M., Rudikoff, S., Ward, J. M. & Gonzalez, F. J. Aryl-hydrocarbon receptor-deficient mice are resistant to 2,3,7,8-tetrachlorodibenzo-p-dioxin-induced toxicity. *Toxicol Appl Pharmacol* **140**, 173–9 (1996).

47. Sorg, O. *et al.* 2,3,7,8-tetrachlorodibenzo-p-dioxin (TCDD) poisoning in Victor Yushchenko: identification and measurement of TCDD metabolites. *Lancet* **374**, 1179–85 (2009).

48. Baccarelli, A. *et al.* Immunologic effects of dioxin: new results from Seveso and comparison with other studies. *Environ Health Perspect* **110**, 1169–73 (2002).

49. Nault, R., Fader, K. A., Lydic, T. A. & Zacharewski, T. R. Lipidomic Evaluation of Aryl Hydrocarbon Receptor-Mediated Hepatic Steatosis in Male and Female Mice Elicited by 2,3,7,8-Tetrachlorodibenzo-p-dioxin. *Chem Res Toxicol* **30**, 1060–1075 (2017).

50. Chen, Q. *et al.* Estimation of background serum 2,3,7,8-TCDD concentrations by using quantile regression in the UMDES and NHANES populations. *Epidemiology* **21 Suppl 4**, S51-7 (2010).

51. Wolfe, W. H. *et al.* Determinants of TCDD half-life in veterans of operation ranch hand. *J Toxicol Environ Health* **41**, 481–8 (1994).

52. Dornbos, P., Crawford, R. B., Kaminski, N. E., Hession, S. L. & LaPres, J. J. The Influence of Human Interindividual Variability on the Low-Dose Region of Dose-Response Curve Induced by 2,3,7,8-Tetrachlorodibenzo-p-Dioxin in Primary B Cells. *Toxicol Sci* **153**, 352–60 (2016).

53. Dornbos, P. *et al.* Characterizing Serpinb2 as a Modulator of TCDD-Induced Suppression of the B Cell. *Chem Res Toxicol* **31**, 1248–1259 (2018).

54. Fader, K. A. *et al.* 2,3,7,8-Tetrachlorodibenzo-p-dioxin (TCDD)-elicited effects on bile acid homeostasis: Alterations in biosynthesis, enterohepatic circulation, and microbial

metabolism. *Sci Rep* **7**, 5921 (2017).

55. Lee, J. *et al.* Male and female mice show significant differences in hepatic transcriptomic response to 2,3,7,8-tetrachlorodibenzo-p-dioxin. *BMC Genomics* **16**, 625 (2015).

56. Tanos, R. *et al.* Aryl hydrocarbon receptor regulates the cholesterol biosynthetic pathway in a dioxin response element-independent manner. *Hepatology* **55**, 1994–2004 (2012).

57. Luo, J., Yang, H. & Song, B.-L. Mechanisms and regulation of cholesterol homeostasis. *Nat Rev Mol Cell Biol* **21**, 225–245 (2020).

58. Goedeke, L. & Fernández-Hernando, C. Regulation of cholesterol homeostasis. *Cell Mol Life Sci* **69**, 915–30 (2012).

59. Li, J. *et al.* Novel insights: Dynamic foam cells derived from the macrophage in atherosclerosis. *J Cell Physiol* **236**, 6154–6167 (2021).

60. Chiang, J. Y. L. Bile acid metabolism and signaling. *Compr Physiol* **3**, 1191–212 (2013).

61. Min, H.-K. *et al.* Increased hepatic synthesis and dysregulation of cholesterol metabolism is associated with the severity of nonalcoholic fatty liver disease. *Cell Metab* **15**, 665–74 (2012).

62. Arguello, G., Balboa, E., Arrese, M. & Zanlungo, S. Recent insights on the role of cholesterol in non-alcoholic fatty liver disease. *Biochim Biophys Acta* **1852**, 1765–78 (2015).

63. Ioannou, G. N., Haigh, W. G., Thorning, D. & Savard, C. Hepatic cholesterol crystals and crown-like structures distinguish NASH from simple steatosis. *J Lipid Res* **54**, 1326–1334 (2013).

64. Angrish, M. M., Dominici, C. Y. & Zacharewski, T. R. TCDD-elicited effects on liver, serum, and adipose lipid composition in C57BL/6 mice. *Toxicol Sci* **131**, 108–15 (2013).

65. Sirtori, C. R. The pharmacology of statins. *Pharmacol Res* **88**, 3–11 (2014).

66. Gu, Q., Paulose-Ram, R., Burt, V. L. & Kit, B. K. Prescription cholesterol-lowering medication use in adults aged 40 and over: United States, 2003-2012. *NCHS Data Brief* 1–8 (2014).

67. Scott M. Grundy *et al.* 2018 AHA/ACC/AACVPR/AAPA/ABC/ACPM/ADA/AGS/APhA/ASPC/NLA/PCNA Guideline on the Management of Blood Cholesterol: A Report of the American College of Cardiology/American Heart Association Task Force on Clinical Practice Guidelines. *J Am Coll Cardiol* **73**, 285–350 (2019).

68. Lee, J. il, Lee, H. W., Lee, K. S., Lee, H. S. & Park, J.-Y. Effects of Statin Use on the Development and Progression of Nonalcoholic Fatty Liver Disease: A Nationwide Nested Case-Control Study. *Am J Gastroenterol* **116**, 116–124 (2021).

69. Athyros, V. G. *et al.* Statins: An Under-Appreciated Asset for the Prevention and the Treatment of NAFLD or NASH and the Related Cardiovascular Risk. *Curr Vasc Pharmacol* **16**, 246–253 (2018).

70. Koushki, K. *et al.* Anti-inflammatory Action of Statins in Cardiovascular Disease: the Role of Inflammasome and Toll-Like Receptor Pathways. *Clin Rev Allergy Immunol* **60**, 175–199 (2021).

71. Balakumar, P. & Mahadevan, N. Interplay between statins and PPARs in improving cardiovascular outcomes: a double-edged sword? *Br J Pharmacol* **165**, 373–9 (2012).

72. Smart, J. & Daly, A. K. Variation in induced CYP1A1 levels: relationship to CYP1A1, Ah receptor and GSTM1 polymorphisms. *Pharmacogenetics* **10**, 11–24 (2000).

73. Dornbos, P. & LaPres, J. J. Incorporating population-level genetic variability within laboratory models in toxicology: From the individual to the population. *Toxicology* **395**, 1–8 (2018).

74. Song, Y., Liu, J., Zhao, K., Gao, L. & Zhao, J. Cholesterol-induced toxicity: An integrated view of the role of cholesterol in multiple diseases. *Cell Metabolism* vol. 33 1911–1925 Preprint at https://doi.org/10.1016/j.cmet.2021.09.001 (2021).

Chapter 2: Identifying Key Genes Implicated in AHR-Mediated Injury

This chapter is an edited version of a previously published research article in *Toxicological Sciences,* Volume 181, No. 2: pages 285-294.

Authors: Amanda Jurgelewicz[1,2], Peter Dornbos[2,3], Melanie Warren,[4] Rance Nault,[2,3] Anooj Arkatkar,[2,3] Hui Lin,[5] David W. Threadgill,[4] Tim Zacharewski[2,3] and John J. LaPres[2,3]

Affiliations: [1]Department of Pharmacology and Toxicology, Michigan State University; [2]Institute for Integrative Toxicology, Michigan State University; [3]Department of Biochemistry and Molecular Biology, Michigan State University; [4]Interdisciplinary Program in Toxicology, Texas A&M University; [5]Environmental Technology Center, The Dow Chemical Company

Abstract

The aryl hydrocarbon receptor has been linked to several metabolic diseases; however, much remains unknown regarding the impact of genetic variation in AHR-driven disease as past studies have focused on a small number of inbred strains. Recently, it has been reported that there is a wide range of interindividual variability amongst humans in response to TCDD, the prototypical ligand of the AHR, and there are similar levels of interstrain responses to TCDD in mice. Therefore, this study utilized a panel of 14 genetically diverse mouse strains exposed to TCDD to leverage the AHR-mediated response across diverse backgrounds to identify genetic modifiers of AHR signaling. A regression-based approach was used to scan for genes regulated by AHR and/or associated with TCDD-induced phenotypes. Furthermore, QTL analysis was also utilized to identify molecular markers that correspond to TCDD-induced phenotypes. This approach identified 7 genes regulated by the AHR based on association to hepatic TCDD burden, 1 gene associated with change in percent body fat across strains and a peak on chromosome 13 associated with changes in body weight across strains. The results of this study exemplify the power in using mouse genetics-based approaches in toxicological studies.

Introduction

The human population is heterogeneous, which results in differences amongst individuals in their responses to various toxicants upon exposure. Many factors can influence individual responses to environmental exposures such as age, sex, disease-state or genetic variability. In classical laboratory models, genetic variability is typically excluded to reduce experimental variability; however, incorporating genetic diversity into toxicological studies provides avenues to map differences in responses to areas of the genome that can impact susceptibility.[1,2] Genetic diversity within *Mus musculus* mice species, which are commonly used in laboratory settings, have been shown to have a number and distribution of genetic polymorphisms even greater than what is seen in the human population.[3,4] Therefore, the availability of genetically diverse mouse panels provides a way to assess genetic variability similar to what is seen in the human population and to identify variants within a population that may impact toxicant-induced phenotypes.

While exposure to AHR ligands have been associated with many adverse health effects in humans such as metabolic syndrome or chloracne, much remains unknown regarding the mechanism behind how these exposures drive these effects. Recent reports have suggested that exposure to TCDD induces a wide range of human interindividual variability in response to AHR activation and similar levels of inter-strain responses to TCDD in mice.[5,6] Inbred mice strains carry distinct *Ahr* alleles with known differences in sensitivity to ligand-induced effects, and it has been suggested that these inter-strain differences can be leveraged to identify novel genes regulated by the AHR.[1,5–7]

Therefore, the aim of this study was to identify novel genes regulated by AHR-mediated signaling in the liver to point to key genes or pathways that may be important for adverse AHR-

mediated phenotypes, such as liver injury. To address this, 14 genetically diverse strains of female mice were treated in the presence and absence of 100 ng/kg body weight TCDD for 10 consecutive days. RNA sequencing was performed to determine strain-specific changes in hepatic gene expression following TCDD exposure, and regression analysis was performed to scan for genes whose expression was associated with 1) hepatic TCDD accumulation, 2) TCDD-induced change in body weight and 3) TCDD-induced change in body fat percentage. QTL analysis was also performed to identify molecular markers associated with TCDD-induced phenotypes. The materials and methods can be found in Chapter 6. The results of this study exemplify the power in using mouse genetics-based approaches in toxicology by identifying key genes with likely links to adverse health effects modulated by AHR signaling.

Results

Inter-strain Differences in AHR-Mediated Gene Expression

To identify novel AHR-regulated genes or modifiers of AHR signaling, RNA sequencing was utilized to assess global changes in gene expression in mouse liver from 14 genetically diverse strains of mice treated with 0 or 100 ng/kg body weight/day of TCDD for 10 consecutive days. The results showed that there were 1024 differentially expressed genes (DEGs) in TCDD-treated mice across the 14 strains with fold changes ≥ 1.5 and adjusted p-values ≤ 0.05 as compared to their respective controls (Figure 2.1). There was considerable variation in the number of DEGs across strains of mice.

Figure 2.1: Differentially expressed genes (DEGs) counts in each mouse strain. The correlation matrix indicates the total and shared number of DEGs across 14 genetically diverse strains of mice. Genes are considered differentially expressed if the |fold change| ≥ 1.5 and Benjamini-Hochberg corrected p-values ≤ 0.05. Darker red indicates a greater degree of correlation or more shared genes between strains.

AHR Allele	Ahr^{B1}	Ahr^{B1}	Ahr^{B1}	Ahr^{B2}	Ahr^{B2}	Ahr^{B2}	Ahr^{B2}	Ahr^{B2}	Ahr^{D}	Ahr^{D}	Ahr^{D}	Ahr^{D}	Ahr^{D}	Ahr^{D}
Strain	C57Bl/6J	BXD100	BXD91	A/J	CBA/J	FVB/nJ	C3Heb/FeJ	Balb/cj	DBA/J	NOD/ ShiLtJ	NZO/HilTJ	129S1/ SvlmJ	BXD40	CC019
Total DEGs	161	14	23	85	19	8	16	6	4	595	4	3	78	8
C57Bl/6J		6	8	5	3	2	6	2	1	11	0	1	3	1
BXD100	6		6	5	3	3	6	3	0	1	1	0	0	1
BXD91	8	6		7	4	3	6	3	3	1	2	1	6	3
A/J	5	5	7		2	3	5	5	2	3	1	1	6	4
CBA/J	3	3	4	2		2	3	2	0	0	0	0	0	0
FVB/nJ	2	3	3	3	2		3	3	1	0	1	0	0	2
C3Heb/FeJ	6	6	6	5	3	3		3	1	1	0	0	3	3
Balb/cj	2	3	3	5	2	3	3		1	0	1	0	2	2
DBA/J	1	0	3	2	0	1	1	1		0	1	0	3	1
NOD/ShiLtJ	11	1	1	3	0	0	1	0	0		0	0	6	1
NZO/HilTJ	0	1	2	1	0	1	0	1	1	0		0	1	2
129S1/SvlmJ	1	0	1	1	0	0	0	0	0	0	0		1	0
BXD40	3	0	6	6	0	0	3	2	3	6	1	1		3
CC019	1	1	3	4	0	2	3	2	1	1	2	0	3	

Note: |Fold-Change| >= 1.5, padj (FDR) <= 0.05

Mice carry 1 of 4 alleles of the *Ahr,* which impact susceptibility to ligand-induced AHR-mediated signaling due to variations in ligand binding capabilities.[8] Therefore, we sought to establish which alleles the mice carry using an automated method to determine if the differences in alleles may, in part, explain the variation in DEGs across strains.[9] It was determined that 3 stains carry the Ahr^{b1} allele, 5 strains carry the Ahr^{b2} allele, and 6 strains carry the Ahr^{d} allele (Figure 2.2A). On average, Ahr^{b1} mice shared 7 DEGs, Ahr^{b2} mice shared 3 DEGs and Ahr^{d} mice shared 1 DEG. As TCDD binding induces expression of AHR battery genes, we also assessed expression of main target genes like cytochrome P450 enzymes, *Cyp1a1, Cyp1a2* and *Cyp1b1* (Figure 2.2B). 8 of the 14 strains had significant induction of *Cyp1a1* and *Cyp1a2* upon TCDD treatment, and all 8 strains carried the high binding affinity Ahr^{b1} or Ahr^{b2} alleles (Figure 2.2B).

Figure 2.2: AHR alleles impact induction of AHR target genes upon TCDD exposure. (A) A phylogenetic tree indicating the genetic similarity between strains. Gray indicates *Ahr*^{b1} allele strains, blue indicates *Ahr*^{b2} allele strains and green indicates *Ahr*^{d} allele strains. (B) Gene expression of AHR target genes, *Cyp1a1, Cyp1a2* and *Cyp1b1*, across the strains of mice. Red intensity indicates expression was more upregulated compared to control and blue intensity indicates expression was more downregulated compared to control.

A.

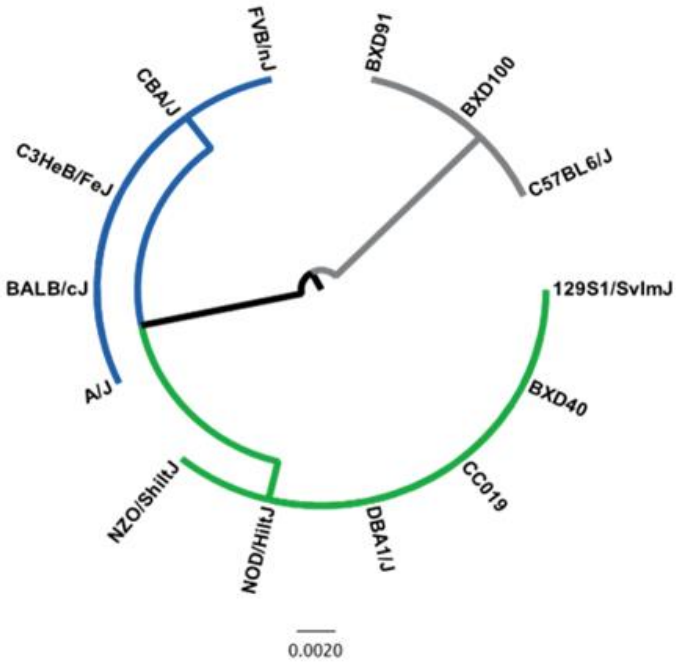

B.

	Strain	Cyp1a1	Cyp1a2	Cyp1b1
Ahr^{b1}	C57Bl/6J	3414.02	10.40	3.27
	BXD100	1138.63	15.73	1.67
	BXD91	2437.20	17.21	6.18
Ahr^{b2}	A/J	23.36	7.66	0.72
	CBA/J	1033.42	11.08	2.30
	FVB/nJ	19.46	5.23	2.11
	C3Heb/FeJ	681.02	12.86	2.82
	Balb/cj	20.06	5.54	1.07
Ahr^{d}	DBA/J	5.16	3.01	0.88
	NOD/ShiLtJ	1.39	1.52	0.92
	NZO/HilTJ	0.81	1.22	0.39
	129S1/SvImJ	3.52	2.51	1.28
	BXD40	2.59	2.92	0.28
	CC019	0.89	1.25	1.11

Although the *Ahr* allele carried by a mouse impacts susceptibility of a strain to AHR-mediated toxicity, differential expression of AHR target genes was not concordant across strains carrying the same allele. For example, strains such as CBA/J and C3HeB/FeJ, which both carry the Ahr^{b2} alleles, had respective 1031.12 and 680.29-fold changes in *Cyp1a1* expression in comparison to the other Ahr^{b2} mice that averaged 20.97 (Figure 2.2B). Furthermore, the number of DEGs carried by strains was variable between mice of the same allele. For example, even though BXD strains are derived, in part, from the C57Bl/6J strain, BXD100 and BXD91 had 14 and 23 DEGs respectively in comparison to 161 DEGs in the C57Bl/6J mice even though all strains carry the Ahr^{b1} allele (Figure 2.1). Interestingly, NOD/ShiLtJ mice had 595 DEGs as an Ahr^{d} allele carrier, which is notably more than any strain carrying a 'responsive' *Ahr* allele (Figure 2.1). Therefore, there are likely additional genetic factors that modulate response to AHR ligands in addition to the *Ahr* allele carried by the mouse.

Hepatic TCDD Accumulation Differs Across Strains

Ligand-activated AHR-mediated gene expression is dose-dependent, so we sought to establish the burden of TCDD present in the livers of the differing strains. Similar to what was seen with gene expression, there was variability in the level of hepatic TCDD accumulation across strains. On average, the level of TCDD sequestered in the liver is impacted by the *Ahr* allele carried by the mouse (Figure 2.3A). The mean level of TCDD in Ahr^{b1} mice is significantly higher than the mean levels found in Ahr^{b2} and Ahr^{d} mice, and similarly, Ahr^{b2} mice sequester more TCDD than Ahr^{d} mice. Although, on average, more responsive alleles sequester more TCDD than the less responsive allele, there was still intra-allelic variability (Figure 2.3B). For example, DBA/1J

and BXD40 mice were found to have significantly higher TCDD burden in comparison to other *Ahr*^{d} mice such as NOD/ShiLtJ, NZO/HiLtJ and CC019. Similarly, CBA/J had significantly higher TCDD burden than all other *Ahr*^{b2} mice. Interestingly, several *Ahr*^{d} mice such as BXD40 accumulated more TCDD than some *Ahr*^{b2} mice such as A/J. This suggests that while the *Ahr* allele affects TCDD sequestration, other genomic factors likely also impact accumulation.

Figure 2.3: Differences in hepatic TCDD accumulation across strains. (A) The average TCDD liver burden (ng/kg) on average between AHR alleles. Asterisk (*) indicates $p < 0.05$. (B) The TCDD liver burden of each strain of mice separated by AHR allele. The letters above the bars indicate significant differences ($P < 0.05$) compared to the mean of: (a) NOD/ShiLtJ, (b) NZO/HiLtJ, (c) CC019, (d) A/J, (e) FVB/nJ, (f) BALB/cJ and (g) C3HeB/FeJ. In all cases, green indicates an *Ahr*^{d} allele, blue indicates an *Ahr*^{b2} allele and gray indicates an *Ahr*^{d} allele and error bars indicate standard error.

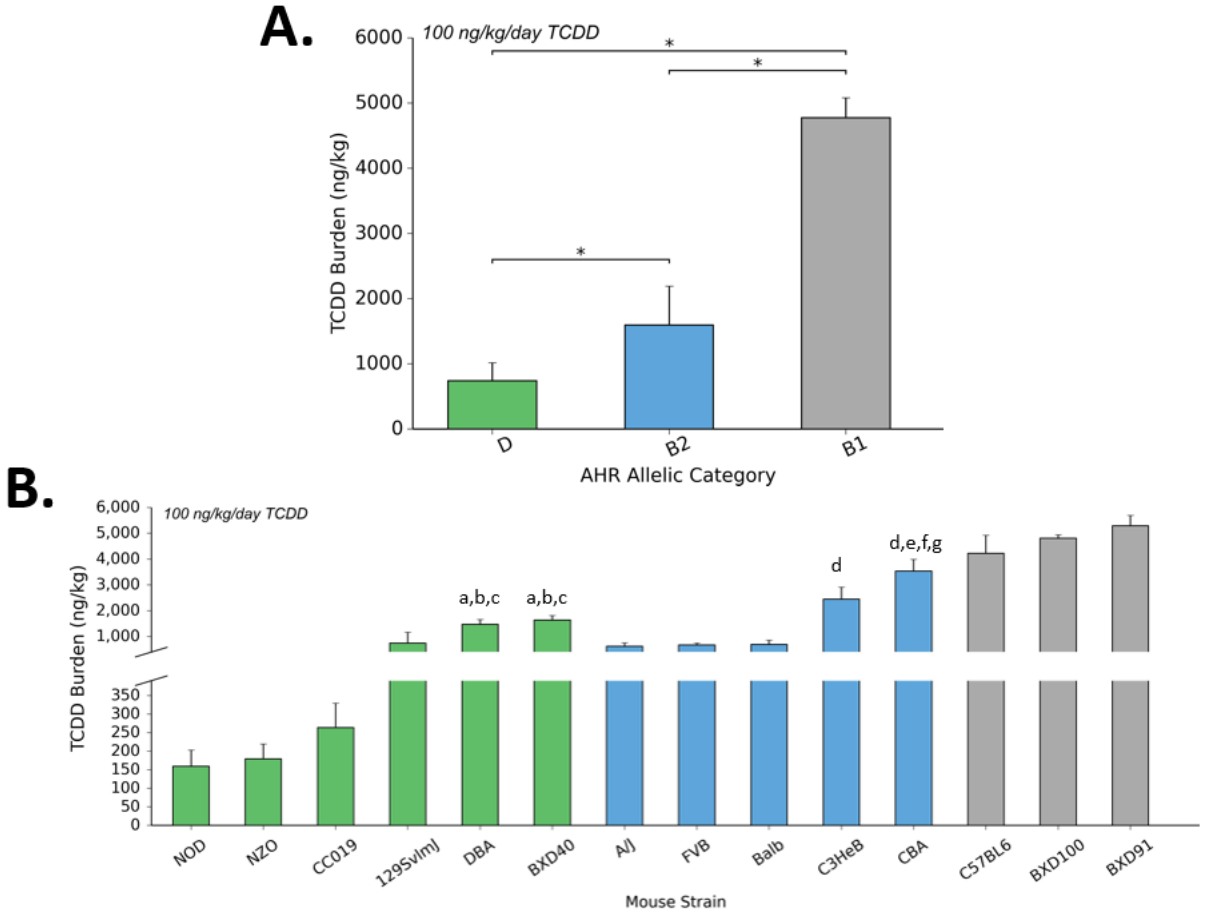

Genes Associated with TCDD Liver Burden

The interstrain variability in gene expression and hepatic accumulation across strains led us to believe that there may be additional genes that could be regulated by AHR-mediated signaling. Linear regression was used to search for gene expression that was associated with TCDD liver burden. The results indicated that there were 7 genes with expression that is associated with TCDD burden in the liver (Figure 2.4). Of note, there were 'positive control' genes found to be significantly associated with TCDD burden that are AHR battery genes including *Cyp1a1* and *Cyp1a2* (Figure 2.4A and G).[10] Furthermore, there were genes associated with TCDD burden that had previously been linked to TCDD exposure such as nuclear factor erythroid 2-related factor 2 (*Nfe2l2* or NRF2) and phosphomannomutase 1 (*Pmm1*) (Figure 2.4E and F).[10–13] Of particular interest were 2 novel genes, neuronal pentraxin 1 (*Nptx1*) and solute carrier family 46 member 3 (*Slc46a3*).

Figure 2.4: Gene expression associated with TCDD liver burden. The plots indicate genes with expression that had significant association to TCDD liver burden for the mouse panel determined by linear regression analysis (P < 0.05). The beta, R2, and adjusted P-value determined by the regression analysis are listed with each gene: (A) *Cyp1a1*, (B) *Nptx1*, (C) *Htatip2*, (D) *Slc46a3*, (E) *Pmm1*, (F) *Nfe2l2* and (G) *Cyp1a2*.

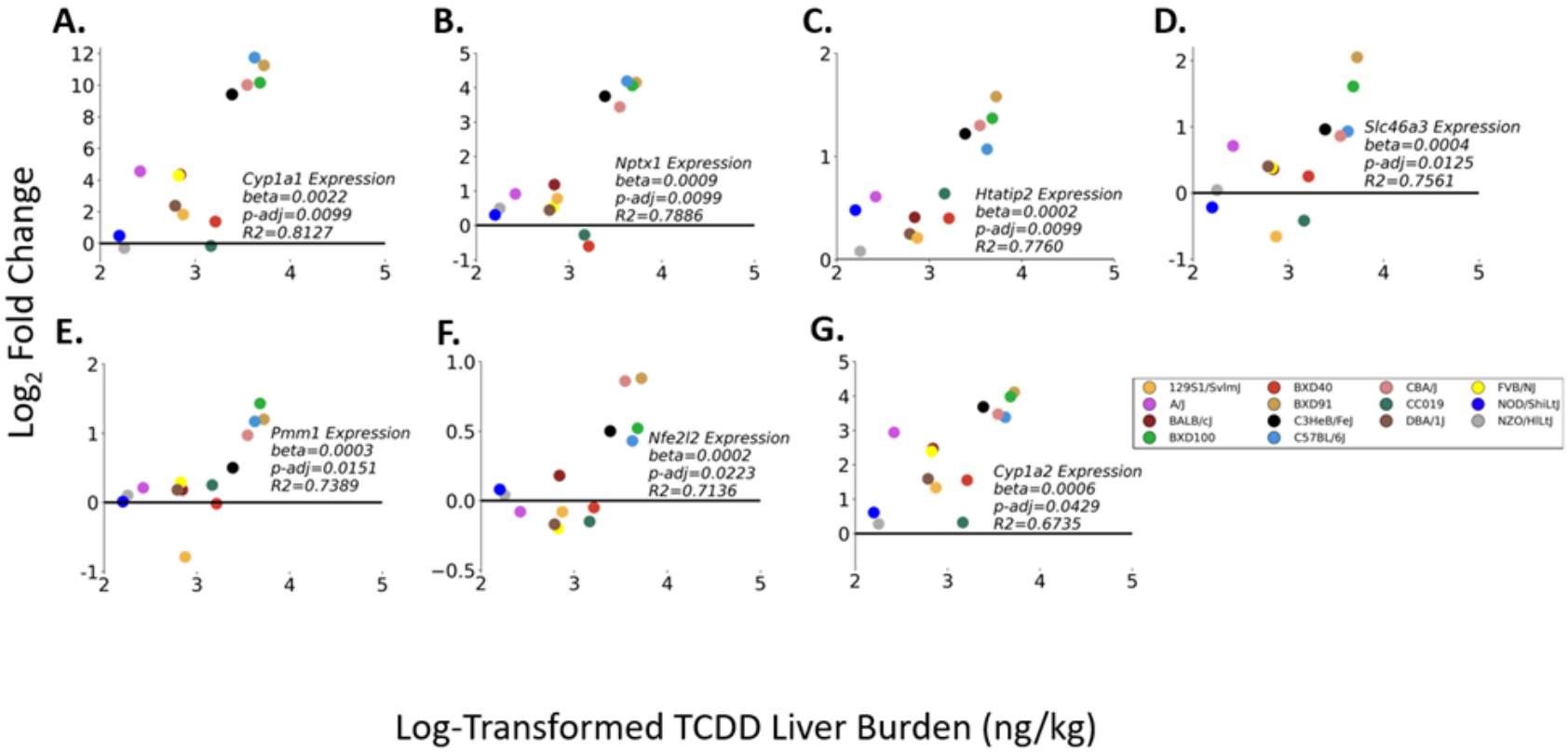

TCDD-Induced Changes in Body Measurements Across Strains

TCDD has been well-established to induce body changes in rodents such as wasting, but we observed that TCDD-induced changes in body fat percentage and body weight were quite variable across strains over the dosing scheme of this study. The change in body fat percentage was variable across strains, ranging from -7% to +5% (Figure 2.5A). Although the *Ahr*^{b1} and *Ahr*^{d} allele mice ranged from +0.2% to -1.4% and +1.6% to -1.2%, respectively, the change in percent body fat for *Ahr*^{b2} mice was less concordant. For example, CBA/J mice gained 4.75% body fat, whereas C3HeB/FeJ mice lost 6.61% body fat. The variability across strains led us to examine if there may be any genes associated with the change in body fat percentage. Regression results indicated that 1 gene, iodothyronine deiodinase 1 (*Dio1*), was associated with TCDD-induced changes in body fat. Notably, *Dio1* catalyzes the conversion of thyroid hormones T4 to T3, and TCDD has been shown to dysregulate expression of *Dio1* in mice liver and thyroid previously.[13]

Figure 2.5: TCDD-induced changes in body fat composition. (A) The differences in body fat percentage in TCDD vs. vehicle control mice. Each dot represents a different strain of mice. (B) The regression plot indicates negative association of *Dio1* expression with the change in fat percentage in mice treated with TCDD. The beta, R^2 and adjusted p-values are indicated on the plot.

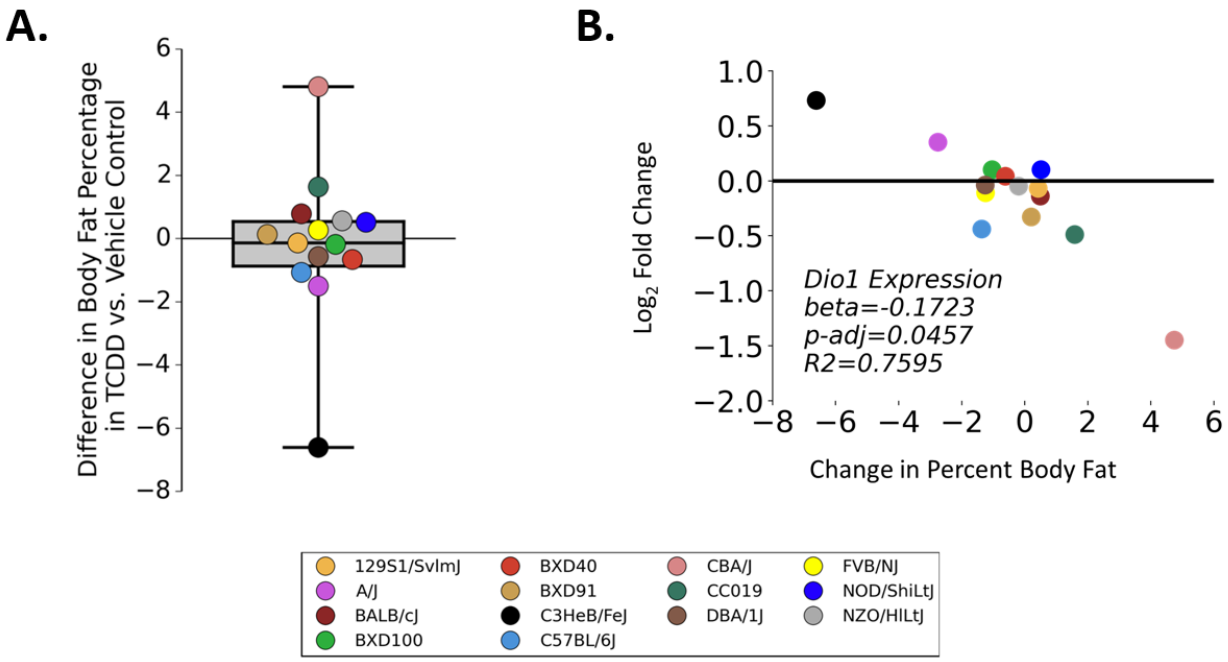

The change in body weight was also variable across strains. The average change in weight percentage ranged from +1% to -6% (Figure 2.6A). Although 4 strains that carry the *Ahr*^{b2} allele ranged from about +1% to -1% weight change, the FVB/nJ strain lost 6% body weight. Interestingly, the change in weight for this strain was greater than all strains carrying the *Ahr*^{b1} allele. Notably, strains such as C3HeB/FeJ mice, while losing body fat, were observed to gain weight; however, while all of these changes are TCDD-induced, the results may be confounded by the pregnancy of the mice. Linear regression did not indicate any gene expression that was significantly associated with change in body weight. Therefore, QTL analysis was performed to see if there may be any molecular markers associated with this phenotype. QTL analysis identified a significant association with Chromosome 13 for inter-strain differences in body weight change (Figure 2.6B). This peak was within 0.5 Mb of HMG-CoA reductase (*Hmgcr*). HMGCR catalyzes the rate-limiting step of cholesterol biosynthesis, and TCDD has been associated with altering circulating cholesterol levels and expression of various enzymes in this pathway previously.[14] These results suggest that *Dio1* and *Hmgcr* may be important genes involved in TCDD-induced changes in body composition.

Figure 2.6: TCDD-induced changes in body weight. (A) The differences in body weight in TCDD vs. vehicle control mice. Each dot represents a different strain of mice. (B) QTL analysis indicated a significant peak within Chromosome 13 ($p < 0.001$). The dotted line indicates the threshold of genome-wide significance determined by permutation testing (n=10,000).

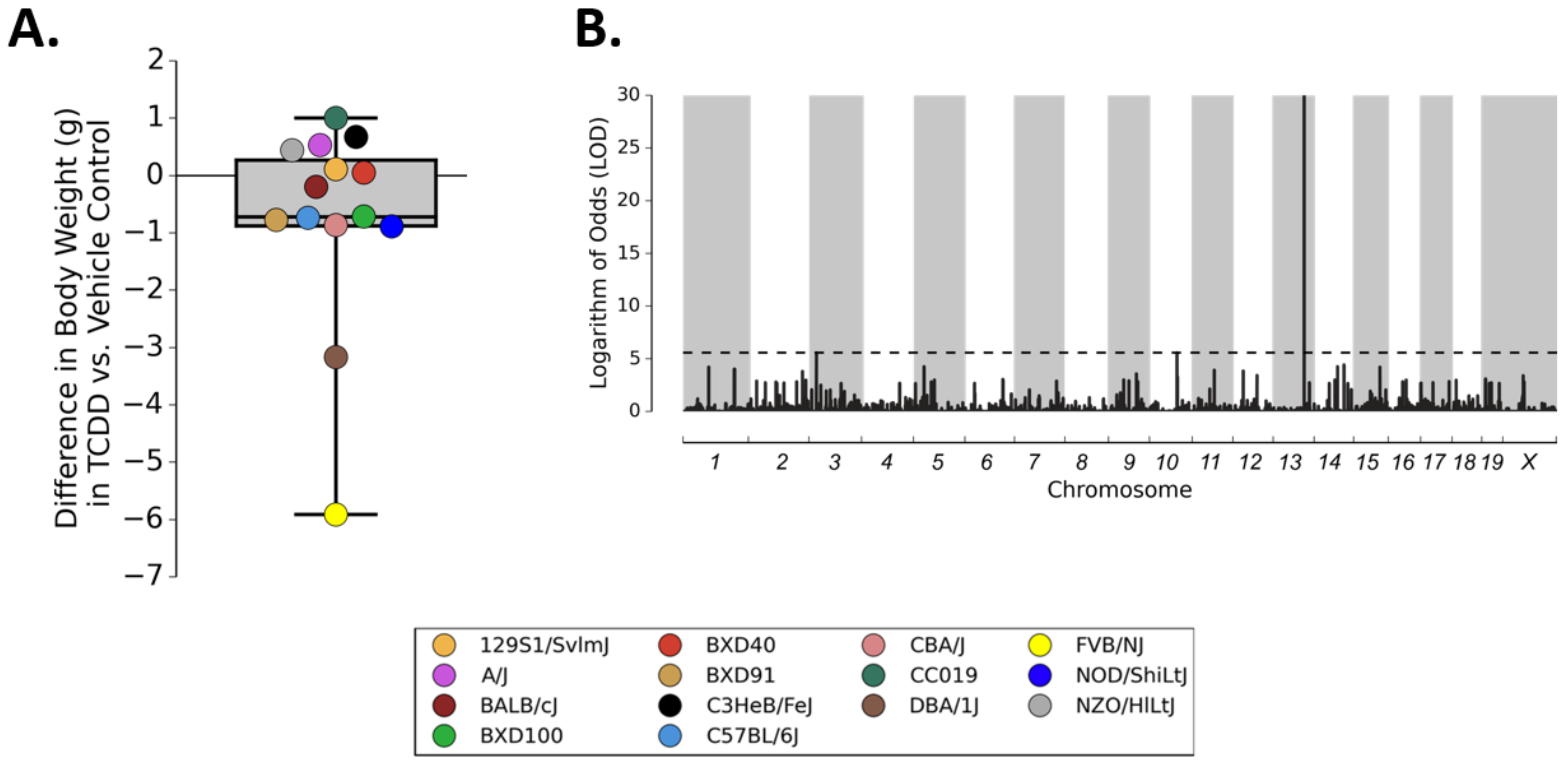

Discussion

Previous reports have suggested that interstrain differences in mice in response to AHR ligands can point to novel genes that may be regulated by the AHR.[1,15] Therefore, discovering novel genes may improve the understanding of the AHR's role in complex disease and potentially lead to treatment options for adverse AHR-mediated phenotypes. In this study, a genetically diverse mouse panel was treated with TCDD to find genes regulated by the AHR in the liver, a target organ of AHR-mediated adverse outcomes. It also aimed to identify genes associated with alterations in body measurements across strains.

This study showcased the impact that genetics can have on physiological response. Although previous reports have established that differing *Ahr* alleles have differing affinities for TCDD, we also observed distinct intra-allelic differences across strains. For example, this study used a few BXD strains, which are a cross between C57Bl/6J (Ahr^{b1}) and DBA/2J (Ahr^{d}) strains. We observed that both BXD100 and BXD91 strains, Ahr^{b1} allele carriers, had TCDD burden levels similar to C57Bl/6J, but had far less DEGs (Figures 2.1; 2.4). However, BXD40, a Ahr^{d} allele carrier, had a TCDD burden level similar to DBA/1J, a close genetic cousin of DBA/2J, but more DEGs compared to DBA/1J and the other BXD strains (Figures 2.1; 2.4). These results suggest that while the *Ahr* allele impacts sensitivity to ligands, other genetic factors much also impact the response.[16,17]

Furthermore, linear regression identified 7 genes that were associated with TCDD liver burden. Of note, 2 of these genes, *Nptx1* and *Slc46a3*, had not been previously linked to TCDD exposure when this study was conducted. Although all 7 genes have different functions, many reports have suggested that they all may play a role in liver disease.[11,12,18–22] Previous reports

have suggested that upregulation of many of these genes is associated with a protective response to liver damage. For example, NAFLD progression can lead to mitochondrial damage that causes an overproduction of reactive oxygen species (ROS). NRF2, a transcription factor, is activated by ROS to produce antioxidant proteins that may alleviate damage induced by NAFLD.[20] Also, *Htatip2*, known as TIP30 or CC3, expression has been shown to inhibit tumor cell proliferation in hepatocellular carcinoma and deficiency was strongly related to hepatocarcinogenesis.[21,22] It is possible that upregulation of genes like NRF2 or TIP30 with TCDD exposure may be a protective response against TCDD-induced liver injury. However, a recent study showed that TCDD-induced induction of *Slc46a3*, which encodes a lysosomal transporter, instead caused triglyceride accumulation and mitochondrial dysfunction in mouse liver leading to steatosis.[19] Therefore, the results of this study provide insight into upregulated pathways that could be therapeutic or adverse in the context of TCDD-induced liver injury, which can be explored further to develop potential treatment options for NAFLD.

Regression and QTL analysis also suggested that *Dio1* and *Hmgcr* are associated with TCDD-induced changes in body fat percentage and body weight, respectively. Although these phenotypic changes may provide insight on a potential mechanism for TCDD-induced wasting, it may also impact our understanding of AHR-mediated liver injury. Previous reports have suggested that DIO1 expression in rodents and humans with chronic liver injury was significantly dysregulated.[23] Also, hypothyroidism has been associated with the development of nonalcoholic fatty liver disease (NAFLD) because thyroid hormone can regulate hepatic lipid metabolism.[24] Furthermore, metabolic dysfunction is highly associated with NAFLD development, including dysregulation of cholesterol.[25–29] Free cholesterol accumulation promotes mitochondrial

dysfunction and cell stress leading to the development of steatosis, inflammation and cell death.[27–29] Therefore, thyroid hormone synthesis and cholesterol biosynthesis have particularly strong links to adverse AHR-mediated phenotypes and are important pathways to explore in the context of TCDD-induced liver injury. Overall, this study not only showcases the power in using genetics-based approaches in toxicology, but it also provided insight into the impact of AHR-mediated signaling in liver damage and may suggest new therapeutic targets for liver-related disease.

REFERENCES

1. Dornbos, P. & LaPres, J. J. Incorporating population-level genetic variability within laboratory models in toxicology: From the individual to the population. *Toxicology* **395**, 1–8 (2018).

2. Harrill, A. H. & McAllister, K. A. New Rodent Population Models May Inform Human Health Risk Assessment and Identification of Genetic Susceptibility to Environmental Exposures. *Environ Health Perspect* **125**, 086002 (2017).

3. Rusyn, I., Gatti, D. M., Wilshire, T., Kleeberger, S. R. & Threadgill, D. W. Toxicogenetics: population-based testing of drug and chemical safety in mouse models. *Pharmacogenomics* **11**, 1127–1136 (2010).

4. Ideraabdullah, F. Y. *et al.* Genetic and Haplotype Diversity Among Wild-Derived Mouse Inbred Strains. *Genome Res* **14**, 1880–1887 (2004).

5. Dornbos, P., Crawford, R. B., Kaminski, N. E., Hession, S. L. & LaPres, J. J. The Influence of Human Interindividual Variability on the Low-Dose Region of Dose-Response Curve Induced by 2,3,7,8-Tetrachlorodibenzo-p-Dioxin in Primary B Cells. *Toxicol Sci* **153**, 352–60 (2016).

6. Dornbos, P. *et al.* Characterizing Serpinb2 as a Modulator of TCDD-Induced Suppression of the B Cell. *Chem Res Toxicol* **31**, 1248–1259 (2018).

7. Smart, J. & Daly, A. K. Variation in induced CYP1A1 levels: relationship to CYP1A1, Ah receptor and GSTM1 polymorphisms. *Pharmacogenetics* **10**, 11–24 (2000).

8. Swanson, H. I. & Bradfield, C. A. The AH-receptor: genetics, structure and function. *Pharmacogenetics* **3**, 213–30 (1993).

9. Dornbos, P., Arkatkar, A. A. & LaPres, J. J. An Automated Method To Predict Mouse Gene and Protein Sequences Using Variant Data. *G3 (Bethesda)* **10**, 925–932 (2020).

10. Stevens, E. A., Mezrich, J. D. & Bradfield, C. A. The aryl hydrocarbon receptor: a perspective on potential roles in the immune system. *Immunology* **127**, 299–311 (2009).

11. Nault, R. *et al.* Dose-Dependent Metabolic Reprogramming and Differential Gene Expression in TCDD-Elicited Hepatic Fibrosis. *Toxicol Sci* **154**, 253–266 (2016).

12. Nault, R., Doskey, C. M., Fader, K. A., Rockwell, C. E. & Zacharewski, T. Comparison of Hepatic NRF2 and Aryl Hydrocarbon Receptor Binding in 2,3,7,8-Tetrachlorodibenzo- *p* -dioxin–Treated Mice Demonstrates NRF2-Independent PKM2 Induction. *Mol Pharmacol* **94**, 876–884 (2018).

13. Boutros, P. C., Bielefeld, K. A., Pohjanvirta, R. & Harper, P. A. Dioxin-Dependent and Dioxin-Independent Gene Batteries: Comparison of Liver and Kidney in AHR-Null Mice. *Toxicological Sciences* **112**, 245–256 (2009).

14. Angrish, M. M., Dominici, C. Y. & Zacharewski, T. R. TCDD-elicited effects on liver, serum, and adipose lipid composition in C57BL/6 mice. *Toxicol Sci* **131**, 108–15 (2013).

15. Chapman, D. E. & Schiller, C. M. Dose-related effects of 2,3,7,8-tetrachlorodibenzo-p-dioxin (TCDD) in C57BL6J and DBA2J mice. *Toxicol Appl Pharmacol* **78**, 147–157 (1985).

16. Greig, J. B., Francis, J. E., Kay, S. J. E., Lovell, D. P. & Smith, A. G. Incomplete correlation of 2,3,7,8-tetrachlorodibenzo-p-dioxin hepatotoxicity with Ah phenotype in mice. *Toxicol Appl Pharmacol* **74**, 17–25 (1984).

17. A Poland & E Glover. Characterization and strain distribution pattern of the murine Ah receptor specified by the Ahd and Ahdb-3 alleles. *Mol Pharmacol* **38**, 306–312 (1990).

18. Zhao, Y. *et al.* As a downstream target of the AKT pathway, NPTX1 inhibits proliferation and promotes apoptosis in hepatocellular carcinoma. *Biosci Rep* **39**, (2019).

19. Kim, J.-H. *et al.* Lysosomal SLC46A3 modulates hepatic cytosolic copper homeostasis. *Nat Commun* **12**, 290 (2021).

20. Zhou, J., Zheng, Q. & Chen, Z. The Nrf2 Pathway in Liver Diseases. *Front Cell Dev Biol* **10**, (2022).

21. Mitsuhiro Ito *et al.* TIP30 deficiency increases susceptibility to tumorigenesis. *Cancer Res* **63**, 8763–8767 (2003).

22. Zhao, J. *et al.* TIP30 inhibits growth of HCC cell lines and inhibits HCC xenografts in mice in combination with 5-FU. *Hepatology* **44**, 205–215 (2006).

23. Bohinc, B. N. *et al.* Repair-Related Activation of Hedgehog Signaling in Stromal Cells Promotes Intrahepatic Hypothyroidism. *Endocrinology* **155**, 4591–4601 (2014).

24. Sinha, R. A., Singh, B. K. & Yen, P. M. Direct effects of thyroid hormones on hepatic lipid metabolism. *Nat Rev Endocrinol* **14**, 259–269 (2018).

25. Mitra, S., De, A. & Chowdhury, A. Epidemiology of non-alcoholic and alcoholic fatty liver diseases. *Transl Gastroenterol Hepatol* **5**, 16 (2020).

26. Godoy-Matos, A. F., Silva Júnior, W. S. & Valerio, C. M. NAFLD as a continuum: from obesity to metabolic syndrome and diabetes. *Diabetol Metab Syndr* **12**, 60 (2020).

27. Arguello, G., Balboa, E., Arrese, M. & Zanlungo, S. Recent insights on the role of cholesterol in non-alcoholic fatty liver disease. *Biochim Biophys Acta* **1852**, 1765–78

(2015).

28. Min, H.-K. *et al.* Increased hepatic synthesis and dysregulation of cholesterol metabolism is associated with the severity of nonalcoholic fatty liver disease. *Cell Metab* **15**, 665–74 (2012).

29. Song, Y., Liu, J., Zhao, K., Gao, L. & Zhao, J. Cholesterol-induced toxicity: An integrated view of the role of cholesterol in multiple diseases. *Cell Metabolism* vol. 33 1911–1925 Preprint at https://doi.org/10.1016/j.cmet.2021.09.001 (2021).

Chapter 3: The Role of HMG-CoA Reductase Repression in TCDD-Induced Liver Injury

This chapter is an edited version of a previously published research article in *Scientific Reports*, Volume 9, No. 1: 15828.

Authors: Peter Dornbos[1,2], Amanda Jurgelewicz[2,3], Kelly A. Fader[1,2], Kurt Williams[4], Tim Zacharewski[1,2] and John J. LaPres[1,2].

Affiliations: [1]Department of Biochemistry and Molecular Biology, Michigan State University; [2]Institute for Integrative Toxicology, Michigan State University; [3]Department of Pharmacology and Toxicology, Michigan State University; [4]Department of Pathobiology and Diagnostic Investigation, Michigan State University

Abstract

In Chapter 2, our mouse panel study indicated that 2,3,7,8-tetrachlorodibenzo-ρ-dioxin (TCDD)-induced changes in body weight were associated with a peak chromosome 13 that was within 0.5 Mb of HMGCR. TCDD exposure has been linked to the suppression of key cholesterol biosynthesis enzymes as well as changes in circulating and hepatic cholesterol levels in mice. Due to emerging reports linking dysregulation of cholesterol to liver injury development, the aim of this study was to understand the role of HMGCR repression in TCDD-induced liver injury in mice. In this study, male and female C57Bl6/J mice were treated in the presence and absence of TCDD and simvastatin, and the results indicated that HMGCR likely plays a key, but sex-specific, role in TCDD-induced liver injury. The results implicated that simvastatin co-treatment alters glycogen metabolism in females and increases the risk of AHR-elicited liver damage in males suggesting that vulnerable populations who take statins may be at greater risk of sex-specific, toxicant-induced injury.

Introduction

In the mouse panel study outlined in chapter 2, there was a significant peak on chromosome 13 associated with TCDD-induced body weight changes that was within 0.5 Mb of *Hmgcr* or HMG-CoA reductase. This enzyme is involved in the rate-limiting step of cholesterol biosynthesis, and its expression is highly regulated in the liver.[1,2] TCDD exposure had been previously associated with repression of various cholesterol biosynthesis enzymes in mice, including *Hmgcr*, and these changes corresponded with reduction in circulating levels of cholesterol and increases in hepatic cholesterol levels.[3–5] Furthermore, *Hmgcr* was of particular interest due to the emergence of reports connecting metabolic disruption, especially dysregulation of cholesterol, to the development of non-alcoholic fatty liver disease.[6,7] Thus, the goal of this study was to investigate the significance of *Hmgcr* in the context of TCDD-induced liver injury.

In this study, we sought to characterize the role of HMCGR repression in TCDD-induced liver injury in mice. Male and female C57BL/6J mice were treated in the presence and absence of TCDD (10 μg/kg) and simvastatin (500 mg/kg food), a HMGCR competitive inhibitor, for 10 consecutive days. The materials and methods for this study can be found in Chapter 6. The results of this study supported that TCDD exposure impacts expression of HMGCR, circulating levels of cholesterol in serum and hepatic levels of cholesterol seen in previous studies. Furthermore, it implicated that HMGCR activity likely plays a key role in TCDD-induced liver injury. While simvastatin co-treatment led to decreased levels of AHR-mediated steatosis, the results suggested that there may be an increased risk of TCDD-induced liver injury and alterations in glycogen metabolism in a sex-specific manner.

Results

Hepatic Expression of Cholesterol Biosynthesis Enzymes

Given the focus on HMGCR, we focused on its expression at the gene and protein level (Figure 3.1). At the gene level, TCDD treatment decreased expression compared to vehicle control in both sexes, but this decrease was not statistically significant (Figure 3.1A). In females, simvastatin alone significantly increased *Hmgcr* expression and a similar, but non-significant, trend was seen in males. In both sexes, simvastatin and TCDD (T+S) co-treatment had expression that was significantly larger than mice treated with TCDD alone. At the protein level, western blot analysis suggested that TCDD treatment significantly decreased HMGCR expression in males regardless of diet (Figure 3.1B). This trend was also seen in females, but it was non-significant. On the contrary, protein-level analysis suggested that simvastatin did not mediate an increase in protein expression of HMGCR that was seen at the gene level.

Figure 3.1: Hepatic gene and protein expression of HMCGR. (A) Gene expression fold changes of *Hmgcr* for male and female mice. N ≥ 7 for all groups. (B) Protein expression of HMGCR for males and females assessed by densitometry analysis of western blots. Analysis is reported as fold change relative to vehicle control, and N=5 for each treatment group. (C) A representative western blot chosen to visualize bands used for densitometry analysis depicting 1 sample from each treatment group. Asterisks (*) indicate statistically significant differences ($p \leq 0.05$) as compared to respective control or between means indicated by brackets.

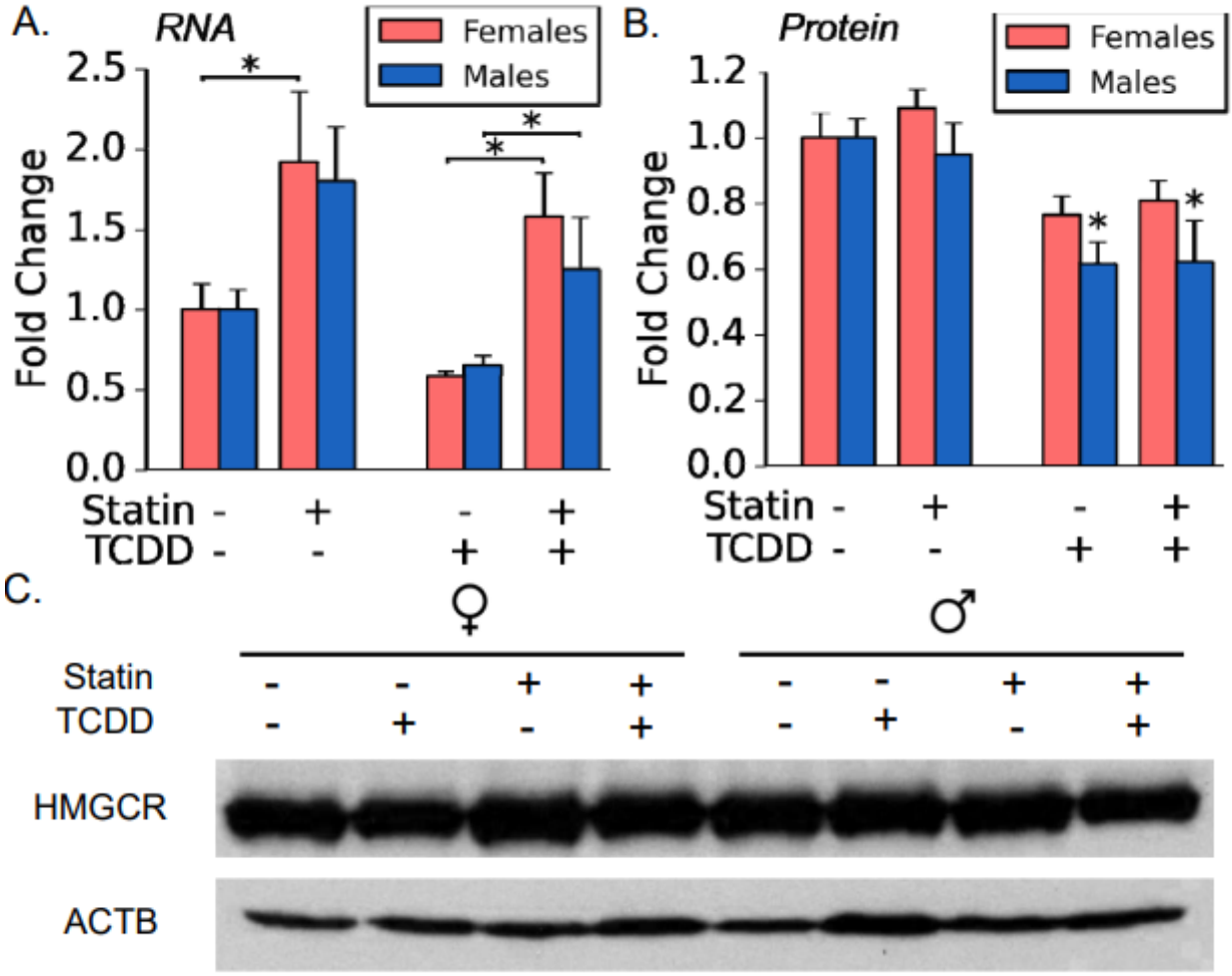

Consistent with previous reports, TCDD treatment in both sexes led to an overall reduction in expression of additional cholesterol biosynthesis-related genes, such as squalene epoxidase (*Sqle*) and 7-dehydrocholesterol reductase (*Dhcr7*) (Table 3.1).[3,4] However, this trend was not statistically significant, similar to what was seen with *Hmgcr*. In general, simvastatin treatment led to an overall increase in expression of genes involved in this pathway. For example, *Sqle* and *Cyp51* expression significantly increased in females.

Table 3.1: TCDD and simvastatin-mediated changes in gene expression. Results are presented as fold changes with standard error in parentheses that are relative to vehicle control mice. In all cases, n ≥ 7 in all groups for gene expression analysis. Superscript letters indicate significant differences ($p < 0.05$) as indicated by ANOVA in comparison to: vehicle (sesame oil)[a], TCDD treatment[b] or simvastatin treatment[c]. Statistical comparisons were not made across sexes.

	Females				Males			
	Standard Chow		Statin Chow		Standard Chow		Statin Chow	
Gene	Sesame Oil	TCDD	Sesame Oil	TCDD	Sesame Oil	TCDD	Sesame Oil	TCDD
Apoa1	1.00 (0.11)	0.26 (0.02)[a]	0.97 (0.12)	0.22 (0.02)[c]	1.00 (0.14)	0.33 (0.05)[a]	1.93 (0.05)[b]	0.36 (0.07)[c]
Cyp1a1	1.00 (0.26)	2959.93 (104.63)[a]	1.08 (0.86)	2625.40 (315.80)[c]	1.00 (0.13)	2514.14 (343.20)[a]	1.46 (0.15)	4070.06 (405.41)[b,c]
Cyp1a2	1.00 (0.04)	16.51 (1.13)[a]	0.76 (0.11)	14.44 (1.19)[c]	1.00 (0.06)	12.85 (2.00)[a]	0.98 (0.06)	17.56 (1.99)[b,c]
Cyp1b1	1.00 (0.21)	505.86 (60.38)[a]	0.81 (0.19)	377 (20.43)[c]	1.00 (0.10)	701.56 (95.72)[a]	0.99 (0.09)	1320.70 (167.30)[b,c]
Cyp4a10	1.00 (0.15)	0.36 (0.04)[a]	0.51 (0.08)[b]	0.19 (0.03)[b,c]	1.00 (0.22)	0.32 (0.06)[a]	1.11 (0.14)	0.78 (0.14)[b]
Cyp4a14	1.00 (0.24)	0.57 (0.08)[a]	0.71 (0.12)	0.27 (0.03)[b,c]	1.00 (0.29)	0.11 (0.02)[a]	1.4 (0.20)	0.35 (0.08)[b,c]
Cyp51	1.00 (0.23)	0.49 (0.03)	2.12 (0.15)[a]	1.59 (0.21)[b]	1.00 (0.11)	0.56 (0.19)	1.86 (0.23)	1.01 (0.19)
Dhcr7	1.00 (0.26)	0.55 (0.10)	1.63 (0.17)	1.46 (0.21)[b]	1.00 (0.12)	0.64 (0.18)	1.67 (0.17)	1.00 (0.21)[b]
Gbe1	1.00 (0.11)	0.51 (0.04)[a]	0.60 (0.04)[a]	0.48 (0.06)	1.00 (0.13)	0.42 (0.06)[a]	0.82 (0.12)	0.63 (0.08)
Gys2	1.00 (0.15)	0.49 (0.04)[a]	0.78 (0.10)	0.28 (0.03)[b,c]	1.00 (0.18)	0.24 (0.04)[a]	1.05 (0.16)	0.36 (0.08)[c]
Hk1	1.00 (0.07)	1.10 (0.06)	0.66 (0.02)[a]	1.04 (0.05)[c]	1.00 (0.08)	1.45 (0.15)	1.03 (0.24)	1.56 (0.12)
Lcat	1.00 (0.31)	0.70 (0.05)	0.63 (0.04)	0.57 (0.06)	1.00 (0.11)	1.19 (0.14)	1.42 (0.14)	1.48 (0.24)
Ldlr	1.00 (0.11)	0.87 (0.05)	0.97 (0.11)	1.26 (0.14)	1.00 (0.15)	0.75 (0.06)	0.95 (0.10)	0.92 (0.23)
Pgm1	1.00 (0.15)	0.99 (0.05)	0.69 (0.04)[a]	0.93 (0.08)	1.00 (0.10)	1.17 (0.20)	0.98 (0.12)	1.50 (0.15)
Ppara	1.00 (0.20)	0.54 (0.05)[a]	0.63 (0.08)	0.32 (0.05)[b,c]	1.00 (0.16)	0.44 (0.04)[a]	0.96 (0.11)	0.85 (0.10)[b]
Pygl	1.00 (0.14)	0.32 (0.03)[a]	0.53 (0.05)[b]	0.24 (0.02)[c]	1.00 (0.11)	0.37 (0.10)[a]	1.01 (0.15)	0.39 (0.05)[c]
Sqle	1.00 (0.45)	0.43 (0.06)	2.95 (0.23)[a]	3.93 (0.38)[b]	1.00 (0.12)	0.78 (0.11)	2.09 (0.27)[a]	1.41 (0.20)[b]
Ugp2	1.00 (0.14)	0.42 (0.03)[a]	0.71 (0.05)	0.39 (0.04)[c]	1.00 (0.15)	0.28 (0.07)[a]	0.80 (0.11)	0.30 (0.03)[c]

Assessing Circulating and Hepatic Cholesterol Levels

Given the impact of TCDD, simvastatin and co-treatment on cholesterol biosynthesis enzyme expression, we also wanted to characterize the impact of these treatments on circulating and hepatic cholesterol levels. The levels of total cholesterol (TC), low-density lipoprotein (LDL) and high-density lipoprotein (HDL) were quantified in serum (Table 3.2). TCDD and co-treated males and females had significantly less TC in serum compared to vehicle control and simvastatin treatment alone. However, TC was not significantly different between TCDD and T+S. Treatment did not significantly impact serum LDL levels in female mice, but T+S-treated male mice had significantly less serum LDL compared to simvastatin-treated mice. The largest TCDD-induced reductions were seen in serum HDL. Both male and female TCDD-treated mice had almost a 50% reduction in serum HDL levels compared to control. Co-treated male and female mice also had significant reductions in serum HDL compared to simvastatin-alone. Interestingly, simvastatin-treated female mice also had reductions in serum HDL compared to control that was not seen in males. The HDL:LDL ratio in female mice fed standard chow was nearly double the ratio in simvastatin-fed female mice (~2.1 vs. ~1.1), which was not seen in male mice.

Table 3.2: **TCDD and simvastatin-mediated changes in cholesterol levels, quantitative pathology, and serum clinical chemistry.** Results are presented as mean weights with standard error in parenthesis. In all cases, sample size (n) is ≥ 5 in all groups. Superscript letters indicate significant differences ($p < 0.05$) as indicated by ANOVA in comparison to vehicle[a], TCDD treatment[b] or simvastatin treatment[c]. Statistical comparisons were not made across sexes.

		Females				Males			
		Standard Chow		Statin Chow		Standard Chow		Statin Chow	
Group	Measurement	Sesame Oil	TCDD	Sesame Oil	TCDD	Sesame Oil	TCDD	Sesame Oil	TCDD
Cholesterol	Low-Density Lipoprotein (mg/dL)	38.1 (1.5)	34.8 (1.0)	52.7 (3.2)	35.6 (1.0)	40.4 (0.7)	33.1 (0.5)	43.2 (0.8)	29.3 (1.6)[c]
	High-Density Lipoprotein (mg/dL)	80.0 (3.8)	43.7 (1.5)[a]	58.1 (2.1)[a]	37.9 (0.9)[c]	63.2 (2.3)	35.1 (1.2)[a]	70.2 (2.1)	39.1 (2.5)[c]
	Total Cholesterol (mg/dL)	136.7 (1.9)	120.4 (1.5)[a]	137.3 (1.3)	120.5 (0.9)[c]	151.7 (1.5)	122.9 (1.7)[a]	170.0 (1.0)	133.6 (2.7)[c]
	Hepatic Free Cholesterol (mg/g)	2.3 (0.1)	3.9 (0.1)[a]	2.2 (0.1)	3.2 (0.2)[b,c]	2.1 (0.1)	3.2 (0.1)[a]	2.1 (0.1)	2.8 (0.1)[b,c]
Pathology	Liver Weight (g)	0.76 (0.02)	0.99 (0.02)[a]	0.80 (0.02)	1.12 (0.04)[b,c]	1.13 (0.04)	1.27 (0.07)	1.18 (0.03)	1.31 (0.05)
	Normalized Liver Weight (mg/kg)	48.48 (0.86)	65.89 (0.63)[a]	50.83 (0.45)	73.47 (1.83)[b,c]	58.58 (1.39)	71.27 (2.67)[a]	59.38 (1.33)	73.80 (1.69)[c]
	Body Weight (g)	15.6 (0.3)	15.1 (0.3)	15.7 (0.3)	15.2 (0.3)	19.5 (0.3)	17.8 (0.4)[a]	19.9 (0.2)	17.7 (0.5)[c]
	GWAT Weight (g)	0.12 (0.02)	0.1 (0.01)	0.10 (0.009)	0.10 (0.01)	0.23 (0.01)	0.22 (0.01)	0.25 (0.005)	0.22 (0.01)
	Normalized GWAT Weight (mg/kg)	7.7 (1.39)	7.09 (0.57)	6.17 (0.60)	6.85 (2.08)	11.79 (0.76)	12.39 (0.24)	12.39 (0.24)	12.65 (0.42)
	Average Histologic Severity Score	0.8 (0.2)	2.0 (0.0)[a]	0.4 (0.2)	1.9 (0.1)[c]	0.4 (0.2)	2.6 (0.2)[a]	0.3 (0.2)	1.5 (0.3)[b,c]
Clinical Chemistry	Alanine Aminotransferase (mg/dL)	44.3 (2.2)	335.1 (21.0)[a]	34.6 (0.6)	345.6 (19.5)[c]	34.0 (1.4)	1844.5 (91.5)[a]	94.2 (3.1)	3010.9 (256.9)[b,c]
	Free Fatty Acids (mmol/mL)	662.7 (19.5)	591.0 (14.4)	470.3 (26.2)	266.6 (25.6)[b,c]	437.4 (8.1)	472.9 (33.2)	325.4 (20.6)	397.0 (32.4)
	Ketone Bodies (mg/dL)	300.6 (11.3)	208.2 (11.2)	263.7 (11.6)	72.2 (2.0)[b,c]	85.6 (3.2)	145.5 (3.8)[a]	83.6 (2.4)	130.0 (5.1)[c]
	Glucose (mg/dL)	165.4 (2.2)	153.7 (3.9)	165.2 (2.4)	142.0 (3.3)	223.7 (4.1)	158.8 (2.7)[a]	221.9 (3.4)	156.6 (3.0)[c]
	Triglycerides (mg/dL)	99.9 (1.3)	107.5 (0.7)	99.0 (1.2)	104.7 (1.8)	115.6 (1.5)	108.4 (1.2)	108.4 (1.3)	101.5 (1.3)

To address this sex-specific difference in serum HDL, we looked at expression of genes involved in HDL components (*Apoa1*) and maturation (*Lcat*) (Table 3.1). TCDD exposure in males and females significantly repressed expression of *Apoa1*, but co-treatment did not alter expression compared to TCDD alone in either sex. Interestingly, simvastatin treatment in males had significantly higher expression of *Apoa1* compared to TCDD alone, which was not seen in females. Furthermore, TCDD alone and simvastatin alone exposure had a trending, but not significant, decrease in *Lcat* expression in females. This decrease was not significantly different from co-treatment and was not seen in males. These results suggest that simvastatin treatment may be influencing HDL formation and maturation in a sex-specific manner.

Hepatic total cholesterol levels were also quantified to determine if cholesterol biosynthesis enzyme repression and changes in cholesterol circulation caused by our treatments also impacted the hepatic levels of cholesterol (Table 3.2). TCDD treatment significantly increased the levels of hepatic cholesterol in males and females compared to control. Similarly, T+S treatment had significantly greater levels of hepatic cholesterol compared to control and simvastatin-treated mice in both males and females. We also observed that T+S-treated mice had significantly less hepatic cholesterol than TCDD-treated mice in both sexes. Overall, our results support the findings of previous studies that indicate TCDD exposure impacts cholesterol homeostasis in mice.[3–5]

Co-Treatment Impacts Liver Injury in a Sex-Specific Manner

In assessing gross liver pathology, TCDD-treated male and female mice had significantly larger liver weight and body weight-normalized liver weight compared to control (Table 3.2). This same trend was also seen in co-treated mice compared to control and simvastatin treatment in both sexes. Interestingly, female co-treated mice had larger liver weight and normalized liver weight compared to TCDD-treated females, which was not seen in males.

Liver tissue sections were stained with Hematoxylin and Eosin (H&E) for general assessment and to perform severity scoring (Figure 3.2A). TCDD exposure led to increased levels of inflammation, hepatocyte necrosis and vacuolization in both sexes compared to control. This corresponded to higher levels of serum alanine aminotransferase (ALT) levels, a marker of liver injury (Table 3.2). Interestingly, co-treated male mice had less inflammation than TCDD-treated male mice, but significantly higher serum ALT levels, which was not seen in females. This corresponded to greater expression of AHR battery genes, including *Cyp1a1, Cyp1a2* and *Cyp1b1* (Table 3.1). This result suggests that simvastatin co-treatment is exacerbating TCDD-induced liver injury in an AHR-mediated manner in male mice.

Figure 3.2: The Impact of TCDD and simvastatin co-treatment on hepatic lipid accumulation. (A) Representative liver sections for Hematoxylin and Eosin (H&E) and Oil Red O (ORO) stains. Scale bars represent 100 µm for H&E and 50 µm for ORO. (B) Percent area of tissue stained with ORO quantified using QuHAnT software. (C) Quantified levels of triglycerides in hepatic lipid extracts. In all cases, n ≥ 5. Asterisks (*) over bars indicate statistically significant differences ($p \leq 0.05$) compared to respective control or between means indicated by brackets.

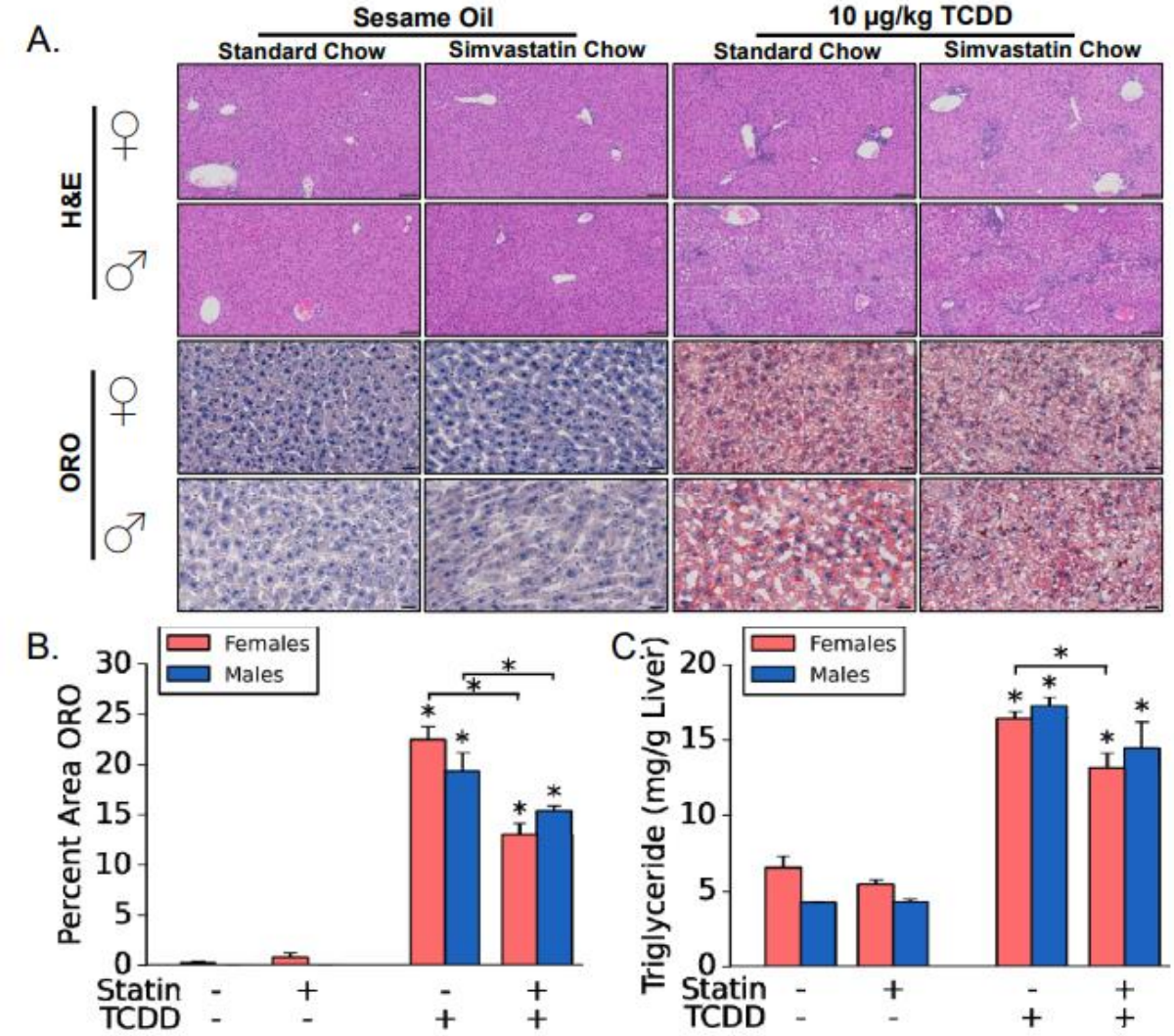

In females, co-treatment led to significantly more vacuolization compared to females treated with only TCDD, which was not seen in males. Hepatic Oil Red O (ORO) stain was used to determine if this was due to changes in lipid accumulation between treatment groups (Figure 3.2A-B). As seen in previous studies, ORO quantification suggested that TCDD treatment increased hepatic neutral lipid levels in both sexes regardless of simvastatin co-treatment (Figure 3.2B).[5,8,9] The quantification results were confirmed by measuring triglyceride content in hepatic lipid extract (Figure 3.2C). Interestingly, T+S-treated mice in both sexes had significantly less ORO staining compared to TCDD alone, and T+S-treated female mice had significantly less triglyceride content compared to TCDD alone.

The increased liver weight and histological differences in T+S-treated females as compared to TCDD alone were not due to lipid accumulation, so we sought to analyze the hepatic glycogen levels in each group. In females, there was significantly more hepatic glycogen in the co-treated group compared to TCDD alone (Figure 3.3A). This was confirmed using a Periodic Acid-Schiff (PAS) stain that can detect polysaccharides such as glycogen (Figure 3.3C). TCDD treatment did not impact hepatic glucose in females, but co-treated mice had significantly less hepatic glucose compared to simvastatin alone (Figure 3.3B). Interestingly, in males, TCDD treatment led to a significant drop in hepatic glycogen and hepatic glucose levels. Co-treated males also had a significant drop in hepatic glucose compared to simvastatin-treated males. To determine why co-treated females may have higher levels of glycogen, expression of various genes involved in glycogen metabolism were assessed (Table 3.1). In females, genes involved in glycogen anabolism including *Gys2*, *Ugp2*, and *Gbe1* were significantly repressed in the liver following TCDD treatment. Similarly, expression of *Pygl*, which regulates glycogen catabolism,

was significantly repressed in TCDD-treated females. Simvastatin treatment alone in females decreased expression of *Gbe1* and *Pygl* in addition to *Hk1* and *Pgm1*, which are involved in glycogen anabolism. However, T+S-treated females only significantly induced further repression of *Gys2* in females compared to TCDD alone though there was trending repression in expression in the other genes, as well. TCDD-treated males had the same significant expression pattern that was seen in females, but simvastatin alone did not impact expression of any of the genes that were repressed in females. Co-treatment also did not impact *Gys2* expression compared to TCDD alone in males. These results suggest that co-treatment is driving a phenotype similar to a glycogen storage disease in female mice.

Figure 3.3: The Impact of TCDD and simvastatin co-treatment on hepatic glycogen. (A, B) Inferred levels of hepatic glycogen and glucose levels. Results are reported as fold changes relative to vehicle control (sesame oil and standard chow). In all cases, n ≥ 5. Asterisks (*) indicate statistically significant differences ($p < 0.05$) as compared to respective control or between means indicated by brackets. (C) Representative liver sections stained with Periodic Acid-Schiff (PAS) stain to confirm differences in glycogen level. Scale bars represent 20 µm.

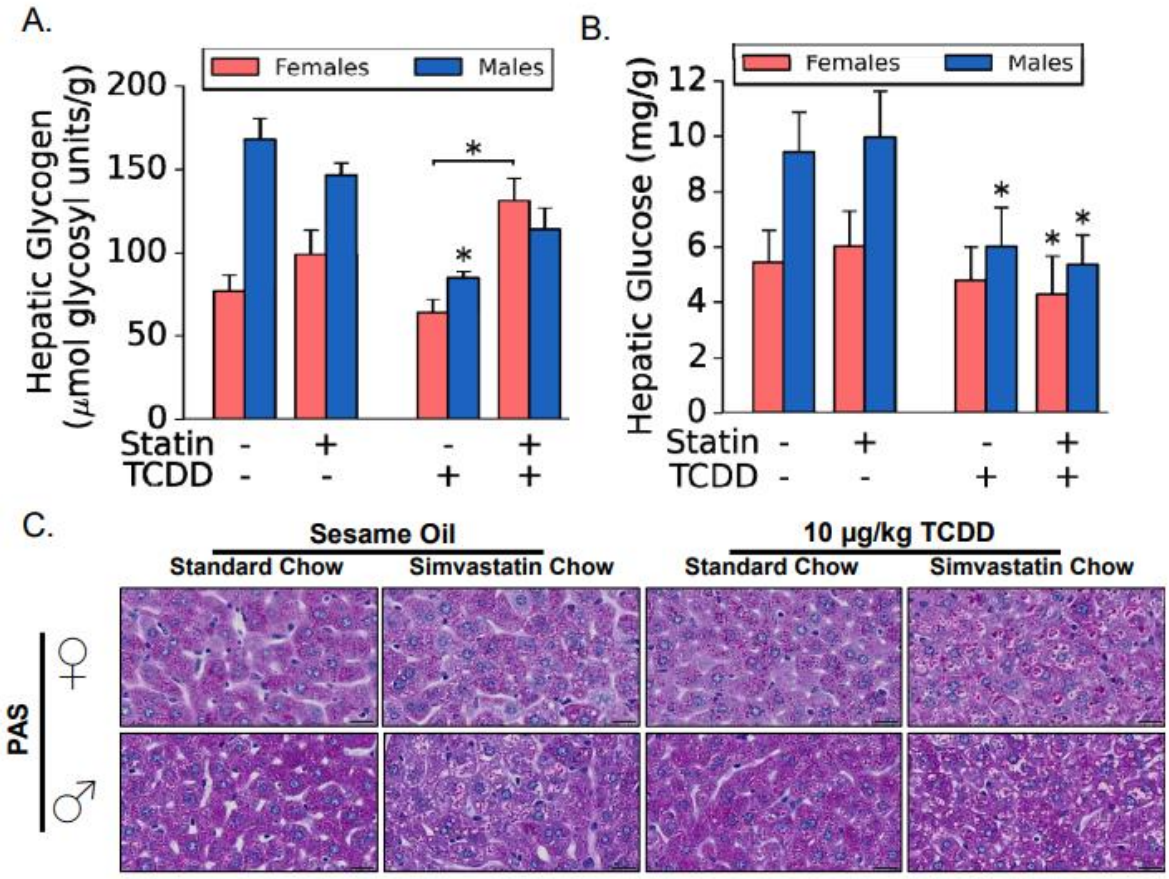

Discussion

Previous reports suggested that alterations in cholesterol homeostasis can induce NAFLD, and TCDD exposure, via AHR activation, can impact cholesterol biosynthesis enzyme expression and levels of circulating and hepatic cholesterol in mice.[3,4,6,7] As *Hmgcr* was linked to TCDD-induced changes in body weight in Chapter 2, this study aimed to deduce if HMGCR modulation also plays a role in TCDD-induced liver injury by treating C57Bl6/J mice in the presence or absence of TCDD and simvastatin, an HMGCR competitive inhibitor.[10]

The impact of TCDD on cholesterol homeostasis in this mouse study supports previous *in vivo* work.[3,4] TCDD exposure led to trending decreases in gene expression of various enzymes utilized in cholesterol biosynthesis including *Hmgcr, Sqle,* and *Dhcr7* that corresponded with significantly decreased levels of HDL and TC in both sexes (Tables 3.1, 3.2). Notably, hepatic HMGCR protein expression was also significantly decreased in males and had a trending decrease in females, which may play a significant role in the decreases in circulating cholesterol (Figure 3.1). Unlike previous studies, LDL levels were unaffected by TCDD treatment, which is likely due to study design differences.[3] Simvastatin treatment did not impact HMGCR protein levels nor TC or LDL levels in serum in both sexes, but it did significantly decrease HDL levels in females. While statin drugs primarily reduce LDL levels in humans, it has been shown that they are less effective at doing so in mice as the predominant lipoprotein in mice is HDL.[11,12] In females, simvastatin treatment had a trending decrease in *Lcat* expression, which is utilized to form mature HDL (Table 3.1).[13] This results suggests that simvastatin-induced repression of *Lcat* may lead to lower HDL levels in females, which in turn, may impact reverse-cholesterol transport.[1,2,13]

TCDD was also shown to increase hepatic cholesterol and lipid levels, as seen in previous

studies (Table 3.2; Figure 3.2).[3,5,8,9] Increases in hepatic cholesterol are associated with liver injury development and steatosis is seen with early stages of liver damage.[6,7,14,15] T+S co-treatment, however, significantly lowered hepatic cholesterol and neutral lipid levels compared to TCDD alone in both sexes. This result supports previous findings that statins may have lipid-lowering capabilities and are protective against hepatic steatosis.[16,17] It has suggested that this could be due to statin-induced activation of PPARα, a major regulator of hepatic lipid metabolism.[16,17] In males, T+S treatment led to increased expression of PPARα target genes, *Cyp4a10* and *Cyp4a14*, compared to TCDD alone, and simvastatin treatment had a trending increase in expression compared to control (Table 3.1). This suggests that simvastatin-induced PPARα activation may play a role in the decrease in AHR-mediated steatosis in males. Interestingly, simvastatin co-treatment had the opposite effect in females, who also had decreased levels of ketone bodies compared to TCDD-treated females, suggesting that there is less lipid mobilization to the liver and that PPARα activation may be sex-specific (Tables 3.1, 3.2).

Interestingly, although co-treatment appears to be protective against AHR-mediated steatosis, there also appeared to be induction of sex-specific liver injury. In females, co-treatment led to significant increases in hepatic glycogen levels compared to TCDD alone, which is a phenotype similar to a glycogen storage disease (Figure 3.3; Table 3.1). This may be due to impaired glycogen catabolism as co-treatment led to a trending decrease in *Pygl* expression compared to TCDD alone, which is involved in the rate-limiting step in this process.[18] Furthermore, the significant decrease in *Gys2* expression in co-treatment vs. TCDD alone suggests that glycogen synthesis is being halted in response to the greater levels of hepatic glycogen. In males, T+S treatment had significantly higher ALT levels in serum and significantly more induction

of AHR battery genes like *Cyp1a1* (Tables 3.1, 3.2). Previous clinical trials have shown that statins have been associated with increased ALT levels with a small minority of patients.[19] However, this result suggests that the increase in ALT levels is associated with increased AHR activity. Given that TCDD-induced liver injury is AHR dependent, this result suggests that simvastatin is exacerbating AHR-mediated, TCDD-induced liver injury in males.[20,21] Overall, this study functionally characterized the sex-specific roles played by HMGCR in TCDD-elicited toxicity in the liver. However, the results suggest that individuals who take statins may be protected from AHR-mediated steatosis, but they may also be at greater risk of sex-specific, TCDD-induced liver injury.

REFERENCES

1. Luo, J., Yang, H. & Song, B.-L. Mechanisms and regulation of cholesterol homeostasis. *Nat Rev Mol Cell Biol* **21**, 225–245 (2020).

2. Goedeke, L. & Fernández-Hernando, C. Regulation of cholesterol homeostasis. *Cell Mol Life Sci* **69**, 915–30 (2012).

3. Angrish, M. M., Dominici, C. Y. & Zacharewski, T. R. TCDD-elicited effects on liver, serum, and adipose lipid composition in C57BL/6 mice. *Toxicol Sci* **131**, 108–15 (2013).

4. Tanos, R. *et al.* Aryl hydrocarbon receptor regulates the cholesterol biosynthetic pathway in a dioxin response element-independent manner. *Hepatology* **55**, 1994–2004 (2012).

5. Fader, K. A. *et al.* 2,3,7,8-Tetrachlorodibenzo-p-dioxin (TCDD)-elicited effects on bile acid homeostasis: Alterations in biosynthesis, enterohepatic circulation, and microbial metabolism. *Sci Rep* **7**, 5921 (2017).

6. Arguello, G., Balboa, E., Arrese, M. & Zanlungo, S. Recent insights on the role of cholesterol in non-alcoholic fatty liver disease. *Biochim Biophys Acta* **1852**, 1765–78 (2015).

7. Min, H.-K. *et al.* Increased hepatic synthesis and dysregulation of cholesterol metabolism is associated with the severity of nonalcoholic fatty liver disease. *Cell Metab* **15**, 665–74 (2012).

8. Nault, R., Fader, K. A., Lydic, T. A. & Zacharewski, T. R. Lipidomic Evaluation of Aryl Hydrocarbon Receptor-Mediated Hepatic Steatosis in Male and Female Mice Elicited by 2,3,7,8-Tetrachlorodibenzo-p-dioxin. *Chem Res Toxicol* **30**, 1060–1075 (2017).

9. Nault, R. *et al.* Dose-Dependent Metabolic Reprogramming and Differential Gene Expression in TCDD-Elicited Hepatic Fibrosis. *Toxicol Sci* **154**, 253–266 (2016).

10. Jurgelewicz, A. *et al.* Genetics-Based Approach to Identify Novel Genes Regulated by the Aryl Hydrocarbon Receptor in Mouse Liver. *Toxicol Sci* **181**, 285–294 (2021).

11. Baigent, C. *et al.* Efficacy and safety of more intensive lowering of LDL cholesterol: a meta-analysis of data from 170 000 participants in 26 randomised trials. *The Lancet* **376**, 1670–1681 (2010).

12. Schonewille, M. *et al.* Statins increase hepatic cholesterol synthesis and stimulate fecal cholesterol elimination in mice. *J Lipid Res* **57**, 1455–1464 (2016).

13. ZHOU, L., LI, C., GAO, L. & WANG, A. High-density lipoprotein synthesis and metabolism (Review). *Mol Med Rep* **12**, 4015–4021 (2015).

14. Maurice, J. & Manousou, P. Non-alcoholic fatty liver disease. *Clinical Medicine* **18**, 245–250 (2018).

15. Dowman, J. K., Tomlinson, J. W. & Newsome, P. N. Pathogenesis of non-alcoholic fatty liver disease. *QJM* **103**, 71–83 (2010).

16. Athyros, V. G. *et al.* Statins: An Under-Appreciated Asset for the Prevention and the Treatment of NAFLD or NASH and the Related Cardiovascular Risk. *Curr Vasc Pharmacol* **16**, 246–253 (2018).

17. Balakumar, P. & Mahadevan, N. Interplay between statins and PPARs in improving cardiovascular outcomes: a double-edged sword? *Br J Pharmacol* **165**, 373–9 (2012).

18. Wilson, L. H. *et al.* Liver Glycogen Phosphorylase Deficiency Leads to Profibrogenic Phenotype in a Murine Model of Glycogen Storage Disease Type VI. *Hepatol Commun* **3**, 1544–1555 (2019).

19. Thapar, M., Russo, M. W. & Bonkovsky, H. L. Statins and liver injury. *Gastroenterol Hepatol (N Y)* **9**, 605–6 (2013).

20. Fernandez-Salguero, P. M., Hilbert, D. M., Rudikoff, S., Ward, J. M. & Gonzalez, F. J. Aryl-hydrocarbon receptor-deficient mice are resistant to 2,3,7,8-tetrachlorodibenzo-p-dioxin-induced toxicity. *Toxicol Appl Pharmacol* **140**, 173–9 (1996).

21. Pierre, S. *et al.* Aryl hydrocarbon receptor-dependent induction of liver fibrosis by dioxin. *Toxicol Sci* **137**, 114–24 (2014).

Chapter 4: Characterizing the Impact of Simvastatin on TCDD-Induced Liver Injury

This chapter is an edited version of a manuscript submitted for publication that is currently under review.

Authors: Amanda Jurgelewicz[1,2], Rance Nault[2,3], Jack Harkema[1,4], Tim Zacharewski[2,3] and John J. LaPres[2,3].

Affliations: [1]Department of Pharmacology and Toxicology, Michigan State University; [2]Institute for Integrative Toxicology, Michigan State University; [3]Department of Biochemistry and Molecular Biology, Michigan State University; [4]Department of Pathobiology and Diagnostic Investigation, Michigan State University

Abstract

In Chapter 3, the results indicated that HMG-CoA reductase repression plays a role in TCDD-induced liver injury, and co-treating mice with TCDD and simvastatin impacted liver injury in a sex-specific manner. In males, co-treatment led to induction of AHR battery genes and higher levels of ALT suggesting that simvastatin co-treatment exacerbates AHR-mediated, TCDD-induced liver injury. The aim of this study was to deduce a possible mechanism(s) for this increased liver injury using single-nuclei RNA sequencing (snRNAseq) in mouse liver. We demonstrated that co-treated mice experienced wasting and increased AHR activation compared to TCDD alone. Furthermore, relative proportions of cell (sub)types were different between TCDD alone and co-treated mice including important mediators of NAFLD progression. Analysis of non-overlapping differentially expressed genes identified several pathways where simvastatin co-treatment significantly impacted TCDD-induced changes, which may explain the differences between treatments. Overall, these results demonstrate how simvastatin can impact the liver in the context of toxicant-induced liver injury.

Introduction

In the study outlined in chapter 3, we showed that HMGCR repression does play a role in TCDD-induced liver injury.[1] Interestingly, we also saw that simvastatin and TCDD (T+S) co-treatment appeared to exacerbate AHR-mediated, TCDD-induced liver injury in male mice compared to TCDD treatment alone.[1] Although statin drugs have been suggested as a potential therapy for NAFLD with their lipid-lowering and anti-inflammatory effects, this result suggested that people who may be exposed to AHR ligands could be at risk of additional injury instead.[2,3] As millions of people take statins, it's important to confirm if simvastatin puts a vulnerable population at greater risk of injury.

The goal of this study was to confirm if simvastatin does exacerbate liver injury, and if so, how this may be occurring. A previous report showed that snRNAseq can be used to identify TCDD-induced alterations in relative proportions of various liver cell (sub)types and changes in cell-specific gene expression.[4] Therefore, snRNAseq was utilized in this study to investigate how simvastatin co-treatment may impact distinct liver cell (sub)types differently than TCDD alone. Male C57Bl/6J mice were treated with TCDD (30 μg/kg) or simvastatin (500 mg/kg food), and liver tissue was used for snRNAseq. The materials and methods for this study can be found in Chapter 6. The results suggested that when TCDD and T+S-treated mice were compared, there were changes in the relative proportions of liver cell (sub)types that are important mediators of NAFLD progression, such as hepatocytes and macrophages. Additionally, there were several treatment-group-specific differentially expressed genes associated with NAFLD pathways. Although distinct markers of liver injury were not significantly different, there was wasting and lethality associated with co-treatment. These results demonstrate that simvastatin may impact liver injury severity

in the context of toxicant-induced liver injury via decreasing the inflammatory response; however, it also suggests that vulnerable populations may be at risk of other adverse effects.

Results

Simvastatin Co-Treatment Exacerbates TCDD-Induced Toxicity

To characterize the impact of simvastatin on TCDD-induced liver injury, mice were treated with TCDD (30 μg/kg) every 4 days for 28 days in the presence or absence of simvastatin (~80 mg/kg body weight/day). Notably, this treatment paradigm was different from the study conducted in Chapter 3 where mice were treated with TCDD (10 μg/kg) for 10 consecutive days. This new treatment paradigm is a well-established model of progressive liver injury that has been shown to induce steatohepatitis with fibrosis at this dose.[4–7] Also, it compensates for the half-life differences of TCDD in humans vs. mice, the short duration of the study considering the bioaccumulative nature of AHR ligands, and it considers the potential cumulative lifetime exposure from diverse AHR ligands.[8–11] Our previous study design resulted in a cumulative dose of TCDD higher than what would be expected for an environmentally relevant exposure, so the dosing schematic was altered to take that into consideration for this study.

During the course of this study, co-treated mice were more severely impacted by their treatment compared to TCDD or simvastatin alone. Simvastatin alone did not impact weight gain compared to control, but there was a difference seen in TCDD alone vs. T+S treatment (Figure 4.1A). TCDD reduced weight gain after 5 doses, while T+S treatment reduced weight gain after only 3 doses with wasting after 4 doses (Figure 4.1A). Unexpectedly, co-treatment also resulted in 2 deaths over the course of the study.

We hypothesized that the wasting was due to increased liver injury in co-treatment compared to TCDD alone as we saw in our previous study. Interestingly, while failure to thrive was exacerbated by co-treatment, there was no difference in liver damage severity. Neither serum ALT levels nor liver weights between TCDD and co-treated groups were significantly different (Figure 4.1B- C). Notably, one mouse had much higher serum ALT compared to the other mice in the co-treated group, and although it was not a significant outlier, the other T+S-treated mice, on average, had significantly lower ALT levels compared to TCDD alone (Figure 4.1B). Furthermore, histopathology between TCDD and T+S-treated mice were also comparable. TCDD induced widespread vacuolization (score 4) with hepatocellular hypertrophy (score 4) and mild mixed inflammatory cell infiltrate (score 2) with minimal necrosis (Figure 4.1D). Lesions were most severe in periportal regions. Co-treatment elicited similar lesions in both character and severity to TCDD-treated mice with the addition of mild biliary hyperplasia besides 1 mouse that did not have biliary hyperplasia and had minimal vacuolization (score 1) and mild-moderate necrosis (score 2-3) (Figure 4.1D). Apart from this one mouse, which was not the mouse with higher ALT levels, all other mice had the same pathologies and severity scoring as the other mice in their respective treatment groups. No significant histopathology lesions were observed in control or simvastatin-treated mice.

Figure 4.1: Simvastatin co-treatment induces wasting. (A) The average body weight of the mice in each respective group measured every 3 days. (B) Measured alanine aminotransferase (ALT) levels (U/L) in serum for each treatment. (C) Corrected liver weight (mg of liver/kg body weight) for each treatment. (D) Representative H&E-stained liver samples for each treatment. Scale bar = 100 µm. Asterisks indicate statistical significance compared to respective control group: * ($P \leq 0.05$), ** ($P \leq 0.01$). Pound symbol indicates statistical significance between TCDD and T+S groups: # ($P \leq 0.05$). $N \geq 5$ mice per treatment group.

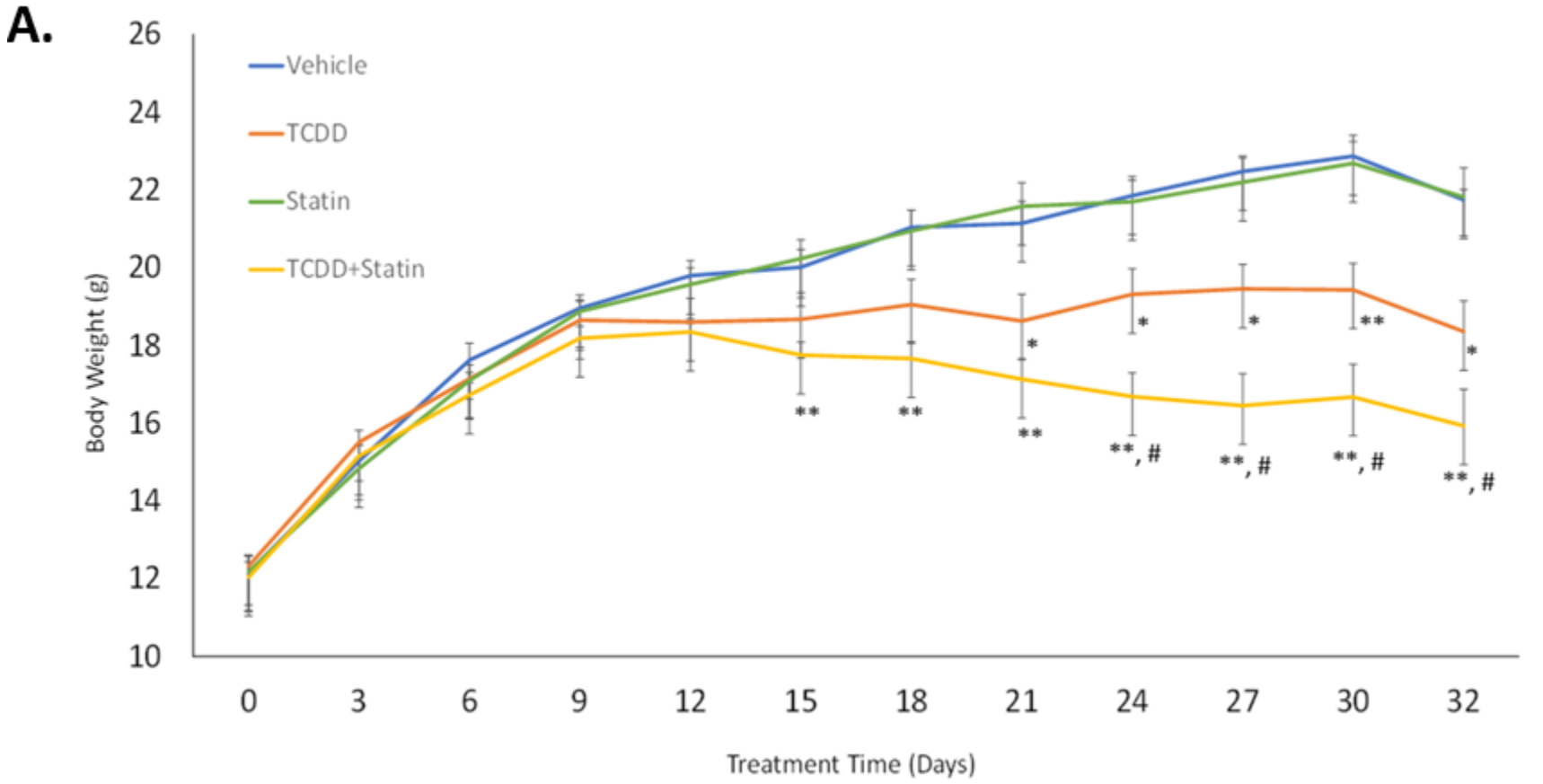

Figure 4.1 (cont'd)

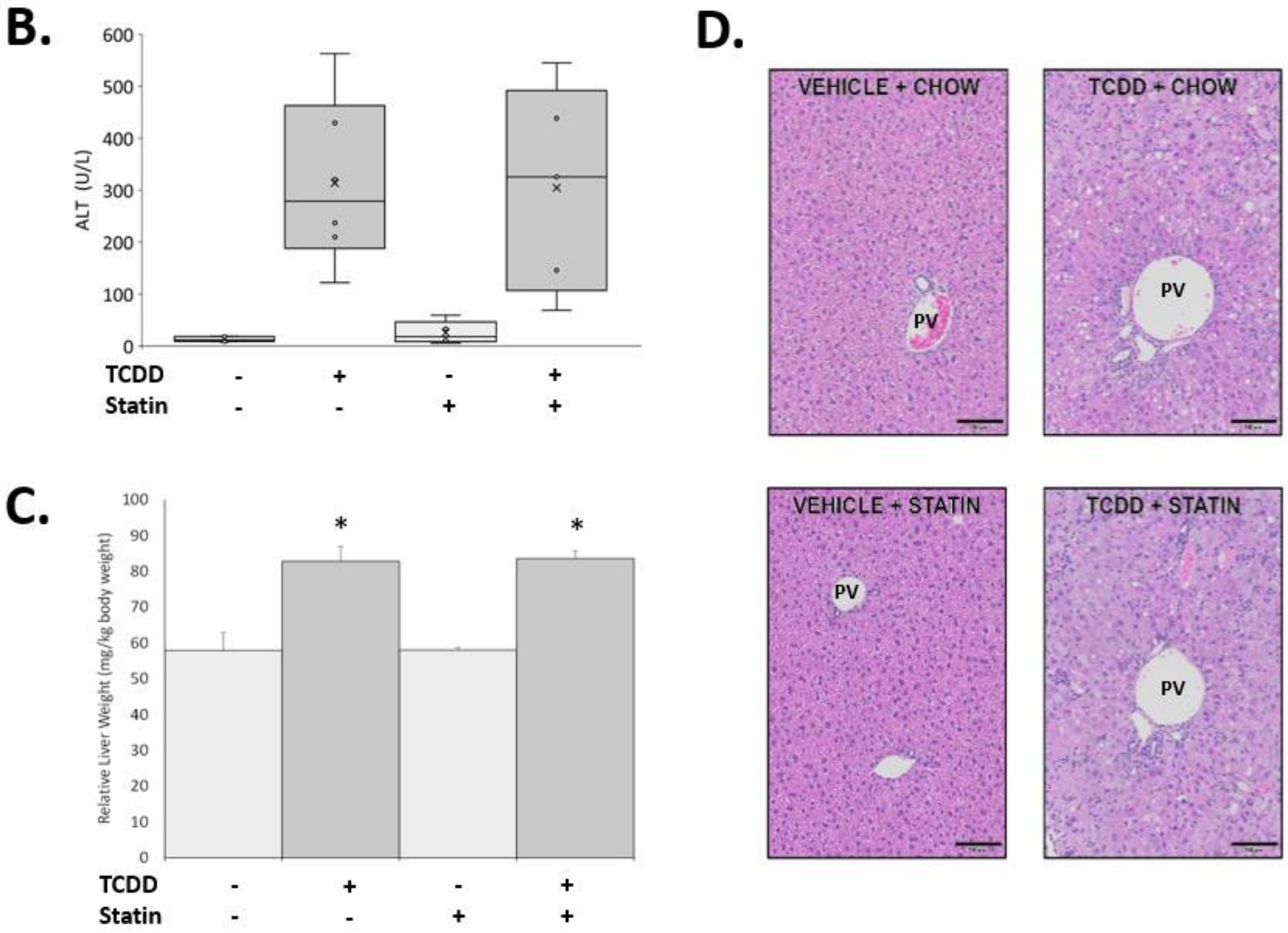

snRNAseq Suggests Differences in Liver Cell Type Proportions Between Treatments

Although T+S-treatment elicited no significant changes in liver pathology using this treatment paradigm compared to TCDD alone, we hypothesized that hepatic cell type and cell-specific gene expression changes may partially explain the increased T+S-toxicity. Furthermore, statin drugs have been suggested to be a treatment option for NAFLD, so we wanted to validate if simvastatin may be exhibiting any lipid-lowering or anti-inflammatory gene expression changes by evaluating how simvastatin co-treatment impacts distinct liver cell types compared to TCDD alone.

A total of 83,229 nuclei (average per group) were analyzed using snRNAseq, and relative proportions of liver cell nuclei clusters across treatments were identified. Simvastatin alone did not alter cell type proportions compared to control mice (Figure 4.2A-B). TCDD alone did elicit shifts in 7 of 10 cell types identified including an increase in macrophages (2.3% to 28.4%), B cells (3.1% to 10.6%) and T cells (2.2% to 7.6%) (Figure 4.2B). This is consistent with previous reports using snRNAseq data as well as F4/80 staining of TCDD-treated liver sections.[4,6,12]

T+S elicited shifts in proportions for 8 of 10 cell types identified compared to control mice, including the same 7 cell types impacted by TCDD alone (Figure 4.2A-B). However, the proportions of B cells, cholangiocytes, centrilobular region (central) hepatocytes and periportal region (portal) hepatocytes differed between TCDD alone and co-treatment. Although co-treated mice had a smaller proportion of central (7.5 to 5.9%) and portal (67.6 to 37.3%) hepatocytes compared to control, this was increased compared to TCDD alone (3.5% and 22.9%, respectively) (Figure 4.2B). There was a large increase in the macrophage population in co-treated mice (2.3% to 20.2%) compared to control as well. However, the 8.2% difference between TCDD alone and

T+S-treated mice was not significant due to one sample driving larger error in the co-treated group. Interestingly, the proportion of liver dendritic cells only increased in the co-treated mice (2.1%) compared to control (0.3%), statin alone (0.3%) and TCDD alone (0.8%) (Figure 4.2B). These results indicated that simvastatin co-treatment was promoting less immune cell infiltration compared to TCDD alone.

Figure 4.2: TCDD alone and T+S co-treatment impact relative liver cell type proportions differently. (A) UMAP visualization of nuclei isolated from livers of mice treated with vehicle control, TCDD alone, simvastatin alone or T+S, clustered based on gene expression profile similarity. (B) Relative proportions of each cell type for each treatment group. Letters indicated statistical significance ($P \leq 0.05$) in comparison to control (a), TCDD alone (b) or simvastatin (c). N=3 mice per treatment group.

A.

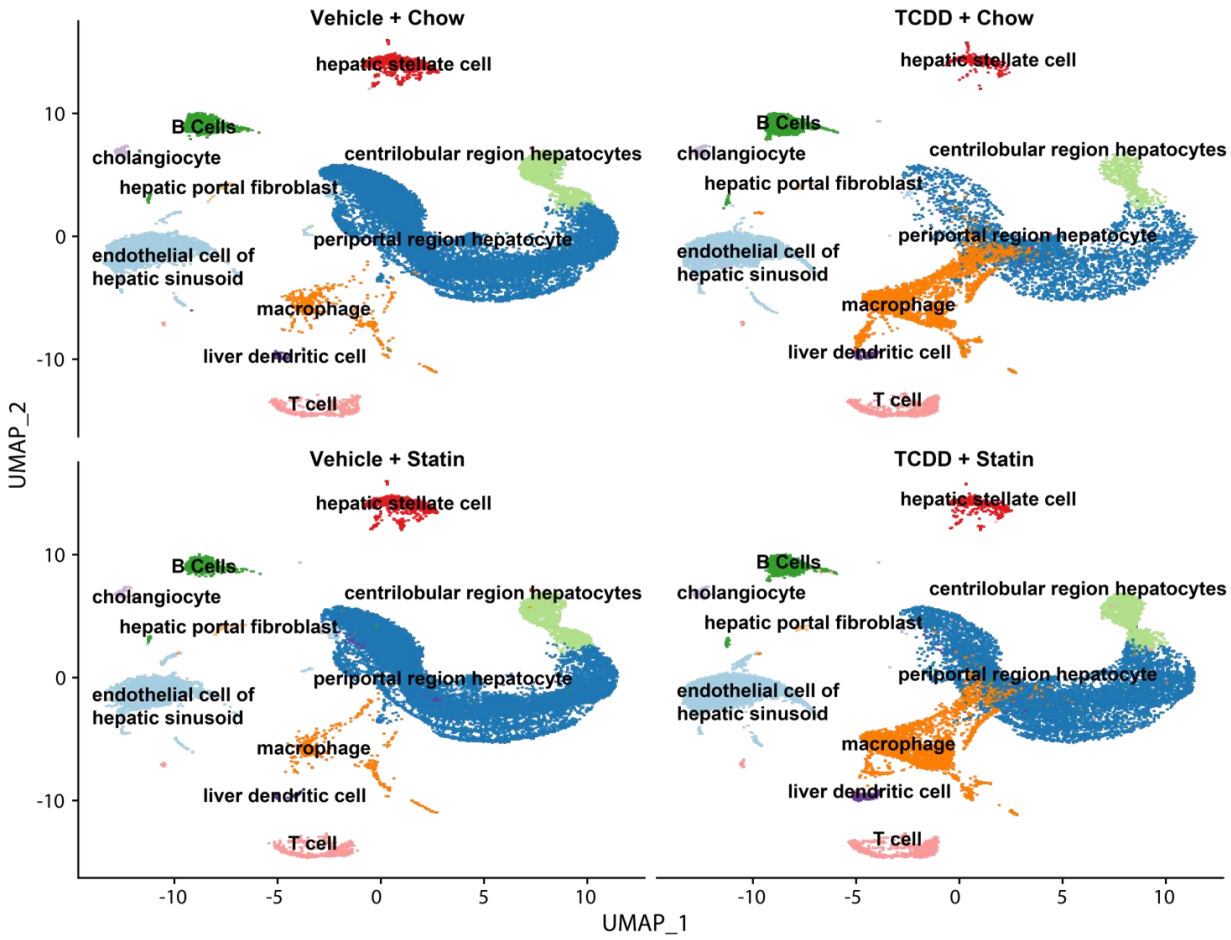

Figure 4.2 (cont'd)

B.

Cell Type	Relative Proportion (%)			
	Control	TCDD	Statin	TCDD + Statin
B Cells	3.1 ± 0.8	10.6 ± 0.1[a]	2.1 ± 0.1	6.5 ± 0.1[a,b,c]
Cholangiocytes	0.7 ± 0.1	1.8 ± 0.1[a]	0.6 ± 0.1	1.2 ± 0.1 [a,b,c]
Central Hepatocytes	7.5 ± 0.2	3.5 ± 0.3[a]	7.0 ± 0.5	5.9 ± 0.4[a,b]
Portal Hepatocytes	67.6 ± 3.3	22.9 ± 4.2[a]	66.3 ± 3.8	37.3 ± 2.2[a,b,c]
Macrophages	2.3 ± 0.2	28.4 ± 1.0[a]	2.1 ± 0.7	20.2 ± 4.0[a,c]
Endothelial Cell of Liver Sinusoid	10.4 ± 0.5	21.9 ± 1.8[a]	11.8 ± 2.2	20.2 ± 1.5[a]
Liver Dendritic Cells	0.3 ± 0.1	0.8 ± 0.0	0.3 ± 0.1	2.1 ± 0.2[a,b,c]
Hepatic Portal Fibroblasts	0.5 ± 0.1	0.4 ± 0.2	0.6 ± 0.2	0.2 ± 0.0
Heaptic Stellate Cells	5.4 ± 1.6	2.1 ± 0.1	7.4 ± 1.0	2.3 ± 0.8[c]
T Cells	2.2 ± 0.3	7.6 ± 1.0[a]	1.9 ± 0.3	6.3 ± 0.3[a,c]

Comparing Changes in Portal Hepatocytes Between TCDD alone and T+S Treatment

The relative proportion of portal hepatocytes was significantly different between TCDD treatment (22.9%) compared to T+S treatment (37.3%) (Figure 4.2B). Hepatocytes, in general, are the first major cell type disrupted in NAFLD due to fat accumulation.[13,14] However, portal hepatocytes, or hepatocytes near the portal triad, are particularly important as TCDD exposure initially exhibits periportal toxicity in the liver.[4,15] Furthermore, cholesterol biosynthesis, which is impacted by both TCDD and statin exposure, primarily takes place in portal hepatocytes.[16–18] Therefore, we hypothesized that there may be alterations in differentially expressed genes (DEGs) in portal hepatocytes between TCDD alone and co-treated mice that may influence processes like the development of steatosis.

As expected, TCDD treatment resulted in decreased gene expression in many enzymes involved in cholesterol biosynthesis compared to control such as *Hmgcs1, Fdft1* and *Cyp51* (Figure 4.3). Furthermore, TCDD treatment also decreased expression of other genes involved in cholesterol homeostasis including genes used in cholesterol re-uptake (*Ldlr*) and cholesterol efflux (*Abca1*) (Figure 4.3). The enzymes involved in cholesterol biosynthesis were more upregulated in co-treated mice compared to TCDD alone (Figure 4.3). In contrast, genes such as *Srebf2*, which regulates cholesterol homeostasis, had significantly lower expression in co-treated mice compared to simvastatin alone (Figure 4.3).

Figure 4.3: Cholesterol homeostasis gene expression. Dot plot of genes involved in cholesterol biosynthesis and homeostasis in portal hepatocytes. Colors indicate significant differences in expression between treatment groups (P ≤ 0.05): green (control); blue (control and TCDD alone); yellow (control and statin alone); gray (TCDD alone and statin alone); and peach (control, TCDD alone and statin alone). N=3 mice per treatment group.

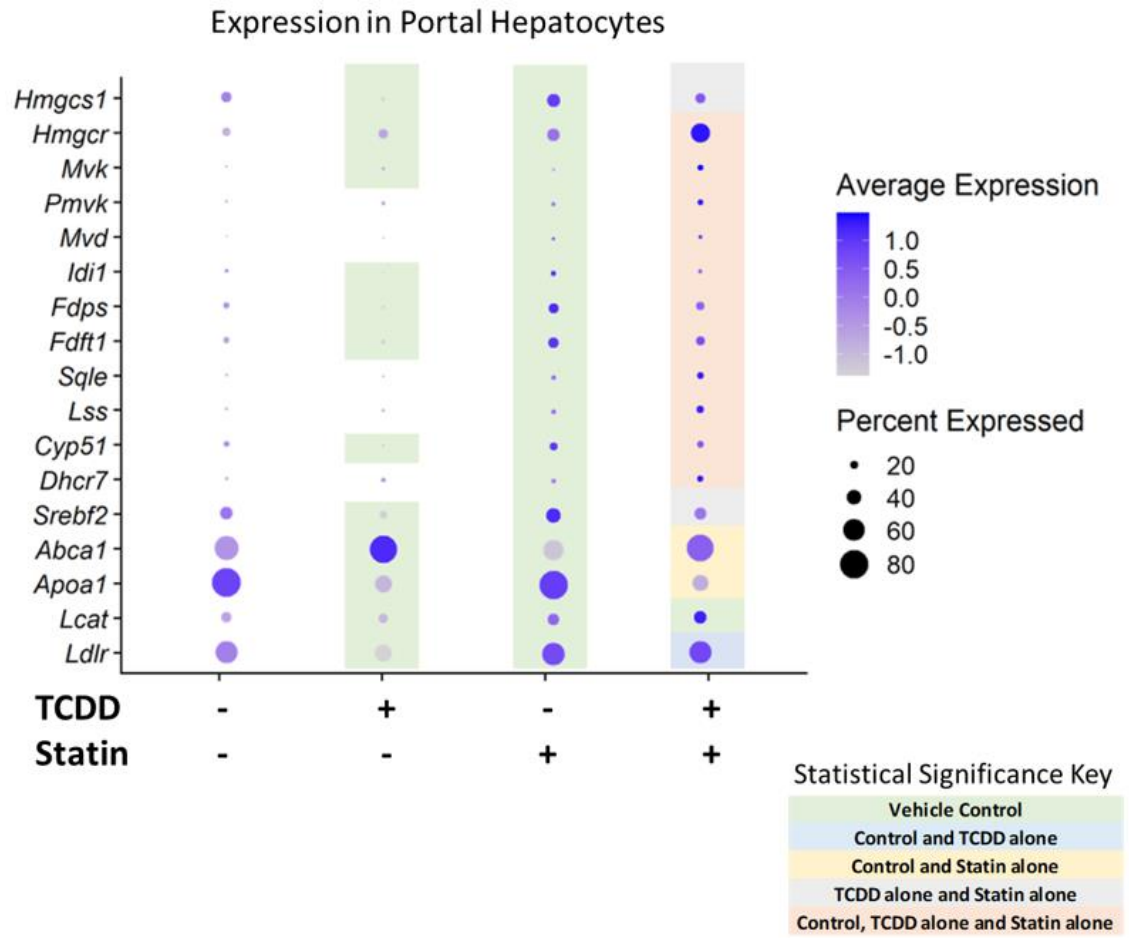

Although there was a difference in the relative proportion of portal hepatocytes between TCDD alone and co-treated mice, the majority of DEGs between these two groups were the same compared to control (Figure 4.4A). However, a large portion of these DEGs had expression levels that were different when comparing co-treatment to TCDD alone, including transporters like *Slco1a4* and enzymes involved in metabolism like *Cyp4a14* (Figure 4.4B). DAVID analysis of these DEGs with different expression levels indicated that pathways involving lipid and cholesterol metabolism were more upregulated in T+S treatment compared to control. This is consistent with the study outlined in Chapter 3 where T+S-treated mice had significantly reduced fat content in the liver.[1]

Non-overlapping DEGs in the TCDD alone and T+S-treated mice groups were also assessed. DAVID analysis indicated that there were unique DEGs in both treatment groups that were involved in lipid metabolism (Figure 4.4C-D). The genes involved in this cluster in the TCDD-treated group, such as *Elovl6*, were downregulated (Figure 4.4C). Notably, *Hmgcs1* and *Srebf2* are also represented in this cluster, which supports the importance of cholesterol homeostasis in TCDD-induced liver injury (Figure 4.4C). In contrast, the genes involved in the lipid metabolism cluster in co-treated mice were upregulated (Figure 4.4D). The non-overlapping genes associated with the lipid metabolism clusters in both groups as well as the changes in expression of shared DEGs involving lipid metabolism between treatment groups may play an important role in differences previously seen in fat accumulation (Figure 4.4B-D).[1] It is possible that the upregulation of genes involved in lipid metabolism may be protective against hepatocyte injury (i.e. lower ALT levels) that was seen in most, but not all, of the T+S-treated mice as this could lead to less fat accumulation like we saw in our previous study (Figure 4.1B). [1]

Figure 4.4: Simvastatin co-treatment impacts pathways involved in lipid metabolism differently than TCDD alone. (A) Venn diagram of the statistically significant (P ≤ 0.05) differentially expressed genes (DEGs) compared to control that are shared between treatment groups. (B) Volcano plot representing the significant DEGs compared to control that were shared between TCDD and T+S treatments where the fold changes for both treatments were also significantly different from each other. The plot shows the $\log_2$ fold change of these DEGs for both TCDD (blue) and T+S (orange) corresponding to their respective p-values. (C) Dot plot of DEGs in the DAVID cluster involving lipid metabolism in TCDD-treated mice. (D) Dot plot of the DEGs in the DAVID cluster involving lipid metabolism in T+S-treated mice. Colors indicate statistical significance (P ≤ 0.05) in expression between treatment groups: green (vehicle); blue (vehicle and TCDD alone); gray (TCDD alone and statin alone) and peach (vehicle, TCDD alone and statin alone). N=3 mice per treatment group.

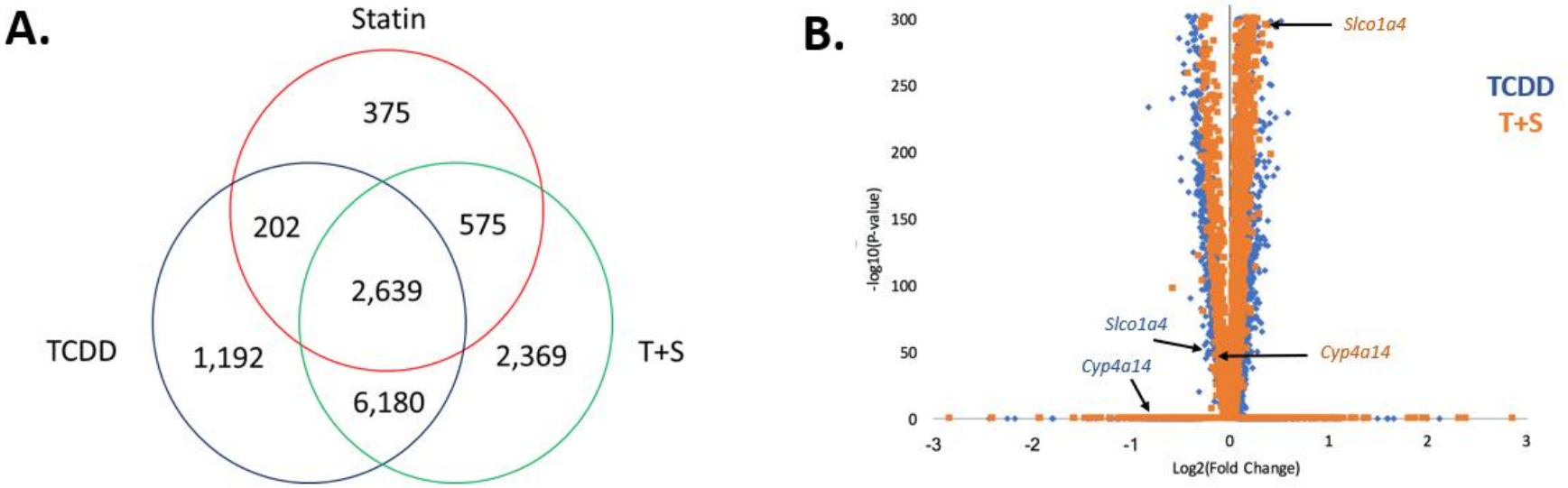

Figure 4.4 (cont'd)

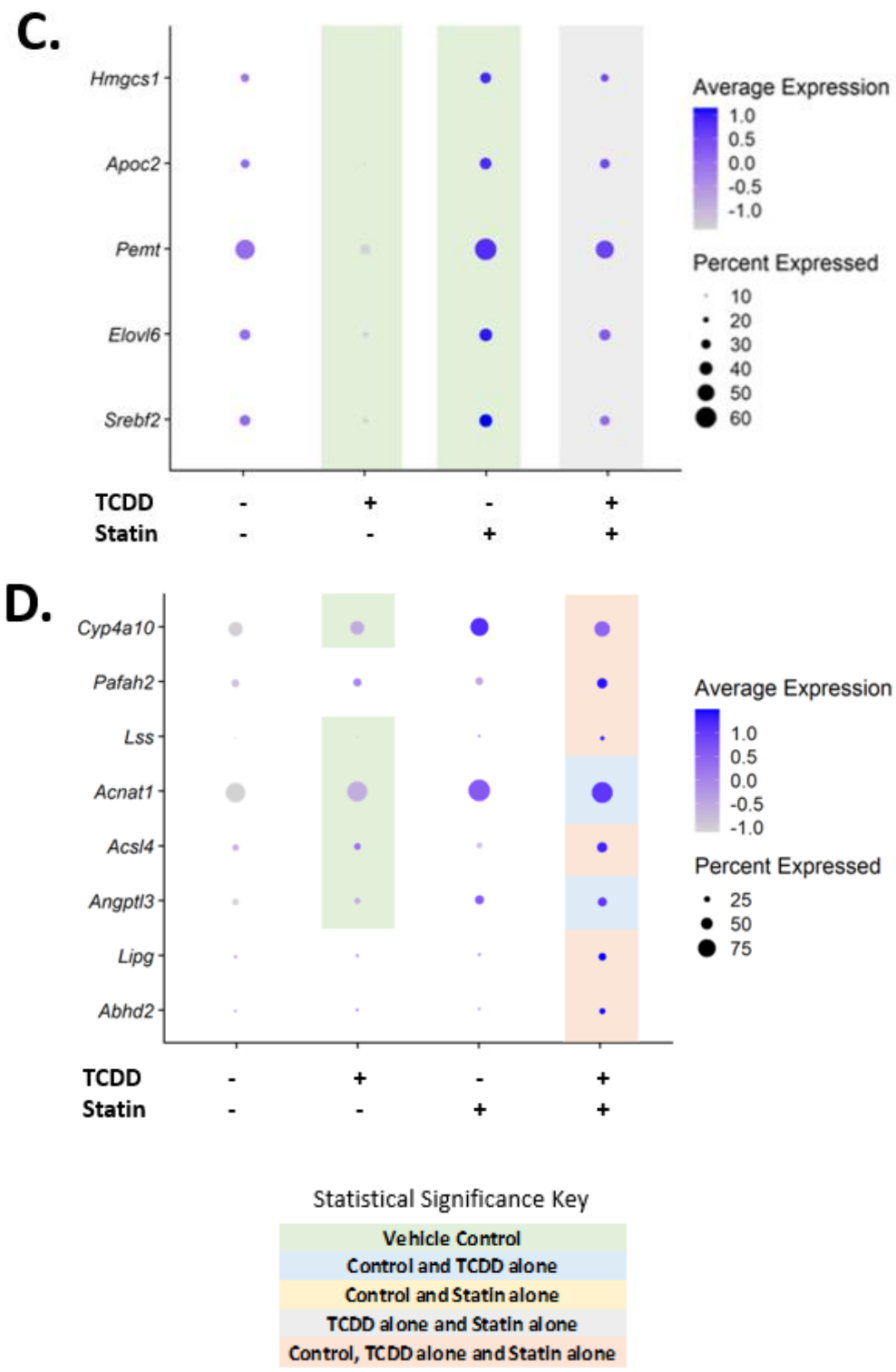

Comparing Changes in Immune Cell Populations Between TCDD alone and T+S Treatment

NAFLD progresses due to the presence of inflammation that is largely controlled by macrophages.[13,14] Hepatic lipid accumulation in hepatocytes can trigger immune cell infiltration and subsequent pro-inflammatory responses.[13,14] Although the relative proportion of macrophages was not significantly different between TCDD alone (28.4%) and T+S-treated (20.2%) mice, simvastatin tended to limit immune cell recruitment or proliferation (Figure 4.2A-B). Due to inflammation being important for liver injury progression, we hypothesized that changes in DEGs in macrophages may also play a role in the differences in immune cell infiltration between treatments.

The majority of DEGs in macrophages were the same between TCDD alone and T+S-treated mice compared to control; however, a portion of these shared DEGs had expression that was different when comparing co-treatment to TCDD alone including genes involved in immune signaling like *Cd74* or *Adk* (Figure 4.5A-B). DAVID analysis of this group of genes indicated that immune system signaling was more repressed following co-treatment compared to TCDD alone. In contrast, unique DEGs in TCDD alone-treated mice associated with the immune response were upregulated (Figure 4.5C). Notably, a portion of these genes were specifically associated with activation of the NF-κB signaling pathway including *Prkcb, Nfkb1* and *Nlrp3* (Figure 4.5C). NF-κB signaling in macrophages may play an important role in TCDD-induced liver injury via NLRP3 inflammasome activation, which has been previously associated with the progression of steatosis to steatohepatitis. [19]

Figure 4.5: Simvastatin co-treatment impacts pathways involved in inflammation differently than TCDD alone. (A) Venn diagram of the statistically significant (P ≤ 0.05) differentially expressed genes (DEGs) shared between treatment groups in macrophages. (B) Volcano plot representing the significant DEGs compared to control that were shared between TCDD and T+S treatments where the fold changes for both treatments were also significantly different from each other. The plot shows the $\log_2$ fold change of these DEGs for both TCDD (blue) and T+S (orange) corresponding to their respective p-values. (C) Dot plot of genes associated with NF-κB signaling in macrophages in TCDD-treated mice. (D) Dot plot of genes in the immune pathway cluster in T+S-treated mice for liver dendritic cells. Colors indicate statistically significant (P ≤ 0.05) differences in expression between treatment groups: green (vehicle); gray (TCDD alone and statin alone) and pink (TCDD alone). N=3 mice per treatment group.

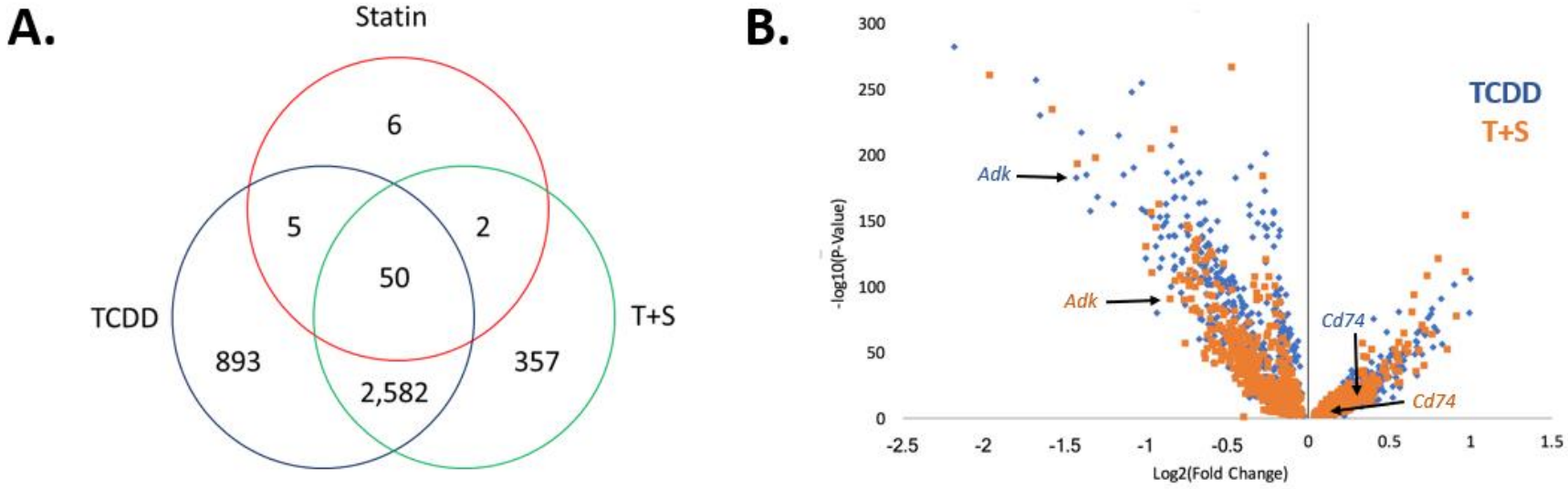

Figure 4.5 (cont'd)

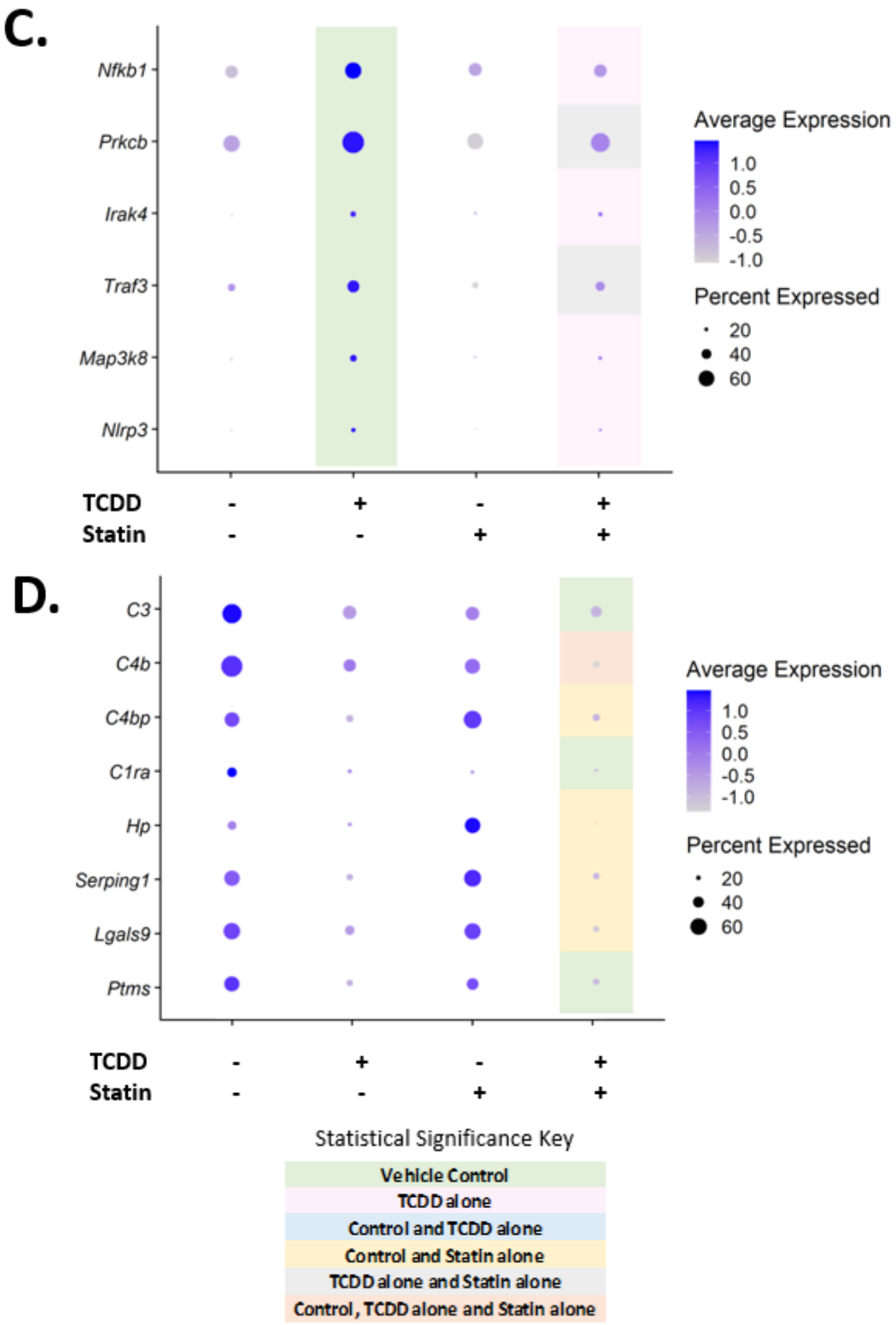

A particularly interesting result of this study was that the proportion of liver dendritic cells significantly increased only in T+S mice (Figure 4.2B). Hepatic dendritic cells can act as a bridge between the innate and adaptive immune process.[20] They have been shown to act as either perpetuators of inflammation in chronic inflammatory states, or interestingly, they can act as protective cells and avoid triggering inflammatory cascades.[20] DAVID analysis of non-overlapping DEGs in liver dendritic cells indicated that immune response, particularly regarding the complement system, was downregulated in co-treatment (Figure 4.5D). Activation of the complement system is involved in immune cell recruitment, so repression of this pathway may be important for the differences seen in the proportion of immune cells between TCDD alone and co-treatment (Figures 4.2B, 4.5D). Furthermore, activation of the complement system is associated with disease severity in humans with NAFLD, so this pathway could also be important for NAFLD severity in rodents.[21] Although liver dendritic cells are a rarer cell type in the liver (Figure 4.2B), they may play an important role in this process.

AHR Activation and Hepatic Signatures of Muscle Wasting

Given the essential role that AHR activation plays in TCDD-induced injury, the impact of simvastatin co-treatment on AHR activation was explored. *Ahr* expression is highest primarily in hepatocytes compared to other liver cell (sub)types, and interestingly, its expression is significantly higher in T+S treated mice compared to TCDD alone in portal hepatocytes (Figure 4.6A-B). The increase *in Ahr* expression also correlates with increased AHR-mediated gene expression, such as *Cyp1a1* and *Cyp1a2* (Figure 4.6B). This trend was also seen in macrophages, but to a lesser degree (Figure 4.6B). Increased expression of AHR battery genes following co-

treatment was also seen in the previous study outlined in Chapter 3.[1] Consequently, increased AHR activity may be involved in the worse prognosis seen in co-treated mice.

Figure 4.6: Simvastatin co-treatment induces AHR activity. (A) UMAP visualization of *Ahr* expression in all nuclei for TCDD and T+S-treated mice. (B) Dot plot of AHR and AHR target gene expression in portal hepatocytes and macrophages. (C) Dot plot of gene expression of GH/IGF-1 axis marker genes in portal hepatocytes. Colors indicate statistical significance ($P \leq 0.05$) in expression between treatment groups: green (vehicle); blue (vehicle and TCDD alone); and orange (vehicle, TCDD alone and statin alone). N=3 mice per treatment group.

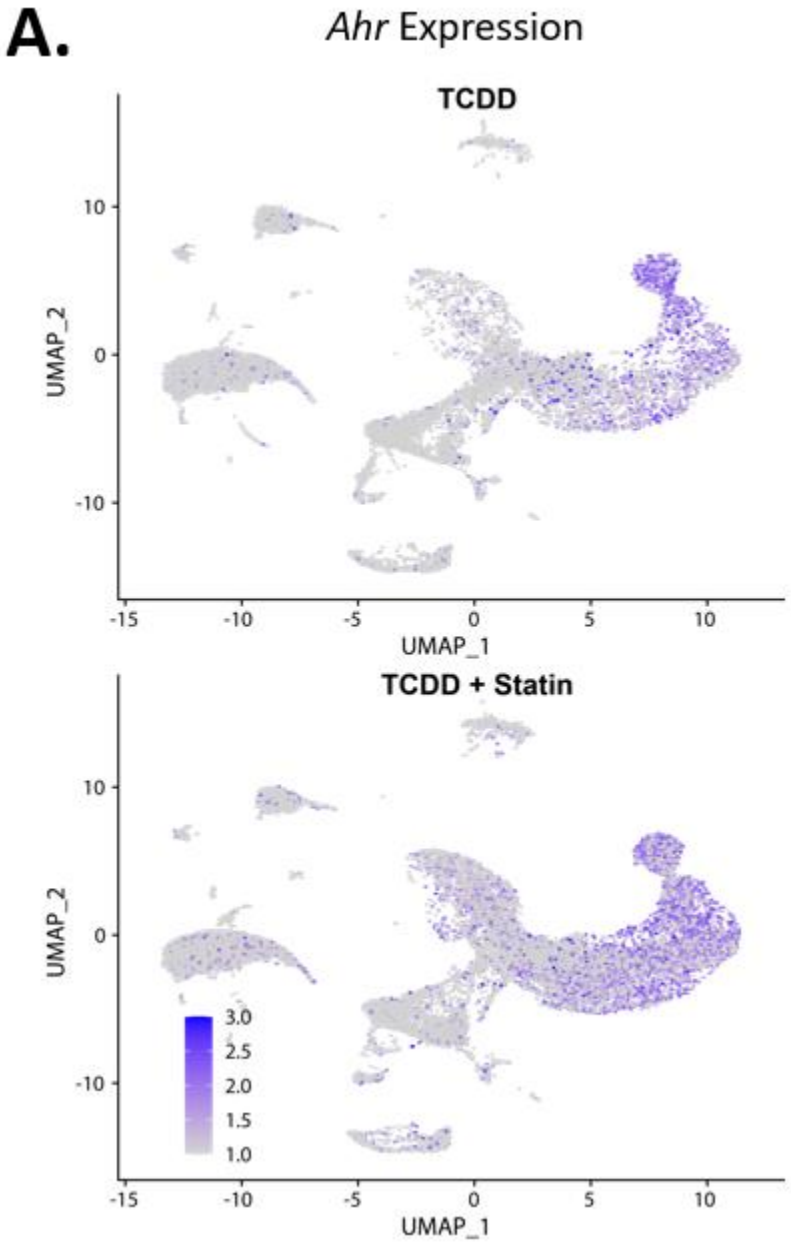

Figure 4.6 (cont'd)

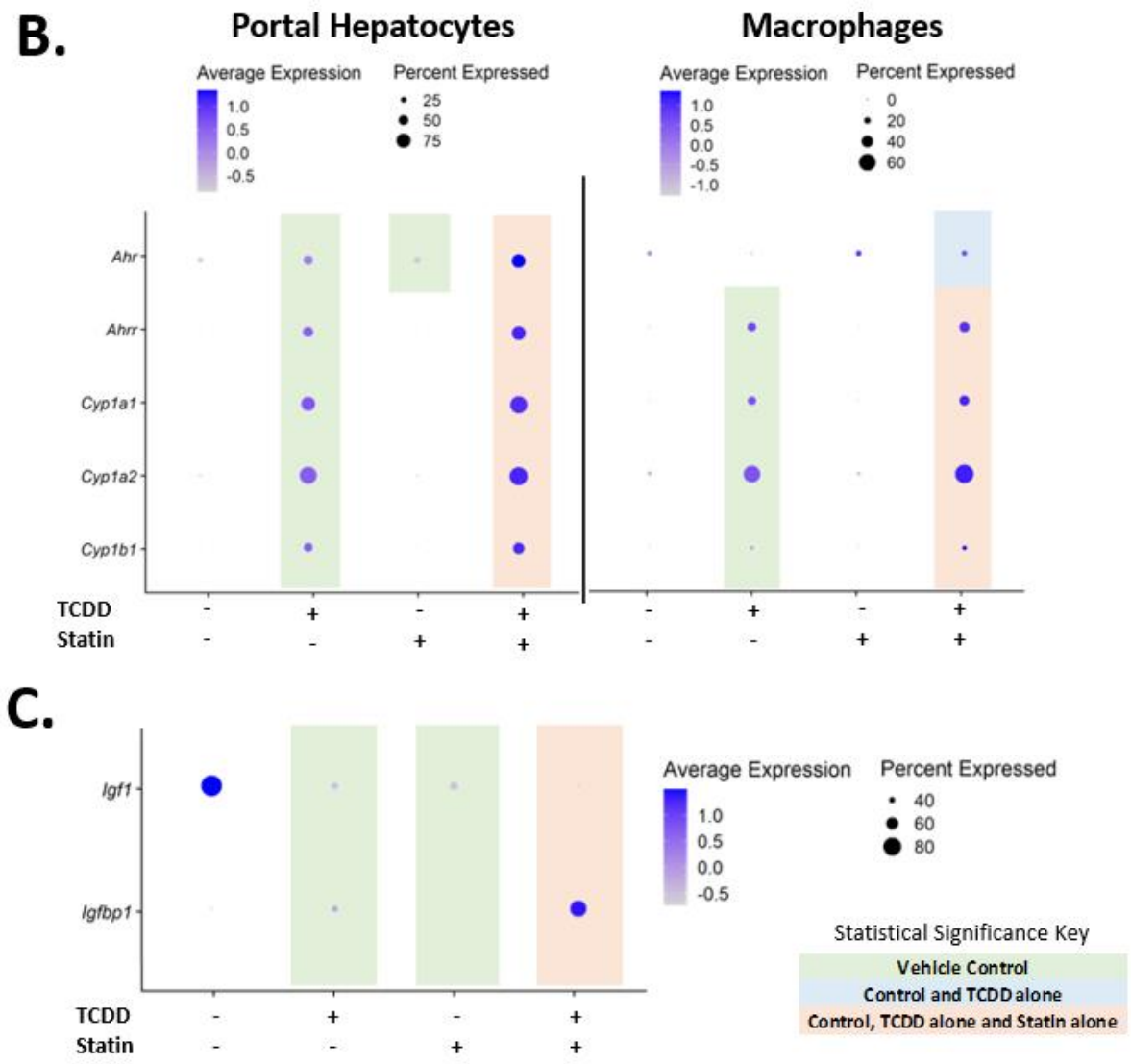

Simvastatin is also linked to muscle pain and muscle damage at high doses or when taken in combination with other drugs.[22] Therefore, we investigated hepatic gene signatures for mechanisms that link AHR activation by TCDD and perturbation by simvastatin to wasting such as the growth hormone (GH) / insulin-like growth factor (IGF)-1 axis. Hepatic steatosis-related alternations in the GH/IGF-1 axis is associated with decreased muscle myofibrillar protein content and muscle strength.[23] Lower IGF1 levels are reported in NAFLD patients, and the liver is the primary organ that contributes to plasma IGF1 concentration.[23,24] *Igf1* expression significantly decreased in T+S mice compared to TCDD alone in portal hepatocytes (Figure 4.6C). A decrease in *Igf1* was also seen in simvastatin alone mice, which corresponds to previous reports.[25] Moreover, overexpression of IGFBP1, a modulator of IGF1 action, is associated with hepatic ER stress, hyperinsulinemia and glucose intolerance.[23,26] *Igfbp1* levels increased in T+S mice compared to TCDD alone (Figure 4.6C) in portal hepatocytes. *Igfbp1* expression has been shown to be upregulated by the AHR in both humans and mice, so an increase in AHR activation in co-treated mice may explain the difference in expression between TCDD and co-treatment.[27,28] While statins have been shown to have no effect on IGFBP-1, there was a small (P=0.04) decrease in expression in the simvastatin alone group compared to control in our study.[25] While these changes in expression are not huge in the liver, skeletal muscle can be examined in future experiments to determine if this possible mechanism is important for the wasting seen in co-treatment.

Discussion

Many studies suggest that simvastatin may be protective against NAFLD. Our study in Chapter 3, however, suggested that simvastatin may exacerbate aspects of TCDD-induced injury. In this study, we aimed to elucidate how simvastatin may exacerbate TCDD-induced liver injury using snRNAseq in mouse liver tissue to determine how treatment may be impacting specific liver cell (sub)types differently than TCDD alone. Co-treatment with simvastatin in this study impacted gene expression in pathways involved in liver injury differently, which may explain differences in pathology between TCDD and co-treated mice seen in Chapter 3. For example, portal hepatocyte snRNAseq signatures suggested that differential expression of key genes encoding proteins important for lipid homeostasis, such as the induction of PPARα target genes like *Cyp4a10* only seen in T+S-treated mice, may play a role in steatosis differences in TCDD vs. co-treated male mice, which supports the results seen in Chapter 3.[1]

An important observation in this study was that co-treatment led to wasting and caused the death of 2 mice compared to TCDD alone. However, there was not a significant increase in liver injury with co-treatment, likely due to following a different treatment paradigm in this study compared to our previous one. While the liver is a key organ impacted by treatment, increased wasting and lethality in co-treated mice are likely due to systemic effects that may also involve other tissues. Due to restrictions at the time this study was conducted, other tissue was not able to be collected to fully address this outcome, so the hepatic snRNAseq results may not solely explain the T+S pathology. However, co-treatment appears to impact the GH/IGF-1 axis, which may impact the liver with subsequent effects on muscle protein and strength. Specifically, differences in hepatic *Igf1* and *Igfbp1* expression between TCDD and co-treatment suggests that

decreased IGF1 signaling may exacerbate muscle wasting, which can be explored in future studies by looking beyond the liver. Although we were unable to examine other tissue to explain the weight loss in co-treatment, this result does support our findings in Chapter 2 that linked HMGCR to TCDD-induced changes in body weight.[29] As simvastatin also impacts HMGCR directly, co-treatment may exacerbate the impact on body weight changes in mice caused by TCDD exposure, supporting that cholesterol biosynthesis plays an important role in TCDD-induced phenotypes.

Simvastatin co-treatment also exhibited differences in immune cell infiltration evidenced by a decrease in immune cell populations and differences in pro-inflammatory pathways in macrophages compared to TCDD alone. Notably, TCDD-induced macrophage gene expression associated with the NF-κB pathway was not present in co-treatment. NF-κB activation plays an important role in chronic liver injury as pro-inflammatory mediators upregulated by activation of this pathway in macrophages can lead to additional injury to hepatocytes.[30,31] Statin drugs have been shown to lower activity of NF-κB and deactivate the NLRP3 inflammasome.[2] Therefore, the ability of simvastatin to partially inhibit this TCDD-induced upregulation of NF-κB-related genes could lead to a weaker inflammatory response in co-treatment. While immune cell infiltration decreased with co-treatment, the liver dendritic cell population increased. An increase in plasmacytoid dendritic cells (pDCs), for example, is associated with protection against immune-mediated acute liver injury in humans and mice.[32] Furthermore, non-overlapping DEGs in liver dendritic cells in co-treated mice suggested that a decrease in the complement system pathway may play a role in protection against immune-related injury. Complement components are responsible for recruitment of inflammatory cells such as macrophages, and NAFLD severity in patients is correlated with accumulation of several components.[20,21] It is possible that liver

dendritic cell recruitment in co-treatment plays an important role in decreasing macrophage and other immune cell recruitment through inhibition of the complement system.[20,21] The combination of liver dendritic cell recruitment and inhibition of TCDD-induced NF-κB pathway activation in macrophages may explain the differences in immune cell infiltration between treatment groups, which may ultimately influence liver injury severity.

Overall, this study provides additional support for the results of the studies outlined in Chapter 2 and Chapter 3. The snRNAseq results provided more insight on how simvastatin co-treatment impacts distinct liver cell populations, which may influence the severity of TCDD-induced liver injury. This study also further supports that *Hmgcr* is a likely candidate for TCDD-elicited changes in body weight as simvastatin co-treatment induced wasting. Importantly, the results of this study provide more context in how simvastatin could work as a treatment option for NAFLD; however, statins could put vulnerable populations at increased risk of other adverse effects that would need to be further analyzed before recommendation.

REFERENCES

1. Dornbos, P. *et al.* Characterizing the Role of HMG-CoA Reductase in Aryl Hydrocarbon Receptor-Mediated Liver Injury in C57BL/6 Mice. *Sci Rep* **9**, 15828 (2019).

2. Koushki, K. *et al.* Anti-inflammatory Action of Statins in Cardiovascular Disease: the Role of Inflammasome and Toll-Like Receptor Pathways. *Clin Rev Allergy Immunol* **60**, 175–199 (2021).

3. Balakumar, P. & Mahadevan, N. Interplay between statins and PPARs in improving cardiovascular outcomes: a double-edged sword? *Br J Pharmacol* **165**, 373–9 (2012).

4. Nault, R., Fader, K. A., Bhattacharya, S. & Zacharewski, T. R. Single-Nuclei RNA Sequencing Assessment of the Hepatic Effects of 2,3,7,8-Tetrachlorodibenzo-p-dioxin. *Cell Mol Gastroenterol Hepatol* **11**, 147–159 (2021).

5. Nault, R. *et al.* Dose-Dependent Metabolic Reprogramming and Differential Gene Expression in TCDD-Elicited Hepatic Fibrosis. *Toxicol Sci* **154**, 253–266 (2016).

6. Fader, K. A. *et al.* 2,3,7,8-Tetrachlorodibenzo-p-dioxin (TCDD)-elicited effects on bile acid homeostasis: Alterations in biosynthesis, enterohepatic circulation, and microbial metabolism. *Sci Rep* **7**, 5921 (2017).

7. Nault, R., Fader, K. A., Lydic, T. A. & Zacharewski, T. R. Lipidomic Evaluation of Aryl Hydrocarbon Receptor-Mediated Hepatic Steatosis in Male and Female Mice Elicited by 2,3,7,8-Tetrachlorodibenzo-p-dioxin. *Chem Res Toxicol* **30**, 1060–1075 (2017).

8. Sorg, O. *et al.* 2,3,7,8-tetrachlorodibenzo-p-dioxin (TCDD) poisoning in Victor Yushchenko: identification and measurement of TCDD metabolites. *Lancet* **374**, 1179–85 (2009).

9. Wolfe, W. H. *et al.* Determinants of TCDD half-life in veterans of operation ranch hand. *J Toxicol Environ Health* **41**, 481–8 (1994).

10. Gasiewicz, T. A., Geiger, L. E., Rucci, G. & Neal, R. A. Distribution, excretion, and metabolism of 2,3,7,8-tetrachlorodibenzo-p-dioxin in C57BL/6J, DBA/2J, and B6D2F1/J mice. *Drug Metab Dispos* **11**, 397–403 (1983).

11. Chen, Q. *et al.* Estimation of background serum 2,3,7,8-TCDD concentrations by using quantile regression in the UMDES and NHANES populations. *Epidemiology* **21 Suppl 4**, S51-7 (2010).

12. Nault, R. *et al.* Single-cell transcriptomics shows dose-dependent disruption of hepatic zonation by TCDD in mice. *Toxicological Sciences* (2022) doi:10.1093/toxsci/kfac109.

13. Dowman, J. K., Tomlinson, J. W. & Newsome, P. N. Pathogenesis of non-alcoholic fatty liver disease. *QJM* **103**, 71–83 (2010).

14. Maurice, J. & Manousou, P. Non-alcoholic fatty liver disease. *Clinical Medicine* **18**, 245–250 (2018).

15. Santostefano, M. J. *et al.* Dose-dependent localization of TCDD in isolated centrilobular and periportal hepatocytes. *Toxicol Sci* **52**, 9–19 (1999).

16. Cunningham, R. P. & Porat-Shliom, N. Liver Zonation – Revisiting Old Questions With New Technologies. *Front Physiol* **12**, (2021).

17. Jungermann, K. Zonation of metabolism and gene expression in liver. *Histochem Cell Biol* **103**, 81–91 (1995).

18. Gebhardt, R. Metabolic zonation of the liver: Regulation and implications for liver function. *Pharmacol Ther* **53**, 275–354 (1992).

19. Wu, X., Dong, L., Lin, X. & Li, J. Relevance of the NLRP3 Inflammasome in the Pathogenesis of Chronic Liver Disease. *Front Immunol* **8**, (2017).

20. Méndez-Sánchez, N., Córdova-Gallardo, J., Barranco-Fragoso, B. & Eslam, M. Hepatic Dendritic Cells in the Development and Progression of Metabolic Steatohepatitis. *Front Immunol* **12**, (2021).

21. Rensen, S. S. *et al.* Activation of the complement system in human nonalcoholic fatty liver disease. *Hepatology* **50**, 1809–1817 (2009).

22. Tomaszewski, M., Stępień, K. M., Tomaszewska, J. & Czuczwar, S. J. Statin-induced myopathies. *Pharmacological Reports* **63**, 859–866 (2011).

23. de Bandt, J.-P., Jegatheesan, P. & Tennoune-El-Hafaia, N. Muscle Loss in Chronic Liver Diseases: The Example of Nonalcoholic Liver Disease. *Nutrients* **10**, 1195 (2018).

24. Chishima, S., Kogiso, T., Matsushita, N., Hashimoto, E. & Tokushige, K. The Relationship between the Growth Hormone/Insulin-like Growth Factor System and the Histological Features of Nonalcoholic Fatty Liver Disease. *Internal Medicine* **56**, 473–480 (2017).

25. Bergen, K., Brismar, K. & Tehrani, S. High-dose atorvastatin is associated with lower IGF-1 levels in patients with type 1 diabetes. *Growth Hormone & IGF Research* **29**, 78–82 (2016).

26. Crossey, P. A., Jones, J. S. & Miell, J. P. Dysregulation of the insulin/IGF binding protein-1 axis in transgenic mice is associated with hyperinsulinemia and glucose intolerance. *Diabetes* **49**, 457–465 (2000).

27. Murray, I. A. & Perdew, G. H. Omeprazole Stimulates the Induction of Human Insulin-Like Growth Factor Binding Protein-1 through Aryl Hydrocarbon Receptor Activation. *Journal of Pharmacology and Experimental Therapeutics* **324**, 1102–1110 (2008).

28. Minami, K. *et al.* Regulation of insulin-like growth factor binding protein-1 and lipoprotein lipase by the aryl hydrocarbon receptor. *J Toxicol Sci* **33**, 405–413 (2008).

29. Jurgelewicz, A. *et al.* Genetics-Based Approach to Identify Novel Genes Regulated by the Aryl Hydrocarbon Receptor in Mouse Liver. *Toxicol Sci* **181**, 285–294 (2021).

30. Akazawa, Y. & Nakao, K. To die or not to die: death signaling in nonalcoholic fatty liver disease. *J Gastroenterol* **53**, 893–906 (2018).

31. Luedde, T. & Schwabe, R. F. NF-κB in the liver—linking injury, fibrosis and hepatocellular carcinoma. *Nat Rev Gastroenterol Hepatol* **8**, 108–118 (2011).

32. Koda, Y. *et al.* Plasmacytoid dendritic cells protect against immune-mediated acute liver injury via IL-35. *Journal of Clinical Investigation* **129**, 3201–3213 (2019).

Chapter 5: Conclusions and Future Directions

Overall Goal

The primary goal of this dissertation was to gain better insight on the connection between alterations in cholesterol homeostasis, AHR-mediated signaling and TCDD-induced liver injury. First, we identified key genes implicated in AHR-mediated injury, leading us to determine that HMGCR is important for TCDD-induced changes in body weight. This led to us characterizing the role that HMGCR plays in TCDD-induced liver injury, and ultimately, how simvastatin impacts toxicant-induced liver injury.

Primary Findings and Future Directions

Specific Aim 1: Identifying Key Genes Implicated in AHR-Mediated Injury

The primary goal of this study was to use a population-based approach to identify novel genes regulated by the AHR that may lead to specific genes or pathways that are implicated in TCDD-induced liver injury. Additionally, it aimed to identify genes that are implicated in TCDD-mediated changes in body weight and body fat percentage. This study examined 14 genetically diverse *Mus musculus* strains that were treated with vehicle control or TCDD (100 ng/kg) for 10 consecutive days.[1]

This study demonstrated that there was a range of responses across diverse genetic backgrounds that suggest factors in addition to the *Ahr* allele carried by a mouse play a role in responses to AHR ligands. There was a range in the number of differentially expressed genes and the level of hepatic TCDD burden that did not entirely correspond to the *Ahr* allele carried by the mice leading to us to perform linear regression to identify which genes were associated with hepatic TCDD burden. This study indicated 7 genes, 2 of which were novel, associated with

hepatic TCDD burden. Furthermore, this study indicated genes that were associated with additional TCDD-induced phenotypes. *Dio1* was associated with TCDD-induced changes in body fat percentage, and *Hmgcr* was associated with TCDD-induced changes in body weight.

While the focus of this dissertation was on characterizing HMGCR in TCDD-mediated injury, additional studies in the future can focus on the role of the additional genes identified in this study, especially the novel AHR-regulated genes, *Nptx1* or *Slc46a3*. For example, *Nptx1* has been shown to play an oncogenic role in several tumors but may inhibit growth and promote apoptosis in hepatocellular carcinoma.[2] Future studies can deduce the role of *Nptx1* in TCDD-induced liver injury and elucidate if it could be a good target candidate for toxicant-induced liver injury. Furthermore, it would also be beneficial to characterize the role of *Dio1* in TCDD-induced liver injury similarly to how we focused on *Hmgcr.* Thyroid hormones play a key role in regulating conditions involved in metabolic syndrome, such as insulin resistance and body weight, and studies suggest that hypothyroidism is prevalent in NAFLD patients.[3] Thus, this could be another likely candidate involved in TCDD-induced liver injury.

Specific Aim 2: Characterizing the Role of HMGCR Repression in TCDD-Induced Liver Injury

The primary goal of this study was to assess the potential role of *Hmgcr* in modulating TCDD-mediated liver injury. This study exposed TCDD-sensitive (*Ahr*^{b1}) mouse strain, C57Bl6/J, to TCDD (10 μg/kg) in the presence and absence of simvastatin, a competitive inhibitor of HMGCR every day for 10 consecutive days.[4] This study was conducted in male and female mice to determine if there were any sex-specific outcomes associated with treatment.

This study supported previous reports indicating that TCDD dysregulated cholesterol

homeostasis and induces hepatopathologies like NAFLD in mice. Interestingly, this study indicated that simvastatin co-treatment led to sex-specific liver injury. In both sexes, simvastatin co-treatment led to decreased AHR-mediated steatosis. However, in females, there was increased hepatic glycogen, and in males, there was exacerbated TCDD-induced liver injury indicated by higher ALT levels and greater induction of AHR battery genes. These results suggested that simvastatin may put vulnerable populations at risk of sex-specific injury.

The follow-up study in specific aim 3 only focused on the outcomes seen in male mice. Therefore, future studies can elucidate a mechanism to determine why simvastatin co-treatment is mimicking a glycogen storage disease in females by analyzing protein expression and activity of enzymes involved in glycogen anabolism and catabolism. It's also important to note that one side effect of glycogen storage disease includes myopathy, which has been linked with statin usage.[5] Additionally, statins have been linked to causing glucose intolerance in rodent muscles.[6] Therefore, future studies could also examine skeletal muscle in addition to liver tissue to elucidate if these conditions may be connected to each other in females.

It is also valuable to indicate if any of these changes seen in co-treatment are also seen in human models. Although supply chain issues prevented their use for the scope of this dissertation, HepaRG cells are a robust and reliable model for toxicity studies. HepaRG cells are more similar to primary human hepatocytes in comparison to other available human liver cell lines when comparing gene expression levels and cytochrome P450 enzyme activity.[7] Using this cell lines has many benefits that can address the human relevance of the changes seen in co-treatment. For example, HepaRG cells can be used for Oil Red O staining allowing us to see if co-treatment decreases steatosis compared to TCDD alone in human hepatocytes.[8] Furthermore,

undifferentiated HepaRG cells can be used to make CRISPR-Cas 9 knockout cell lines. By knocking out AHR, for example, it can be confirmed if the simvastatin-induced changes in co-treated liver are AHR dependent as we saw greater AHR-mediated transcription compared to TCDD alone. It would also be useful to see if different statins have the same effects as we saw with simvastatin. While it may not be feasible to repeat these studies in mice for each statin, using HepaRG cells would be a less costly alternative in addition to being more applicable to how different statins may impact the human liver.

Specific Aim 3: Characterizing the Impact of Simvastatin on TCDD-Induced Liver Injury

The primary goal of this study was to elucidate a mechanism for how simvastatin exacerbates TCDD-induced liver injury in male mice. This study treated C57Bl6/J mice with TCDD (30 μg/kg) every 4 days for 28 days in the presence and absence of simvastatin. Liver tissue was collected from these mice and single-nuclei RNA sequencing was performed to determine how simvastatin co-treatment impacts distinct liver cell (sub)types differently from TCDD alone, which could impact liver injury severity.

This study indicated that simvastatin co-treatment alters the relative liver cell (sub)type proportions compared to TCDD alone. There was a trending decrease in immune cell infiltration with co-treatment, but the portion of liver dendritic cells only increased in co-treatment compared to all other treatment groups. Functional annotation analysis indicated that repression of genes involved in NF-κB signaling in macrophages and repression of genes involved in the complement system in dendritic cells may play an important role in this process. Interestingly, although snRNAseq results suggested that simvastatin co-treatment may be beneficial for the

liver, it was also associated with wasting and lethality that may be due to enhanced AHR activity.

In future studies, it is important to elucidate why co-treatment would lead to wasting. Although this result does support that *Hmgcr* is linked to TCDD-induced body weight changes as indicated in specific aim 1, the snRNAseq results in the liver were not enough information to deduce an explanation for a systemic effect. It is unclear if the wasting is a result of decreased fat or lean muscle mass, so performing whole-body scans of the mice under these treatments would help address where the loss in weight is coming from. Furthermore, future studies can focus on examining other tissues in addition to the liver, such as skeletal muscle. Performing bulk-RNA sequencing on skeletal muscle can help elucidate how treatment is impacting pathways associated with myopathy, and it can help confirm if the GH/IGF-1 axis may be an important pathway involved in this wasting. As this initial study was only performed in males, repeating this study in females would also help address the results seen in Chapter 3.

It would also be important in future studies to confirm if this adverse phenotype is seen at lower concentrations of TCDD treatment. While the dosing schematic in this study is more environmentally relevant, we have not looked at the impact of simvastatin co-treatment at lower doses of TCDD.[9] Again, further research would also be needed to confirm these results in the human population as this data suggests that people who may take statins as a treatment for NAFLD could be at risk of developing adverse side effects.

Overall Conclusion

While it is known that TCDD elicits injury via AHR activation, much remains unknown about the mechanisms behind how exposure to TCDD or other AHR ligands can drive these

adverse effects. This thesis aimed to bridge this gap by showing how dysregulating cholesterol through HMGCR repression is connected to TCDD-induced liver injury. Also, this thesis provides a more concrete understanding of how statin drugs impact the liver in the context of toxicant-induced liver injury. While statins have been suggested to be a treatment for NAFLD, the findings of this thesis showcase how statins directly impact specific liver cell types involved in the development and progression of NAFLD. It also emphasizes that using statins as a treatment for NAFLD requires further investigation to ensure that vulnerable populations are not at greater risk for adverse health effects. Through further investigation of the results outlined in this thesis, we hope that it can eventually lead to therapeutic treatment options for NAFLD. Cases of NAFLD will continue to grow as cases of metabolic disorders continue to rise, so we hope that these results may lead to new pharmaceutical treatments or ways to adapt existing drugs, such as statins, to become safe options for treatment.

REFERENCES

1. Jurgelewicz, A. *et al.* Genetics-Based Approach to Identify Novel Genes Regulated by the Aryl Hydrocarbon Receptor in Mouse Liver. *Toxicol Sci* **181**, 285–294 (2021).

2. Zhao, Y. *et al.* As a downstream target of the AKT pathway, NPTX1 inhibits proliferation and promotes apoptosis in hepatocellular carcinoma. *Biosci Rep* **39**, (2019).

3. Eshraghian, A. Non-alcoholic fatty liver disease and thyroid dysfunction: A systematic review. *World J Gastroenterol* **20**, 8102 (2014).

4. Dornbos, P. *et al.* Characterizing the Role of HMG-CoA Reductase in Aryl Hydrocarbon Receptor-Mediated Liver Injury in C57BL/6 Mice. *Sci Rep* **9**, 15828 (2019).

5. Tomaszewski, M., Stępień, K. M., Tomaszewska, J. & Czuczwar, S. J. Statin-induced myopathies. *Pharmacological Reports* **63**, 859–866 (2011).

6. Seshadri, S. *et al.* Statins exacerbate glucose intolerance and hyperglycemia in a high sucrose fed rodent model. *Sci Rep* **9**, 8825 (2019).

7. Hart, S. N. *et al.* A Comparison of Whole Genome Gene Expression Profiles of HepaRG Cells and HepG2 Cells to Primary Human Hepatocytes and Human Liver Tissues. *Drug Metabolism and Disposition* **38**, 988–994 (2010).

8. Anthérieu, S., Rogue, A., Fromenty, B., Guillouzo, A. & Robin, M. Induction of vesicular steatosis by amiodarone and tetracycline is associated with up-regulation of lipogenic genes in heparg cells. *Hepatology* **53**, 1895–1905 (2011).

9. Nault, R. *et al.* Dose-Dependent Metabolic Reprogramming and Differential Gene Expression in TCDD-Elicited Hepatic Fibrosis. *Toxicol Sci* **154**, 253–266 (2016).

Chapter 6: Materials and Methods

Materials and Methods for Chapters 2-4

Mouse Panel Study

All animal handling was in accordance with Texas A&M University's Institutional Animal Care and Use Committee. Fourteen mouse strains were used: 1) C57BL/6J; 2) A/J; 3) BALB/cJ; 4) FVB/NJ; 5) C3HeB/FeJ; 6) CBA/J; 7) DBA/1J; 8) NOD/ShiLtJ; 9) NZO/HiLtJ; 10) 129S1/SvlmJ; 11) BXD40; 12) BXD91; 13) BXD100; 14) CC019/TauUNC. Animals were obtained from The Jackson Laboratory (Bar Harbor, Maine) and mated at 6-8 weeks of age. Females were checked daily for vaginal plugs. Pregnancy-related endpoints were to be a focus in other studies, but the focus of this study was only on liver-related phenotypes. If a plug was present, mice were separated, weighed and randomly placed into a 2,3,7,8-tetrachlorodibenzo-ρ-dioxin (TCDD) dose group: vehicle control (0), 1 or 100 ng/kg/day. TCDD was administered to mice using peanut butter as the vehicle daily for 10 consecutive days. Maternal body weights and composition were recorded at gestation day 1 (D1; initial dose) and D11 (euthanasia). Body composition was performed using an EchoMRI-100H Body Composition Analyzer. Both weights and body composition results were reported as mean ± SEM. On day 11 (D11), mice were anesthetized with avertin, euthanized via CO_2 asphyxiation, and tissues were snap frozen in liquid nitrogen. Pregnancy success was assessed by the presence of absorption sites or embryos within the uterus under a dissection microscope; only pregnant mice were included in downstream analysis. LabDiet 5058 chow and water were provided *ad libitum* during mating and throughout treatment. Mice were maintained under constant 12-h light/dark cycles, temperature (74°F ± 2°F set point), and humidity (average 51%; range 39-52%) during mating and pregnancy.

TCDD and Statin Exposure

Chapter 3: All animal experiments were approved by Michigan State University (MSU)'s Institutional Animal Care & Use Committee and were carried out in accordance with this approval and all relevant guidelines and regulations. Age-matched male and female C57BL/6J mice were ordered from Charles River Laboratories (Kingston, NY) and delivered to MSU on postnatal day 25 (PND25). Mice were acclimated to the facility for 7 days prior to treatment. Mice were housed in Innovive Innocages (Innovive, San Diego, CA) with ALPHA-Dri bedding (Shepherd Specialty Papers, Chicago, IL) under constant 12-hour light/dark cycles, temperature and humidity. Upon arrival, mice were randomly placed into a treatment group: A) sesame oil (vehicle control; Sigma Aldrich) + standard mouse chow (Harlan Teklad Rodent Diet 8940); B) TCDD (10 μg/kg; Accustandard, New Haven, CT) + standard mouse chow; C) sesame oil + chow containing simvastatin (500 mg/kg food; Harlan Teklad Rodent Diet 8940; Sigma Aldrich, St. Louis, MO); or D) TCDD + chow containing simvastatin. The simvastatin-laced chow was prepared at Envigo (Huntingdon, UK). Mice were acclimated to the simvastatin-laced chow for 3 days prior to treatment with TCDD. Chow was provided *ad libitum* for each treatment group. Each treatment group had a sample size of 8 mice with the exception of the male TCDD + standard chow group due to 1 mouse dying in-transit prior to the experiment start point. The average (mg/kg body weight/day) and standard deviation of simvastatin exposure for females and males over the 13-day period was 77.2 ± 2.8 and 73.6 ± 1.2, respectively. Although this dose range in mice corresponds to approximately 350 mg/day in humans, simvastatin is 5-8 times less efficacious in mice in comparison.[1] Therefore, the effective dose used in this study is within range of what is relevant in humans with moderate to severe hypercholesterolemia. TCDD treatment did not

significantly impact consumption of simvastatin-laced chow. Following the dosing regime, the mice were sacrificed on day 11 following a 6-hour fasting period. Tissues were either frozen in liquid nitrogen or fixed in 10% phosphate buffered formalin (Thermo Fisher, Waltham, MA).

Chapter 4: All animal experiments were approved by Michigan State University (MSU)'s Institutional Animal Care & Use Committee and were carried out in accordance with this approval and all relevant guidelines and regulations. Male C57Bl/6 mice were ordered from Charles River Laboratories and were delivered to Michigan State University on postnatal day 25 (PND25). Mice were acclimated for 7 days prior to treatment. Mice were housed in Innocages (Innovive, San Diego, CA) with ALPHA-Dri bedding (Shepherd Specialty Papers, Chicago, IL) under constant 12-hour light/dark cycles, temperature, and humidity. Upon arrival, mice were randomly placed into a treatment group: (A) sesame oil (vehicle control; Sigma Aldrich) with standard mouse chow (Harlan Teklad Rodent Diet 8940); (B) TCDD (30 μg/kg/day every 4 days for 28 days for 7 total treatments; AccuStandard, New Haven, CT) with standard mouse chow; (C) sesame oil with chow containing simvastatin (500 mg/kg/food, Harlan Teklad Rodent Diet 8940; Sigma Aldrich, St. Louis, MO); or (D) 30 μg/kg TCDD every 4 days for 28 days with chow containing 500 mg/kg simvastatin. The simvastatin-laced chow was prepared at Envigo (Huntington, UK). Mice were acclimated to the simvastatin-laced chow for 3 days prior to treatment with TCDD. Chow was provided *ad libitum* for each treatment group. Each treatment group had a sample size of at least 6 mice. Group D started with 7 mice and ended up with 5 due to 2 mice dying over the course of the study. The average dose of simvastatin (mg/kg/body weight/day) for the mice over the 32-day period was calculated to be 76.4 ± 3.1 and 85.9 ± 3.5 for statin alone and co-treatment,

respectively, estimated from the daily chow consumption per cage. TCDD did not impact consumption of simvastatin-laced chow. Although this dose range in mice corresponds to approximately 350 mg/day in humans, simvastatin is 5-8 times less efficacious in mice in comparison.[1] Therefore, the effective dose used in this study is within range of what is relevant in humans with moderate to severe hypercholesterolemia. On day 32, the mice were sacrificed following a 6-hour fasting period. Tissue samples were frozen in liquid nitrogen or fixed in formalin for histopathology.

TCDD Liver Burden Analysis

TCDD accumulation was measured in liver tissue via gas chromatography-mass spectrometry (GC/MS) at The Dow Chemical Company. TCDD was measured in the livers of all 14 strains of the mouse panel that were assessed with 1 ng/kg/day (n=3) or 100 ng/kg/day (n=3) of TCDD. A subset of strains (n=9) was randomly chosen to assess the level of TCDD in the vehicle control groups. The sample extraction and purification procedures were developed at the Dow Chemical Company (Midland, MI) based on US Environmental Protection Agency method 8290. Briefly, 50 mL of 5% benzene in hexane solution, 10 ng of ^{13}C-YCDD (Wellington Environmental, lot no. MD0480912), and 30 mL of concentrated HCl (trace metal grade) were added to each sample in sequence. Lab control spike (LCS) sample, which contains 10 ng of native TCDD (Wellington Environmental, lot no. 90STN1013) and 0.5 g of corn oil and method blank (MB) sample (0.5 g of corn oil) were analyzed along with each set of samples. All samples were shaken for 1 hour on a shaking bed, vented to release pressure, and then shaken overnight. After shaking, the organic layer was transferred to a new bottle for subsequent sample purification (column

clean-up). Acid/base silica column and alumina column were utilized for sample purification. The sample extracts were then purged to dryness and reconstituted with 20 µL of ^{13}C-1,2,7,8-tetrachlorodibenzofuran (TCDF) (Wellington Environmental, lot no. 020701), which was treated as the injection standard to account for the recovery of the internal standard (^{13}C-TCDD). All samples were quantified using either gas chromatograph/high efficiency triple-quadrupole system (GC/MS/MS, Aligent 7000 series) or low-resolution single quadrupole GC/MS (HP 5973/6890), depending on the dosing level of TCDD. Both instruments were equipped with a 30 m x 0.25 mm DB-5 ms column and data were quantified via a isotopic dilution approach using either chemstation (Agilent) or masshunter (Agilent) software. Results of all quality control samples (MB and LCS) have passed method criteria indicating satisfying analytical quality. The average level of TCDD in the vehicle control group was 2.8 ng/kg liver.

Histological Analyses

Chapter 3: All histological processing and staining was performed by the MSU Investigative Histopathology Laboratory. Formalin-fixed liver was vacuum infiltrated with paraffin using a Tissue-Tek VIP 2000 and embedded with the HistoCentre III embedding station (Thermo Fisher, Watlham, MA). A Rechert Jung 2030 rotary microtome (Reichert, Depew, NY) was used to section tissue at 4-5 µm. Sections were then placed on slides and dried for 2-24 hrs at 56°C. Dried liver sections were strained with hematoxylin and eoxin (H&E) for general morphometric analysis and periodic acid-Schiff (PAS) stain to detect glycogen. Histological severity scoring of H&E stained liver sections was performed by a certified pathologist and based on the following scale: 0 (no lesions present); 1 (mild and random foci of inflammation); 2

(intermediate inflammation with presence of necrotic hepatocytes) and 3 (marked inflammation and greater presence of necrotic hepatocytes as compared to other scores). In all cases, n ≥ 7 for each dose group during the histological scoring. Frozen tissues were sectioned at 6 µm and stained with oil red O (ORO) to detect neutral lipids as previously described.[2] An Olympus Virtual Slide System VS110 was used to digitize the slides at 20x magnification (Olympus, Center Valley, PA). The Olympus OlyVIA software (Olympus) was used to visualize the digitized slides. The percent area of liver tissue stained with ORO was quantified using the Quantitation Histological Analysis Tool (QuHAnT) was previously described.[3] The optimal hue, saturation and value (HSV) thresholds used for feature extraction were 0 to 50 and 225 to 250 (hue), 30 to 255 (saturation) and 0 to 255 (value).

Chapter 4: All histological processing and staining was performed by the MSU Investigative Histopathology Laboratory. The protocol for H&E staining was the same protocol as outlined in Chapter 3. Histological severity scoring of H&E stained liver sections was performed by a certified veterinary pathologist using the following criteria: 1, minimal, less than 25% of tissue; 2, mild, 25% to less than 50%; 3, moderate, 50% to less than 75%; 4, marked, 75%-100%.

Hepatic Lipid Extraction

Hepatic lipids were extracted as previously described.[4] Frozen liver was homogenized in 10x volume of extraction buffer (18 mM Tris (pH 7.5), 300 mM D-Mannitol, 50 mM EGTA, 0.1 mM phenylmethylsulfonyl fluoride) using a Mixer Mill 300 (Life Sciences, Carlsbad, CA). 500 µL of homogenate was added to 4 mL of 2:1 chloroform:methanol and mixed end-over-end shaking overnight at room temperature. Water (800 µL) was added and the sample was mixed by

vortexing and the phases were separated by centrifugation (3000 x g for 5 min). 2 mL of organic phases was transferred to a new tube and evaportated over nitrogen to dryness. Following an incubation at 45°C for 5 min, the lipid residue was dissolved in 300 µL of isopropyl alcohol with 10% Triton X-100. Commercially available reagents were used to analyze triglycerides (Pointe Scientific, Canton, MI) and total cholesterol (FUJIFILM Wako Diagnostics, Richmond, VA) with a SpectraMax M2 microplate reader (Molecular Devices, San Jose, CA). The sample size (n) was 5 for each group and mice were randomly selected.

Hepatic Glycogen and Glucose Assay

The level of glycogen and free glucose were determined as previously described.[5] Frozen liver (~50 mg) was homogenized in 250 µL of 6% perchloric acid using a Polytron PT21000 (Kinematica AG, Luzern, Switzerland). A portion of the homogenate was used to measure background glucose while another portion (50 µL) was combined with 25 µL of 1M $NaHCO_3$ and 125 µL amyloglucosidase solution (2 mg/mL; Sigma Aldrich, St. Louis, MO). The mixtures were incubated with shaking at 37°C for 2 hours. Background-corrected glucose levels in the amylglucosidase-treated samples were used to infer hepatic glycogen levels. Glucose was assessed using commercially available reagents (FUJIFILM Wako Diagnostics, Richmond, VA) and a SpectraMax M2 microplate reader (Molecular Devices, San Jose, CA)> The sample size (n) was 5 for each group and mice were randomly selected.

Western Blot Analysis

Frozen liver was homogenized in radioimmunoprecipitation assay (RIPA) buffer using a

Mixer Mill 300 (Life Sciences, Carlsbad, CA). The protein concentration in the supernatant was determined with a Bradford Assay following a 10 min centrifugation (16,000 x g).[6] Sodium dodecyl sulfate-polyacrylamide gel electrophoresis (SDS-PAGE) was used to separate 60 µg of total protein, which was subsequently transferred into a nitrocellulose membrane. The membrane was blocked with 5% non-fat dry milk dissolved in Tris-Buffered Saline with 0.05% Tween 20 (TBST) and probed with monoclonal anti-mouse HMGCR antibody (1:1000; Abcam, Cambridge, MA) or a monoclonal ACTB antibody (1:3000; Santa Cruz Biotechnology, Dallas, TX) overnight at 4°C. Following 3 x 5-min washes with TBST, the membrane was exposed to a monoclonal mouse anti-rabbit IgG-HRP (1:1000; Santa Cruz Biotechnology, Dallas, TX) or a mouse IgG kappa binding protein-HRP (1:3000; Santa Cruz Biotechnology, Dallas, TX) where appropriate. Following 3 x 5-min washes with TBST, the blots were developed using the Pierce enhanced chemiluminescence (ECL) Western Blotting Substrate (Thermo Fisher, Waltham, MA). The Image Studio Lite software (LI-COR, Lincoln, NE) was used for the densitometry analysis. HMCGR expression was normalized to ACTB prior to analysis. Fold changes are relative to the mean of the vehicle control mice on standard diet. The sample size was 5 for each group and mice were randomly selected.

Serum Clinical Chemistry

All serum clinical chemistry performed was done using commercially available reagents following the manufacturer's protocols. Kits used included serum total cholesterol, low-density lipoprotein, alanine aminotransferase and glucose (FUJIFILM Wako Diagnostics, Richmond, VA) as well as high-density lipoprotein (Crystal Chemical, Houston, TX). In all cases, a SpectraMax M2

microplate reader was used (Molecular Devices, San Jose, CA). N ≥ 5 for each mouse group.

Phylogenetic Analysis

Genomic and amino acid sequences were predicted using the automated Mouse Gene and Protein Sequence Predictor.[7] Multiple sequence alignments were performed using Multiple Alignment using Fast Fourier Transform (MAFFT) algorithm.[8] Clustal-formatted alignment and phylogenetic tree outputs were created based on the output from MAFFT software. Phylogenetic trees were visualized with FigTree v1.4.2.

Heritability Analysis

Heritability was assessed as previously described.[9] Briefly, a regression model was fit to estimate the proportion of variance in the dependent variable (i.e., hepatic TCDD burden) that is not attributed to variance across independent variable replication (i.e., interstrain variability). The 95% CIs of the multiple R^2 value was calculated via bootstrapping (n=1000) using the bias corrected and accelerated method implemented in the boot library in R.[10]

Linear Regression

Regression was used to analyze DEGs across the 14 strains (n=932), meaning 1) at least one strain displayed |fold change| ≥ 1.5 and 2) at least 1 strain displayed significant change in expression of the gene as compared with vehicle ($p < 0.05$). Linear, least-squared regression was performed to scan for genes where expression associated with TCDD burden, body fat percentage or body weight. In all cases, Python version 2.7.10 was used during regression

analysis.[11] P-values were adjusted for 5% false detection rate (FDR) using the Benjamini-Hochberg correction.[12]

Quantitative Trait Loci (QTL) Analysis

QTL analysis was performed using Gene Network's online-based WebQTL program (www.genenetwork.org/webqtl/main.py).[13] Scans for QTLs were performed using the mean change in total body weight. The mapping was performed using the data from the 10 strains that are members of the Mouse Diversity Panel: 1) C57BL/2J; 2) 129S1/SvlmJ; 3) NOD/ShiLtJ; 4) A/J; 5) NZO/HILTJ; 6) C3HeB/FeJ; 7) CBA/1J; 8) DBA/1J; 9) FVB/nJ; 10) BALB/cJ. The whole-genome interval mapping was performed using the default settings of 2000 bootstrap tests. The threshold of significance was determined via permutation test (n=10,000). The log of the odds (LOD) ratio was calculated as outlined in the WebQTL glossary of terms (i.e., LRS/4.61).

RNA Isolation in Liver Tissue

Frozen liver (approximately 50 mg) was homogenized in 1 mL of TriZOL in chrome-steel beads using a Mixer Mill 300 (Life Sciences, Carlsbad, CA) for 4 mins. Following, total RNA was extracted per the manufacturer's instructions with an additional 5:1 phenol:chloroform extraction step (Sigma Aldrich, St. Louis, MO). RNA purity (260/280 ratio) and concentration (ng/µL) were assessed with a NanoDrop 1000 spectrophotometer. RNA quality was determined using an Aligent 2100 Bioanalyzer for RNA samples sent for bulk-RNA sequencing. All RNA samples sent for bulk-RNA sequencing had RNA integrity numbers ≥ 7.

Bulk-RNA Sequencing

Sequencing: RNA samples from the 14 strains of mice treated with either vehicle control (n=3) or 100 ng/kg/day (n=3) were sequenced by Novogene (Sacramento, CA). RNA quality was verified on an Agilent 2100 Bioanalyzer (Santa Clara, CA) prior to sequencing. RNA was fragmented via sonication with a BioRuptor (Diagenode, Denville, NJ). Library preparation was performed using a NEBNext Ultra RNA kit (New England Biolabs, Ipswich, MA). An additional quality control step was performed to assess concentration, molarity and fragment size prior to sequencing. The samples were sequenced using the PE150 sequencing strategy with reagents from Illumina (San Diego, CA).

Processing: Read pair processing and analysis was performed as previously described.[14] Read quality was assessed using FastQC v0.11.5 (www.bioinformatics.babraham.ac.uk/projects/fastqc) and adapter trimming was performed using Trimmomatic v0.38.[15] Strain-specific reference pseudogenomes (Build 37) and corresponding MOD files were downloaded from www.csbio.unc.edu/CCstatus/index.py?run=Pseudo and was used for alignment using Bowtie2 v2.3.2.[16] Alignment for reads for BXD strains (BXD30, BXD91 and BXD100) whose pseudogenomes were not available was performed using the pseudogenomes of parental strains C57BL/6J and DBA/2J. Coordinates of aligned reads were converted to common mm9 reference genome coordinates using the Lapels package (github.com/shunping/lapels). Alignments made to 2 reference genomes (eg, BXD mice) were merged using the Suspenders package (github.com/holtkma/suspenders). Gene counts were determined using HTSeq-count v0.6.1.[17] Differential expression was performed between treatment groups within strains using DESeq2

v3.8.[18] Genes were considered differentially expressed when |fold change| ≥ 1.5 and adjusted p-value (FDR) ≤ 0.05. Sequencing data is deposited in the gene expression omnibus (GEO; GSE167328).

Quantitative Real Time Polymerase Chain Reaction (qRT-PCR)

Total RNA (2 µg for liver homogenate) was converted to cDNA using oligo(dT) primers and GoScript reverse transcriptase (Promega, Madison, WI) in the mouse panel study or using reverse transcriptase superscript III (Invitrogen, Waltham, MA) in the first statin study. SYBR green master mix (Applied Biosystems, Waltham, MA) was used to analyze relative gene expression. Gene expression was normalized to the geometric mean of 3 housekeeping genes: *Hprt, Actb* and *Gusb.* All PCR was performed using one of 3 machines: QuantStudio 3 RT-PCR System (Thermo Fisher, Waltham, MA), DNA Engine Opticon 2 (Bio-Rad, Hercules, CA) or QuantStudio 7 Flex Real-Time PCR System (Thermo Fisher, Waltham, MA). The $2^{-\Delta\Delta ct}$ method was used to calculate fold changes and all values were relative to the mean of their respective control mice for each strain. N=3 for each strain in the mouse panel study and n ≥ 7 in the first statin study.

Nuclei Isolation

Nuclei were isolated from frozen liver samples (n=3) as previously described (https://doi.org/10.17504/protocols.io.3fkgjkw).[19] Briefly, livers were diced in EZ Lysis Buffer (Sigma-Aldrich, St. Louis, MO), homogenized using a disposable Dounce homogenizer, and incubated on ice for 5 minutes. The homogenate was filtered, transferred to a microcentrifuge tube and nuclei were isolated by centrifugation (500 x g and 4^{o} C, 5 minutes). The supernatant

was removed and nuclei were resuspended in fresh EZ Lysis Buffer and incubated on ice (5 mins.) ice followed by centrifugation. The nuclei pellet was washed twice with nuclei wash and resuspend buffer (1x phosphate-buffered saline, 1% bovine serum albumin, 0.2-U/μL RNAse inhibitor) with 5-minute incubations on ice. After washing, the pellet was resuspended in nuclei wash and resuspend buffer containing DAPI (10 μg/mL). The nuclei were filtered (40 μm) and underwent fluorescence-activated cell sorting using a BD FAC-Saria Ilu (BD Biosciences, San Jose, CA) with a 70 μm nozzle at the MSU Pharmacology and Toxicology Flow Cytometry Core.

Single-Nuclei RNA Sequencing (snRNAseq)

Nuclei were immediately processed for snRNASeq, which was performed as previously described.[19] Briefly, 10x Genomics Chromium Single Cell 3' v3 libraries were submitted for 150-bp paired-end sequencing at a depth ≥ 60,000 reads/cell using a NovaSeq 6000 System (Illumina, San Diego, CA) at the MSU Research Technology Support Facility. Following sequencing quality control, Cell Ranger v3.0.2 (10X Genomics) was used to align reads to a custom reference genome (mouse mm10 release 93 genome build) which included introns and exons to consider pre-mRNA and mature mRNA. Raw counts were further analyzed on Seurat v.3.1.1.[20] Each sample was filtered for genes expressed in at least 3 nuclei, nuclei that expressed at least 100 genes and ≤ 1% mitochondrial genes. Clustering of nuclei was performed using Seurat integration tools at a resolution of 0.05 and were annotated using a semiautomated strategy. Marker genes for individual nuclei clusters were also manually examined to verify annotation. Raw and processed data have been deposited in the Gene Expression Omnibus (GEO) with accession ID GSE211018 following the Minimum Information about Animal Toxicology Experiments (MIATE;

https://doi.org/10.25504/FAIRsharing.wYScsE).

DAVID Functional Annotation Analysis

Functional annotation clustering of differentially expressed genes from individual mouse strains was assessed using the gene functional classification tool on the Database for Annotation, Visualization and Integrated Discovery (DAVID, v.6.8).[21,22] Enrichment scores of the generated clusters ≥ 1.3 were considered significant.

Statistical Analyses

Unless otherwise noted in their respective sections, all statistical analyses were performed using R version 3.0.2 besides the relative cell type proportions in Chapter 5 that were calculated using Astatsa.[23] Histograms and q-q plots were used to assess distributions prior to statistical analyses. Outliers within dose-groups were assessed with Grubb's test; significant outliers ($P < 0.05$) were removed prior to downstream analysis. Potential significant differences across dose groups and strains were calculated with a t test or analysis of variance (ANOVA) with a Tukey's pair-wise *posthoc* test where appropriate.

REFRENCES

1. van de Steeg, E. *et al.* Combined analysis of pharmacokinetic and efficacy data of preclinical studies with statins markedly improves translation of drug efficacy to human trials. *J Pharmacol Exp Ther* **347**, 635–44 (2013).

2. Kopec, A. K. *et al.* PCB153-elicited hepatic responses in the immature, ovariectomized C57BL/6 mice: comparative toxicogenomic effects of dioxin and non-dioxin-like ligands. *Toxicol Appl Pharmacol* **243**, 359–71 (2010).

3. Nault, R., Colbry, D., Brandenberger, C., Harkema, J. R. & Zacharewski, T. R. Development of a computational high-throughput tool for the quantitative examination of dose-dependent histological features. *Toxicol Pathol* **43**, 366–75 (2015).

4. Luyendyk, J. P., Sullivan, B. P., Guo, G. L. & Wang, R. Tissue Factor-Deficiency and Protease Activated Receptor-1-Deficiency Reduce Inflammation Elicited by Diet-Induced Steatohepatitis in Mice. *Am J Pathol* **176**, 177–186 (2010).

5. Nault, R. *et al.* Dose-Dependent Metabolic Reprogramming and Differential Gene Expression in TCDD-Elicited Hepatic Fibrosis. *Toxicol Sci* **154**, 253–266 (2016).

6. LOWRY, O. H., ROSEBROUGH, N. J., FARR, A. L. & RANDALL, R. J. Protein measurement with the Folin phenol reagent. *J Biol Chem* **193**, 265–75 (1951).

7. Dornbos, P., Arkatkar, A. A. & LaPres, J. J. An Automated Method To Predict Mouse Gene and Protein Sequences Using Variant Data. *G3 (Bethesda)* **10**, 925–932 (2020).

8. Katoh, K., Kuma, K., Toh, H. & Miyata, T. MAFFT version 5: improvement in accuracy of multiple sequence alignment. *Nucleic Acids Res* **33**, 511–8 (2005).

9. Dornbos, P. *et al.* Characterizing Serpinb2 as a Modulator of TCDD-Induced Suppression of the B Cell. *Chem Res Toxicol* **31**, 1248–1259 (2018).

10. Canty, A. & Ripley, B. D. Boot: Bootstap R (S-Plus) functions. *R package version 1.3-28* Preprint at (2017).

11. van Rossum, G. & Drake, F. L. Python Reference Manual. Preprint at (1995).

12. Benjamini, Y., Heller, R. & Yekutieli, D. Selective inference in complex research. *Philos Trans A Math Phys Eng Sci* **367**, 4255–71 (2009).

13. Jintao Wang, Robert W. Williams & Kenneth F. Manly. WebQTL: web-based complex trait analysis. *Neuroinformatics* **1**, 299–308 (2003).

14. Green, R., Wilkins, C., Ferris, M. T. & Gale, M. RNA-Seq in the Collaborative Cross. *Methods Mol Biol* **1488**, 251–263 (2017).

15. Bolger, A. M., Lohse, M. & Usadel, B. Trimmomatic: a flexible trimmer for Illumina sequence data. *Bioinformatics* **30**, 2114–20 (2014).

16. Langmead, B. & Salzberg, S. L. Fast gapped-read alignment with Bowtie 2. *Nat Methods* **9**, 357–9 (2012).

17. Anders, S. & Huber, W. Differential expression analysis for sequence count data. *Genome Biol* **11**, R106 (2010).

18. Love, M. I., Huber, W. & Anders, S. Moderated estimation of fold change and dispersion for RNA-seq data with DESeq2. *Genome Biol* **15**, 550 (2014).

19. Nault, R., Fader, K. A., Bhattacharya, S. & Zacharewski, T. R. Single-Nuclei RNA Sequencing Assessment of the Hepatic Effects of 2,3,7,8-Tetrachlorodibenzo-p-dioxin. *Cell Mol Gastroenterol Hepatol* **11**, 147–159 (2021).

20. Butler, A., Hoffman, P., Smibert, P., Papalexi, E. & Satija, R. Integrating single-cell transcriptomic data across different conditions, technologies, and species. *Nat Biotechnol* **36**, 411–420 (2018).

21. Huang, D. W., Sherman, B. T. & Lempicki, R. A. Bioinformatics enrichment tools: paths toward the comprehensive functional analysis of large gene lists. *Nucleic Acids Res* **37**, 1–13 (2009).

22. Huang, D. W., Sherman, B. T. & Lempicki, R. A. Systematic and integrative analysis of large gene lists using DAVID bioinformatics resources. *Nat Protoc* **4**, 44–57 (2009).

23. R Development Core Team. R: A Language and Environment for Statistical Computing. Preprint at (2015).